WIND RESOURCE ASSESSMENT, DESIGN AND PERFORMANCE OF HORIZONTAL AXIS WIND TURBINE FOR MISRATA- LIBYA

A THESIS SUBMITTED TO
THE GRADUATE SCHOOL OF NATURAL AND APPLIED SCIENCES
OF
UNIVERSITY OF TURKISH AERONAUTICAL ASSOCIATION

BY

ABDULHAMID BENGHUZZI

IN PARTIAL FULFILLMENT OF THE REQUIREMENTS
FOR
THE DEGREE OF DOCTOR OF PHILOSOPHY
IN
MECHANICAL AND AERONAUTICAL ENGINEERING

AUGUST 2020

Approval of the thesis:

WIND RESOURCE ASSESSMENT, DESIGN AND PERFORMANCE OF HORIZONTAL AXIS WIND TURBINE FOR MISRATA- LIBYA

submitted by **ABDULHAMID BENGHUZZI** in partial fulfillment of the requirements for the degree of **Doctor of Philosophy** i**n Mechanical and Aeronautical Engineering, University of Turkish Aeronautical Association** by,

Assoc. Prof. Dr. Suat Dengiz
Dean, Graduate School of **Natural and Applied Sciences** _____

Prof. Dr. İbrahim Halil Güzelbey
Head of the Department, **Mechanical and Aeronautical Eng** _____

Assist. Prof. Dr. Mohamed ELMNEFI
Supervisor, **Aeronautical Eng, THK University** _____

Examining Committee Members:

Assoc. Prof. Dr. Mustafa KAYA
Aerospace Eng, AYBU _____

Assoc. Prof. Dr. Munir ELFARRA
Aerospace Eng, AYBU _____

Assist. Prof. Dr. Mohamed ELMNEFI
Aeronautical Eng, THK _____

Assist. Prof. Dr. Durmuş Sinan KÖRPE
Aeronautical Eng, THK _____

Assist. Prof. Dr. Erol GÜLTEKİN
Mechanical Eng, THK _____

Date: 24.08.2020

I hereby declare that all information in this document has been obtained and presented in accordance with academic rules and ethical conduct. I also declare that, as required by these rules and conduct, I have fully cited and referenced all material and results that are not original to this work.

Name, Last name :

Signature :

ABSTRACT

WIND RESOURCE ASSESSMENT, DESIGN AND PERFORMANCE OF HORIZONTAL AXIS WIND TURBINE FOR MISRATA LIBYA

Benghuzzi, Abdulhamid
Doctor of Philosophy, Mechanical and Aeronautical Engineering
Supervisor : Assist. Prof. Dr. Mohamed Elmnefi

August 2020, 113 pages

The increase in electrical energy consumption and pollution from power plants have affected the Libyan state budget. It has led to an increased search for many methods to producing electric energy. It is motivated to search and study the wind speed available in the Misrata city. This study run far for five years, analyzed at altitudes 10, 30, and 50 meters from the surface of the earth using the Weibull probability density function. Besides, using the present value cost method to find the cost per kilowatts, then doing simulation for two-blade and three-blade by using the Q blade program compared with previous experimental S809 and then compared with simulation done by the Matlab program where is the comparison showed that the simulation it had resulted from Matlab simulation is more accurate than Q blade simulation in most points. According to this design, a blade of a turbine with 5 meters that mean wind speed 8 m/s of the Misrata location with a fixed twist angle and change the chord at different values of the lift coefficient. Also, determine the cost per Kw by related the rated power for each design with shape, scale, and capacity factor parameters Misrata location. In addition to these designs by changing the twist angle and fixed chord for two blades and three blades experimental S809 and

observed the optimal power at mean wind speed for Misurata location. Finally, designing 5 meters by choosing five sections from the geometric design of three blades S809 with fixed chord and developing three types of twist angle and also determining the cost by related the rated power obtain from each design with shape, scale and capacity factor parameters of Misrata location as a result of this study, Misrata location is encouraged to generation electric from the wind turbine. It shows that the best productive energy at a mean wind speed of Misrata location that it obtained from fixed chord and change twist angle of experimental three blades S809

Keywords: Analysis of Wind Energy Cost of Energy, Design Axis Wind Turbine.

ÖZ

RİSK KAYNAĞI DEĞERLENDİRMESİ, YATAY EKSENİN TASARIMI VE PERFORMANSI MISRATA LIBYA İÇİN RÜZGAR TÜRBİNİ

Doktora, Makine ve uçak Mühendisliği Bölümü
Tez Yöneticisi: Dr. Öğr. Üye. Abdulhamid Benghuzzi
Ortak Tez Yöneticisi: Doç. Dr. Mohamed Elmnefi

Ağustos 2020, 113 sayfa

Elektrik santrallerinden kaynaklanan elektrik enerjisi ve kirlilik tüketiminin artırılması, Libya devlet bütçesinde bir etkiye yol açtı. Elektrik enerjisi üretmek için birçok yöntem arayışında artışa neden oldu. Misrata şehrinde bulunan rüzgar hızını araştırmak ve incelemek için motive edilmiştir. Bu çalışma, Weibull olasılık yoğunluk fonksiyonu kullanılarak rüzgârın yer yüzeyinden 10, 30 ve 50 metre yükseklikte analiz edildiği beş yıl boyunca çalıştı. Ayrıca, kilowatt başına maliyeti bulmak için mevcut değer maliyet yöntemini kullanarak, daha önce deneysel S809 ile karşılaştırıldığında Q blade programını kullanarak iki bıçak ve üç bıçak için simülasyon yapmak ve daha sonra karşılaştırma yapılan Matlab programı tarafından yapılan simülasyon ile karşılaştırmak Matlab simülasyonundan kaynaklanan simülasyonun çoğu noktada Q blade simülasyonundan daha doğru olduğunu gösterdi. Bu tasarımın ardından Misrata yerinin 8 m/s rüzgar hızı sabit bir bükülme açısına sahip 5 metrelik bir türbin kanadı ve akkoru kaldırma katsayısının farklı değerlerinde değiştirin. Ayrıca, her tasarım için nominal gücü, şekil, ölçek ve kapasite faktörü parametreleri Misrata konumu ile ilişkilendirerek kW başına maliyeti belirleyin. Ayrıca, iki bıçak ve üç bıçak için büküm açısını ve sabit akkoru değiştirerek diğer tasarım deneysel S809 ve Misurata konumu için ortalama rüzgar hızında optimum gücü gözlemledi. Son olarak, 5 metre tasarım, sabit akorlu üç bıçak

S809'un geometrik tasarımından beş bölüm seçti ve üç tip büküm açısı geliştirdi ve aynı zamanda her tasarımdan elde edilen yazılı güç ile şekil, ölçek ve kapasite faktörü parametreleriyle ilgili maliyeti belirledi. Misrata lokasyonu Bu çalışmanın bir sonucu olarak Misrata lokasyonu rüzgar türbininden elektrik üretmeye teşvik edilmektedir. Bu sabit akor ve değişim üç bıçak S809 değişim büküm açısı elde ettiği Misrata konum ortalama rüzgar hızında en iyi üretken enerji göstermektedir.

Anahtar Kelimeler: Rüzgar Enerjisi Analizi, Enerji Maliyeti, Tasarım Ekseni Rüzgar Türbini.

Dedication

To my family

ACKNOWLEDGMENTS

In the name of Allah, the Most Beneficent and the Most Merciful. Praise to be cod Alone .He blesses the whole world with the most merciful and compassionate and attains his noble prophet peace up on him, could not have accomplished this work as presented here had it not been for the expert support and constant encouragement from my supervisor Dr. Mohamad Salem ELMNEFI, who supervised this study and provided me with support, encouragement, scientific observations and motivation. As well as being a brother and friend. I extend my thanks and gratitude to Dr. Monier ELFARRA, who supports me throughout this study. I thank Dr. Sinan KORPE for his scientific observations. In the last, I would like to extend my deepest and sincere thanks to my family for their moral support. I know without their love, conviction, and prayers, I would never be able to perform this scholarly activity.

TABLE OF CONTENTS

LIST OF TABLES

TABLES

LIST OF FIGURES

FIGURES

LIST OF ABBREVIATIONS

ABBREVIATIONS

AoA	Angle of Attack
BEM	Blade Element Momentum
PDF	Cumulative Distribution Function
EPF	Energy Pattern Factor Method
HAWT	Horizontal Axis Wind Turbine
IRENA	International Renewable Energy Agency
NACA	National Advisory Committee for Aeronautics
NREL	National Renewable Energy Laboratory
CDF	Probability Density Function
P15-50	Polaris Wind Turbine
PVC	Present Value Cost Method
VAWT	Vertical Axis Wind Turbine
V27-225	Vestas Wind Turbine
V39-500	Vestas Wind Turbine
WWEA	World Wind Energy Association

LIST OF SYMBOLS

SYMBOLS

F_x	Axial force [N]
a	Axial Induction factor
á	Angular induction factor
C	Chord length [m]
Cf	Capacity factor
D	Drag force [N]
CD	Drag coefficient
U	Free stream velocity [m/s]
r	Local radius [m]
L	Lift force [N]
C_L	Lift coefficient
ṁ	Mass flow rate [kg/s]
B	Blade number
P	Pressure [kPa]
P	Power [kW]
C_P	Power coefficient
U_{rel}	Relative wind speed [m/s]
R	Radius blade tip [m]
Re	Reynolds number
T	Torque [Nm]
F	Tip loss correction factor

GREEK LETTERS

GREEKLETTER	
ρ	Air density [kg/m^3]
α	Angle of attack[deg]
Φ	Angle of relative wind velocity[deg]
Ω, ω	Angular velocity of the rotor [rad/s]
θ_P	Blade pitch angle [deg]
θ_T	Blade twist angle[deg]
ν	Kinematic viscosity of air [m^2 /s]
σ	solidity
λ	Tip speed ratio

CHAPTER 1

INTRODUCTION

Fuel sources are one of reasons that lead to pollution the earth. Many researchers are working around the world to find clean and renewable energy sources. A fuel cell uses the chemical energy of hydrogen or another fuel to produce electricity in clean and efficient way. If hydrogen is the fuel, for electric then water and heat are the only products [1, 2]. Most researchers in energy fields are interested in wind energy in their study to improve it because it is one of the free energy sources [3, 4]. During the past centuries, studies in electricity and energy have been developed in many countries around the world [5].

Annually, the demand for electricity consumption in Libya increases annually, which is a reason to concentrate on the alternative energy sector because it is available in Libya [6, 7]. Solar energy and wind energy is one of the best alternatives to obtain power electricity [8]. The average solar radiation in Libya is about 7.5 Kwh/m^2/day, with around 3000 to 3500 hours of sunshine a year. The average wind speed is between 6 m/s and 7.5 m/s at 40 m height. This is important measure of the distribution of the sun and wind over an area 1,750,000 km^2. It can contribute supply in the future for Libyan electricity and most countries that are close to Libya. Libya depends on oil and gas to produce electricity, as the demand for the need for greater quantities of oil and gas increases, which will have a detrimental effect on the economy in Libya [6, 7, 8].

In the first plans of growth in Libya. Lines of electricity should be connected to all areas, so the average power consumption per person can be calculated, which is one of the main factors to measure the growth scale in modern countries. These days, the production of electricity has become very expensive, especially for agricultural

applications. The cost of Libyan electricity in the agrarian and manufacturing has taken a high value from the government budget in the past thirty years [6, 8]. The amount of plans for electricity delivery contractors is nearly 17,144 million Libyan dinars for the section of electrical power production (1.420 LYD equals 1 USD) [7]. There were a few critical studies about wind energy that are carried at different locations in Libya [6, 7, 8, 9]. They have selected a small wind farm of 1.5MW to be a pilot wind project. They have checked out different locations in Tripoli[7, 9]. The result, an average of wind speed was found as 6.9 m/s at 10m height with an available power of 399 W/m^2. Their findings were promising for the project of wind farms [10]. They have checked out the utilization of renewable energy in Libya [1, 2, 6, 7, 11], and they concluded that Libya is rich in renewable energy and wind energy; however, it needs a more comprehensive energy strategies and more investments in the financial and educational sector.

They have acquired wind speed measurements for 12 months precisely at Benina's location in Libya [12, 6, 7, 8]. The results showed an average wind speed of about 11 m/s at 10 m height, which indicates the high wind energy potential in Benina's location. Recently [4, 13], four areas have been selected, which are placed close to the Libyan coast and conducted the technical and economic assessment of wind power generation using real measured wind data. The results have shown that the electricity cost of all the locations is less than the price of electricity average in the world [7, 8].

Other studies were about the wind potential in different centuries, such as Turkey [14], Italy [15], Algeria [16], Iran [17] and India [18, 19, 20]. Officially, it has also been implemented.

The aim of this work is to study the potential for electrical power generation from wind energy using the analysis of information about wind speed. It acquired from the meteorological station of Misrata city and knowledge of wind energy potential in this location using wind energy as an additional source for power generation in the city of Misrata. After that, this work will contribute to the saving of electrical energy, and it will reduce the emission of greenhouse gases. For example, carbon

dioxide (CO_2), Methane (CH_4) and Nitrous Oxide (N_2O) since these gases are the main factors to increase global warming [4, 18, 21].

Blade shape design also has a critical effect on power acquisition. The wind produces from variation in air pressure. The flow variation in speed and pieces in the world is also influenced by the variation in area [1, 22]. These days generating electrically by converting mechanical energy to wind energy by moving the rotor by the wind to generate electric power [4], the dynamics of wind turbines are related utilized to their engineering and Reynolds number [23]. The most used in trade is HAWT [24].Not just the market demand for large scale wind turbines; however, also the demand for small scale wind turbines has also developed due to the growing energy demand in the world [23, 25]. A small-scale wind turbine is defined as a wind-powered electric generation with a rated power of lower than 50 kilowatts, generally purposed to supply electricity for domestic use and small farms. The intention of designing the small wind turbines is related to the mean wind speed in the Misrata region to provide electrical energy to buildings and Farmlands, which have no connection to the country's electrical network or no electric power available [23, 25]. To get a good design for a wind turbine of a suitable horizontal axis for this location, the applied theory of blade element momentum (BEM) should be used, airfoils S809, the Matlab program, and the Q blade program [26, 27].

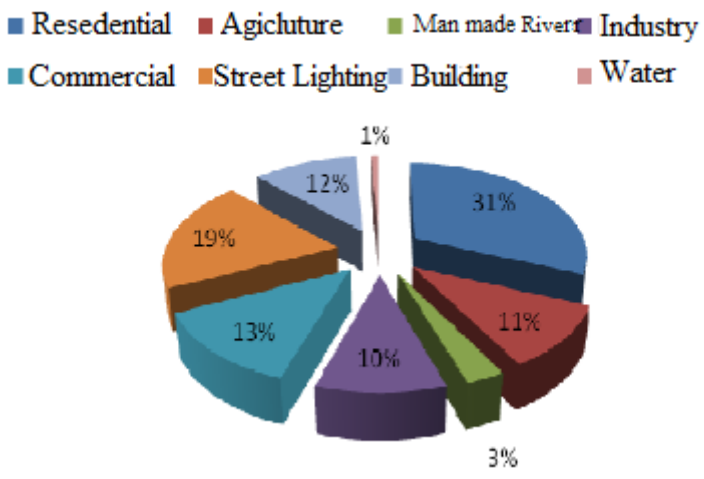

Figure 1.1: Percentage of electric consumption in Libya in 2012 [1].

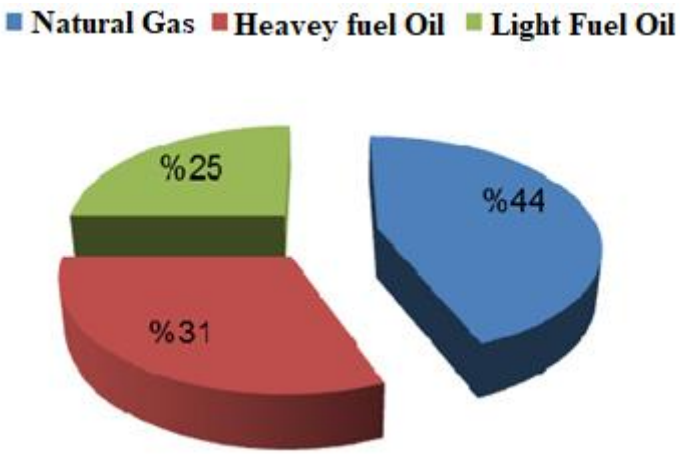

Figure 1.2: Fuel and gas consumption in Libya in 2012 [1].

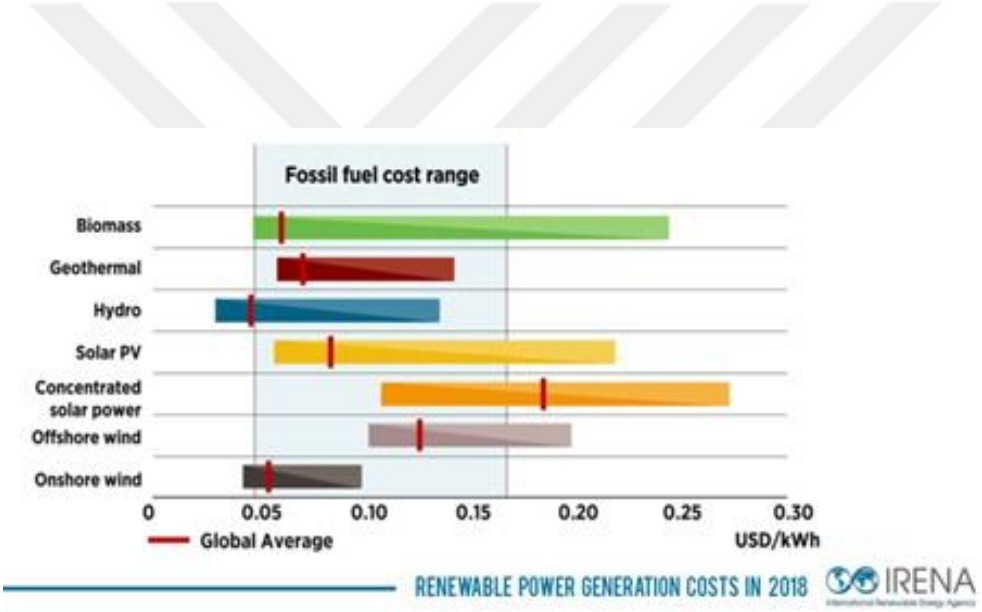

Figure 1.3: Comparison costs between reneable and fossil fuil in 2018

1.2 Overview

Wind Turbines work by collecting the mechanical energy of the wind and converting it to electricity. The wind moves the blades, which rotate to the shaft. Then, the wind relates to a generator and product electricity [25]. Wind blades can be set on the land

or coast in vast bodies of water, such as oceans and lakes. In 2010 established data from EWEA (European Wind Energy Association) [4]. There were 70,488 wild wind energy and 1,132 offshore wind energy, as shown in Figures 1.3 and 1.4.

On the other hand, the EU is taking care of advanced technological turbines; that is why it is becoming vast and most efficient. Acquiring the same quantity of energy can be generated with a small turbine [25]. The average size of wild wind energy, which was made in 2014, can work annually more than 1,500, which is the average of the local European Union. The average offshore wind energy of 3.6 Mw can power more than 3,312, which is the average of domestic EU. The year 2014 showed that the growth of wild wind energy is more economical than that of offshore wind energy. However, in the next years, the turbines of offshore wind energy were produced on an enormous scale because the prices were decreasing; thus, the manufacturing of the turbine of offshore wind energy increases in 2014. According to EWEA, there is 19.5 MW of wind energy built per 1,000 Km of land area in the EU. It was the most significant densities in Denmark and Germany [28]. Even though 25 counters of the 27, EU member countries now still use wind power. There are still essential quantities of wind available in countries such as France, the United Kingdom, and Italy. The total wind power that is installed in Europe at the end of 2012 reached 7% of the EU-27's annual electricity demand. Wind supplies 26% of electricity generated in Denmark, while Portugal and Spain generate around 16% of their electricity from wind power, then Ireland (12%) and Germany (11%) [29, 30].

Wind energy turbines are divided into two types, one of them is horizontal with the axis, and the second one is vertical with the axis. A horizontal axis machine has its blades moving on an axis parallel to the land [31]. Vertical axis machine blades; move on an axis vertical with the land. There are many forms of designs for each type, and each one has advantages and disadvantages [32, 33, 34]. However, there is a small number of vertical axis machines used commercially [25, 27, 31].

Figure 1.4: Onshore wind farm turbine [35]

Figure 1.5: Offshore wind farm turbine [35]

1.3 Objectives of the Study

This work aims to study the possibility of electrical power generation from the wind energy by using the analysis of information of wind speed obtained from the meteorological station of Misrata city and achieving the best results for power. That corresponds to the mean wind speed of the region at 8 m/s with different designs.

- To analyze wind speed by studying wind energy potential, also extrapolate wind speeds at different altitudes, using Weibull distribution function
- Evaluate the power output, and analyze the cost of wind energy, using the present value cost method
- To make validation of the power curve among Q blade program, Matlab program, and experimental S809 measurements by applied BEM theory.
- To estimate the power curve of the wind turbine, thrust, and power coefficient, by using a design that has axis three blades of the wind turbine in different chords with fixed twist angle also Determine the cost of energy per Kw for each design by using parameters of K and C for Misrata city and present value cost method.
- To compare the curves of power, thrust, and power coefficient of experimental S809 as a result for changing the twist angle at various values and fixed chord with the mean wind speed for Misrata city, and compared the cost of electricity per kW for best design with the cost of power per kW for S809 experimental by using parameters of K and C for Misrata city and present value cost method.

1.4 Structure of the Thesi

The need to design axis wind turbines for two reasons is the increasing demand for energy and the search for alternative renewable energy. This work will take comprehensive the study of the location. In the beginning,

studied previous research and methods of measuring wind speed, dynamics forces of wind energy, Analyze the wind speed of the site and find the resulting potential and calculating the energy cost per kilowatts. Investigate the blade element theory with correction factors, using validation among Q blade software simulation, Matlab code simulation agnest NREL VI power curve following that designs of wind turbines by change chord with fixed twist angle using different lift coefficients , change twist angle with fixed chord and other design using proper TSR to lead observe maximum power results at mean wind speed of location, also determine cost per kilowatts.

CHAPTER 2

LITERATURE REVIEW

A study in Hatiya Island in Bangladesh indicates that winds during most of the year are around 58% in the site because the wind speed reaches 6 m/s. This wind speed is enough to generate electricity from small turbines [25]. A study was conducted in Belicik in Turkey, and it appears the use of the Weibull probability density function to calculate the output of wind potential [13, 36, 37]. The data were collected from the meteorological station using the Matlab program to obtain good results. It is noted in the study that the increase in the speed of wind and energy obtained by the Bilecik site from 2010 to 2014 in summer and fall in winter and autumn. This data should be done for different sites and different altitudes, also calculating the cost of the site to obtain accurate data.

In Iraq, a study was conducted using the Weibull distribution and wind power estimated for three different sites in Iraq: Baghdad, Basrah and Dhi Qar, after collecting and synthesizing all these data from (Weather under Ground website) [13, 36, 37]. To perform statistical analysis for each station from 2009 to 2010, using mathematical processes and estimation of wind energy. Also, designing a special software that was built to calculate Weibull because the distribution was optimal for wind speed statistics and for the shape parameter (k), scale parameter (c) by using Maximum Likelihood Estimation (MLE) and the least-squares method (LSM) [13, 36, 37]. It was observed that the distribution of wind speed for different intervals showed that the superiority of the maximum method was better than the squares method. Therefore, this method should be used rather than the other for acquiring correct data (Weather Under Ground website) about the studies for many years, and for the three stations, the highest wind speed in the low sites from (2 - 4) m/s[38].

Libya is one of the largest countries in Africa to produce oil and to improve its economy [6]. Most of the economic sectors in Libya depend on oil in order to work, especially the electricity sector, because all the factories are used fuel and gas to operate the electricity industry[8]. Libya currently produces about 33 terawatt-hours of electricity to cover the domestic market. The demand in energy is expected to increase after years of destruction to develop more energy locations and will lead to an increase in the consumption of oil and gas. After that, revenues of oil and gas will decline and impact the state budget [8]. Therefore, Libya should use alternative energy to cover the deficit of future energy and preparing trainers and engineers to use it [7, 6, 8]. Alternative energy in Libya is expected to increase in the next years[6]. Therefore, the government has conducted studies that concentrate on renewable energy, including wind energy and solar energy [1, 2, 11]. About 30% of the total energy will be consumed in 2030. The whole production of electricity in 2012, which is obtained from 14 main stations of power has been nearly 33,980 Gwh, and it has a consumption estimated to be approximately 6,003,262,899 m^3 (Natural Gas), 2,388,932 m^3 of (Light Fuel Oil), and 805,472 m^3 of (Heavy Fuel Oil). The demand for Libyan power is increasing every day, and this number is possible to reach at 250% in 2020 compared to 2012 [6, 8]. In Libya, the production price of 1628 kWh of electricity is equivalent to each barrel of oil. Cost of product price can be calculated by price per barrel of oil in the world market. In 2030 energy, demand in Libya is expected to be approximately 120 Gwh. Therefore, it will need to be covered about 194 thousand barrels per day, and this will be deducted from the exports of Libyan oil, which will negatively affect the state budget. Hence, Libya must rely on available renewable energy[1, 2, 8, 11]. To reduce uncertainty related to the wind energy expense output. The pattern factor method (EPF) is recommended to be used to estimate wind speed parameters [39]. The rotor shape in the wind turbines plays an important role as the lift force depends on the shape of the blade because it can convert the external energy into mechanical energy, where was used the blade element momentum theory [23]. The design of a 5 kW for blade and take two types of NACA for the airfoil and studying of the parameters to design

the blade that helps computer program to obtain a coefficient of performance[40, 41]. It is an excellent way to predict and know the performance of the blade of wind energy turbines [25].

2.1 Wind Energy

Wind energy is one of the widely used renewable sources of renewable electricity because it is generated from a natural resource which abundant on the earth [1, 2, 3]. Its use indicates the fastest growth, and it may compete with the cost of conventional electricity [42]. The wind is the result of air actions, which include the result of force from different heating and cooling of the earth. Wind movement that is generated by airflow is called wind power. The availability of air on the surface of the earth to move it. It can be raising the wind, and it influences the rate of wind in the atmosphere, the force of gradient, the force of Coriolis, centrifugal force, and the force of friction. The air that flows from excessive pressure to less pressure is known by using the force of the pressure gradient. The strength of the Coriolis is again to its region called is the deviant force. Through using this movement, it finds from the center of rotation under the impact of the force and it is known as centrifugal force. The winds that are not active construction and try to decrease wind speed are called friction force [38]. This power is enormous on the earth, and it is loaded by turbines [25]. This force of wind friction reduces the winding height from 450 to 600 meters above the earth. Wind energy is created by using air that is infecting the force. The part that helpful of wind power can be changed to mechanical energy or electrical energy. The first use of wind power depends on the early time and old time. Recently, this technology carries on to activities and progress to be always right.

2.2 Measurement of Wind Speed

Electricity can be made from a wind turbine. Therefore, it can assign in a place that location is related to the wind characteristics at the same time. The advantages of the

wind depend on many parameters, such as wind speed, the direction of wind, pressure, and temperature. All these parameters are determined using the measurements made on site. Wind measurements are achieved by using directorate meteorology because they have devices that can measure the wind speed, wind rotation, temperature, pressure, and relative humidity of this location [38].

Wind height must be 60 meters and 30 meters at least inside the measuring station; the records obtained from those measurements should be transferred to the central directorate of meteorology. The wind speed is measured with a tool that is called an anemometer. Measurements of wind speed are executed normally by using anemometers with ladles, as shown in Figure (2.1). In fact, anemometers of ladles have three steel ladles. The wind that hits these ladles is rotated on the connecting ladles. When wind speed is rotated, the wind velocity is determined to depend on the amount of rotation formed in the shaft related to unit time. Direct winds do not affect the measured wind speed because the ladles with anemometers change with the different wind direction.

Figure 2.1: Metrological weather station [43]

2.3 Estimation of Wind Energy Potential

In order to produce electricity from wind power, it is necessary to estimate the potential of wind energy at the site where the foundation will be built prior to the installation of wind energy. After calculation the wind potential , the wind turbines to be installed in that region will be selected [23, 25]. Calculation of speed distribution at site to calculate the wind potential. The most important methods that are applied are Weibull and Rayleigh to calculate the wind speed distributions in the location.

The Weibull distribution method is an important commonly used method that is applied to calculate the wind speed distribution of the location because it is a method for two-parameter, which give a similar outcome with the measured data [38]. Weibull distribution function. In fact, other methods can be applied to calculate the speed distribution of the wind; one is called the Rayleigh speed distribution method. A Rayleigh distribution function [38].

2.4 Wind Turbines

Some systems change kinetic energy to electrical power. In the recent period, the wind turbines have emerged as windmills to generate mechanical power. Before that, the first windmill was used in north France. A system was applied by Prof. James Blyth in Scotland in 1887 to produce electricity from windmills. The primary wind turbine produces electricity; therefore, it has been instituted by Charles F. Brush in 1888 in America. The built wind turbines systems have kept growing so far during these dates in many countries, such as Germany, Denmark, and America [25].

Recently, wind turbines mostly consist of main parts like Tower, Nacelle, Rotor Hub, Rotor Blades, Gearbox, Generator, and Yaw System. Therefore, it has a wind turbine, as shown in Figure (2.2).

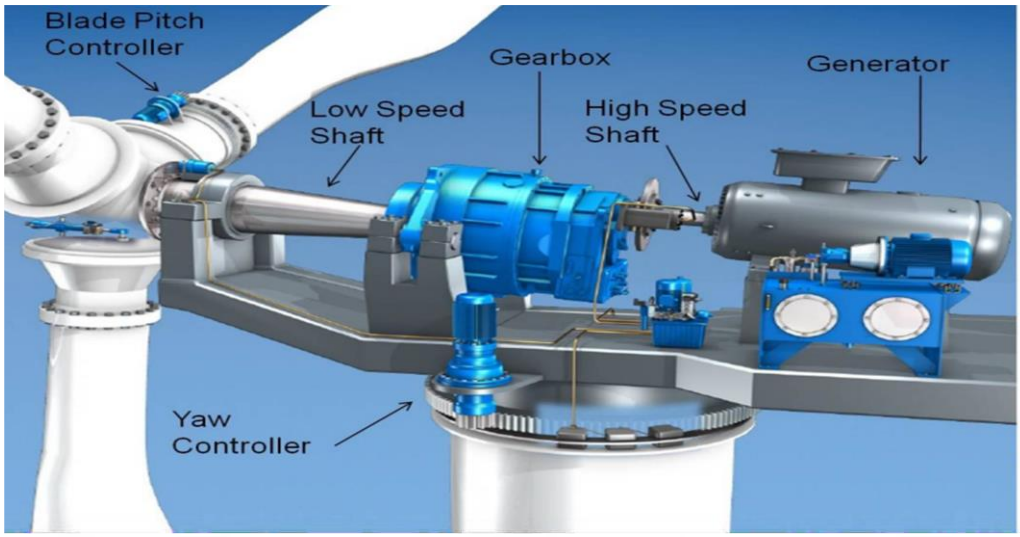

Figure 2.2: Wind turbine parts [35]

2.5 Classification of the Wind Turbines

Wind turbines are classified as single-blade, double-blades and three-blades according to the number of blades, upwind field, and downwind field.

Now, the format of the wind turbines classification is the status of the rotor axis that is related to the ground. It is most widely used as a classification of wind turbines [23, 25]. Therefore, it has three groups, which are:

- Wind turbines with a horizontal axis
- Vertical axis of the wind
- Inclined turbines axis wind turbine

2.5. 1 Horizontal Axis Wind Turbines

The blades of horizontal axis wind turbines are attached to a horizontal shaft. It is designed as a vertical shape to the wind direction [15, 23, 45]. The parts are placed on the top of the tower in these types of turbines the blades of horizontal axis wind turbines need to back to the wind direction because there is a rotating technique in

these turbines [15, 23, 27, 45, 31]. A horizontal axis of the wind turbine is shows in Figure (2.3).

Figure 2.3: Axis wind turbine [35]

2.5.2 Vertical Axis of the Wind Turbines

The blades of the vertical axis of wind turbines are attached to a perpendicular shaft, as it is shows in Figure (2.4). These types of turbines are also called Darrieus turbines, and they have been improved and

by G.J.M. Darrieus for the first time. Because of this, the vertical wind turbine blades is rotate on their axis. Therefore, the wind blows from any direction, and it does not need to obtain to the wind direction [15, 25]. In addition, the construction and repair of these types of turbines are inexpensive and easy to use when compare to horizontal axis turbines because wide parts for mechanical compounds and electrical compounds are on the surface of the ground. Blades of vertical axis turbine blades are exposed to wind speed less than horizontal axis wind turbines [25, 38]. Therefore, the blades are near to the surface of the ground. Also, it has efficiency lower than

horizontal axis wind turbines because increasing the blade altitude is too expensive and that it is not suitable for using to generate electricity [23, 25, 31].

Figure 2.4:Vertical axis wind turbine [32]

2.5.3 Inclined axis wind turbines

These turbines shows in figure (2.5) of limited use, Angle arms are placed between the rotation axis and blade to distribute mechanical loads [32].

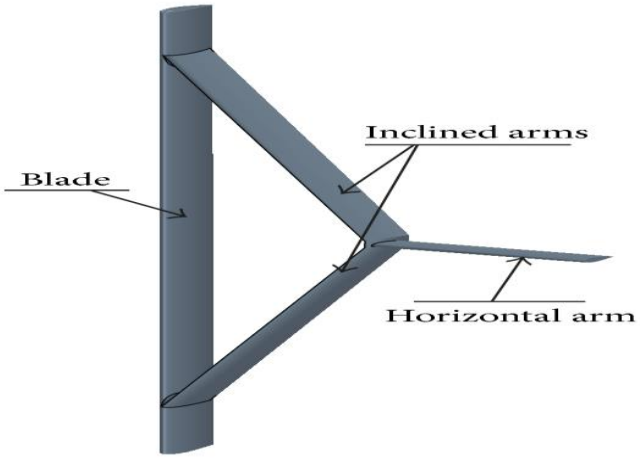

Figure 2.5: Inclined arms of the axis wind turbine [32]

2.6 Production of Electrical Energy from Wind Turbines in the World

Global energy demand has been estimated at one-third higher these days. In the future, it is expected that despite the increase for energy obtained from conventional energy sources and nuclear power. Therefore, the total produced energy will decline, such as environmental problems, increasing incentives, and rising fossil fuel prices. Interest in renewable energy sources will rise quickly in the future [1, 2, 11]. The total rate of the electricity produced in the world from renewable sources, which is expected to rise to 31%. Wind-based electricity production facilities have shown a good improvement in last years when compared to other power generation facilities based on other renewable sources. Figure (2.6) shows the capacity of wind power production facilities between 1996 and 2014. Today, the capacity of energy-generating in the world from wind power speed is 2.5% and is supposed to be about 8-12% 2020 [24].

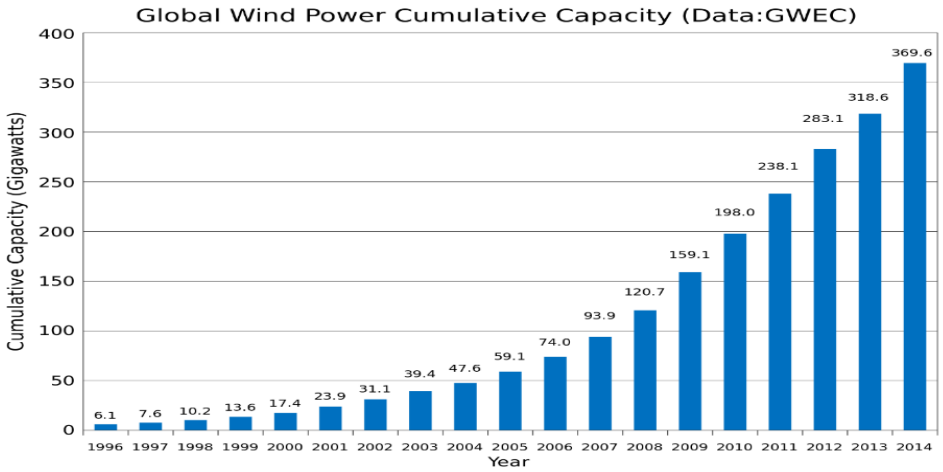

Figure 2.6: Capacity of power production facilities between 1996 to 2014 [44]

Figure (2.7) shows the overall capacity of all wind turbines that are installed worldwide at the end of 2018; it is reached 600 Gig watts by using preliminary statistics published by World Wind Energy Association (WWEA) today. Also, it added 53.900 MW in the year 2018 that is slightly more than in 2017 when it was installed 52.552 MW. The year of 2018 was the second year in a row with a growing

number of new installations, but the rate was low of 9.8% after that was growing 10.8% in 2017. All turbines can cover installing wind by the end of 2018 to 6% from the global electricity demand.

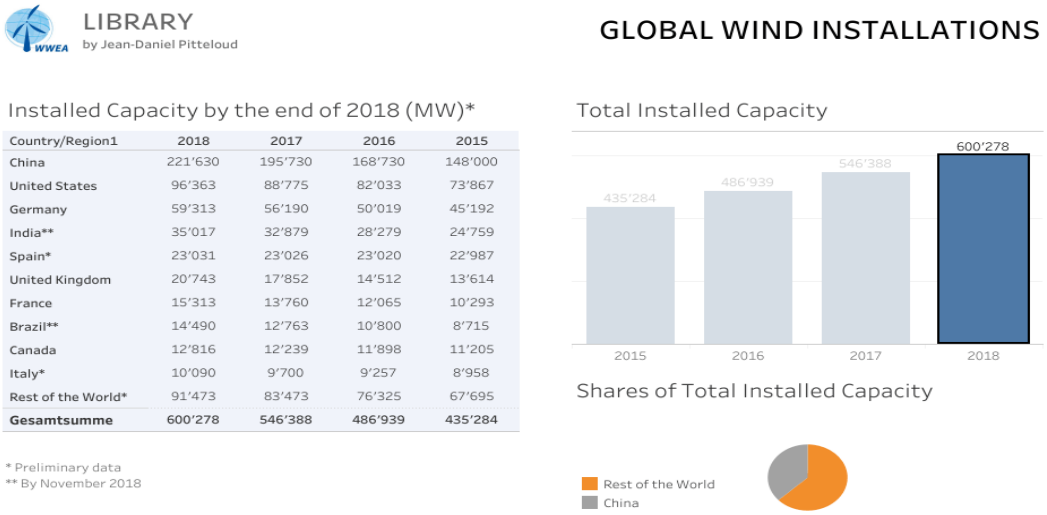

Figure 2.7: Overall capacity of all wind turbines that are installed worldwide up to 2018

2.7 Operating Regions

Wind turbines have three operating zones. Each region, the turbine has a different operational objective depending of the average wind speed [38]. There is the summary below, and the ideal power captured in each region is illustrated in Figure (2.8).

Region (1) very law wind speed is less than sill minimum, it is called the cut-in speed, the power Extracted is zero.

Region (2), between the cut-in and the rated speed, where turbines will spend most of their operational life in a designed wind speed zone. Therefore, the main goal is to maximize the capture of power in this zone.

Region (3), rated region is a constant output generated unto the cut-off speed is obtained, specified for the up of wind speed where wind energy should be limited to the estimated power to avoid damage to turbine components. Thus, the turbines reduce their efficiency to restrict the capture of power to the estimated rated power of the generator [46].

Beyond region (3) where the wind speed is too, fast for the safe operation of wind turbines. Therefore, the turbine is taken out the process of operation to safe its parts and hence the power Extracted is zero [23].

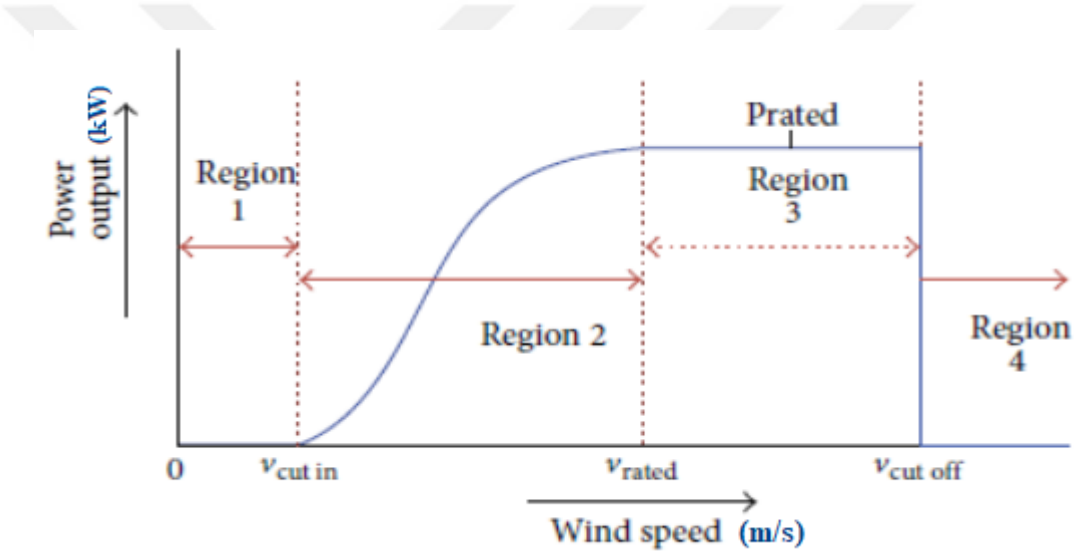

Figure 2.8: The typical power curve of the wind turbines [47]

2.8 General Control and Cost

The major target for using wind turbines is to produce energy at a lower price. Some factors affect the price of energy, such as the location, the distribution of wind speed, and the efficiency of turbines [23, 31]. The control system has some factors that can control the unit affect to know the price of power the capture of the power and the

components stress lifetime. In order to go down the price of energy, we should control the system:

1- By increasing power capture:

(A) Power limits took according to the operational location (i.e., limiting energy capture in the location I and III);

(B) By operating constants for each location.

I. To maximize the power in location II, the blade pitch degree is adjusted to the optimum angle, which will maximize the dynamic torque generated and uses the Torque generated to control the rotor speed to achieve the right goal.

II. In location III, the torque change of the generator is not allowed significantly (e.g., within 5% of the specified torque) to reduce fluctuations of energy.

2 - Extend the operational life of wind turbines. Even though regular maintenance to wind turbines. The life of the wind turbine can be increased by reducing stress loads on its components (blades, movement group, and tower) [23].

To go down the energy price using both approaches to increase power and reduce the stress load. Ideally, a single multipurpose implementation is required. The standard operation uses a separate controller for these operations by using specific rules.

2.9 Materials and Structure for Wind Turbine Rotor Blades

With the speed of technology, the companies have taken an interest in producing wind turbines and finding engineering methods that improve the wind turbine efficiency, such as blades-made materials and the engineering design of the blades. One of the essential features for the development of wind turbines is durability, weather tolerances, and optimum usage of wind energy [23, 46]. Therefore, the search for composite materials while contributing to good specifications. A wide range of materials is being applied in the construction wind of turbines. High

efficiency of wind turbines can only be achieved by selecting the appropriate materials for each unit. Therefore, physical development and behavior are tested in all circumstances. Officially, there are five preferred methods for selecting materials in all cases. These methods are called economic characteristics, performance characteristics, features measurement values, analysis of value, analysis of damage, and analysis of economic benefits. The plastic of Glass reinforced is a type of compound material most commonly used for wind turbines with rotary blades [23]. These composite materials have been preferred to be used because they are easier to use and economical compared to fiber-reinforced plastic in providing lightness in turbine blades, high resistance, and erosion resistance. Carbon fiber reinforced plastic has limited usage in rotor blades. Although these composite materials offer strength and lightness compared to glass-reinforced plastic, however, their high price is still a significant disadvantage.

2.10 Power Extraction from Wind Turbines

There is a large amount of power in the wind speed; it is available like kinetic energy, which can be obtained as usable power. The total estimated power in

Cylindrical for wind power (P), is defined in the following formula:

$$P = \frac{1}{2} \rho A V^3 \quad (2.1)$$

Where (r) is the radius of the area (A), ρ is the air density, and V is wind speed. Figure (2.9) shows a turbine which is used to extract energy from the wind; it comes in a turbine at V_1 it converts energy from the wind and causes a reduced exit speed. Where $V_{2,}$ the same mass of air, should be leaving the space when entering the turbine. The next air column should be stretched where the wind leaves turbines. This leads to the expansion of the flow tube and increases the energy that is obtained from the air column. In order to increase the column should be expanded.

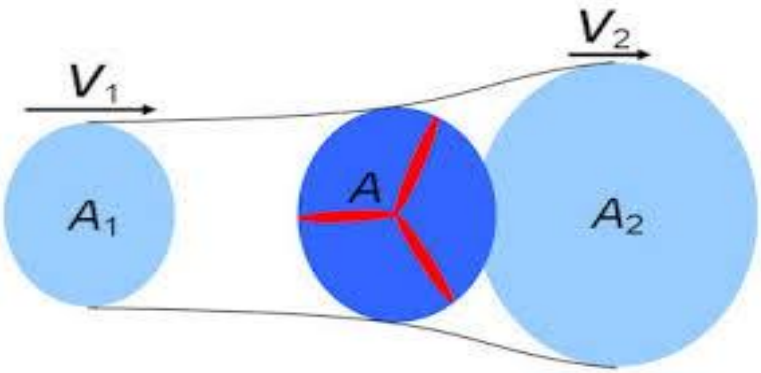

Figure 2.9: Extract of wind energy [48]

In the 19th century, Albert Betz calculated the most theoretical percentage of power that can be acquired from the movement of air. The process assumed an ideal blade with no hub and completely axial flow. The blade is used was without mass, and the flow was considered to be incompressible. With assumptions used, Betz calculated that ideally limits 59.3% of the power can be acquired from wind obtained using a wind turbine. Based on this analysis, there is no possible method to obtain more power from the wind system.

2.11 Aerodynamics of Wind Turbines

Before discussing specific aerodynamic processes in wind turbines, some basic aerodynamic concepts should be introduced. These concepts will be highlighted in the case of external flow on a cylinder [23, 49].

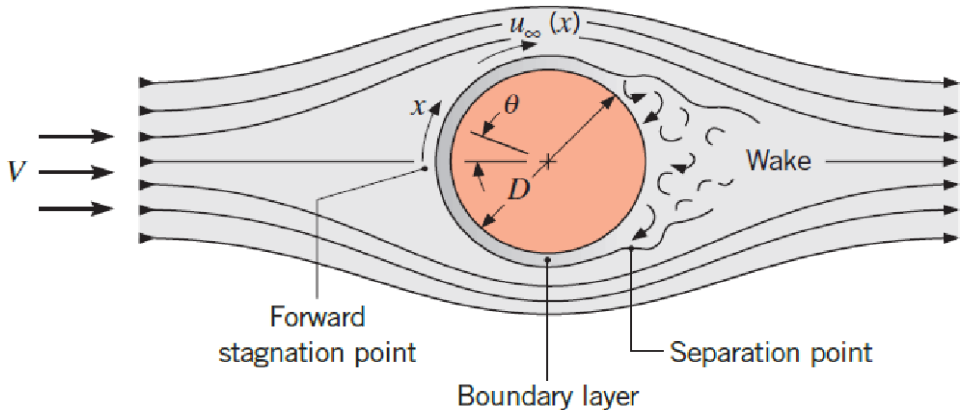

Figure 2.10: Out flow on the cylinder [50]

It can streamline the concept of the primer. A streamline is a line that is tangential to the immediate speed at each location. The lines display in Figure (2.10) are model of streamlines; it is turned around the cylinder apart from the streamline that opposes the center of the cylinder. The forward stagnation point because the speed of a fluid particle is recorded zero, and there is no fluid activity at the stagnation point. As the flow around the cylinder is symmetrical, the stagnation point is on the end centerline of the cylinder, as displayed in the figure. Bernoulli explains with streamlines, and higher speeds result in lower pressure. Therefore, the forward stagnation point has the most pressure effect on the cylinder.

Another of the important concepts shown in Figure (2.11) is the boundary layer, which is defined as the distance from the cylinder surface where the fluid speed is still affected by the body. The boundary layer of the edge is defined as the site where speed 99% of the value of free stream speed. Because of the high pressure at the stagnation point, the flow accelerates under a favorable pressure gradient on the part for the cylinder of the surface. The pressure should finally reach a lower value; after that, the flow of pressure begins to slow due to an adverse gradient. This pressure gradient finally leads to flow reflection, as shows in Figure (2.11).

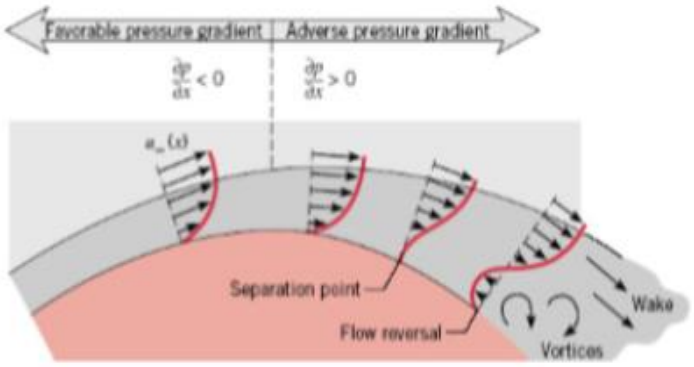

Figure 2.11: Pressure gradient finally leads to flow reflection [50]

The location of the boundary layer separated from the cylinder surface body is defined as the separation point location. The location after flow was separated is defining as the wake site, and the flow is an advantage by very troubled vortices (flow as high turbulent) Figure (2.12).

The location of this separation point is related to a factor defined as the Reynolds' number. The (Re) number is known by this formula:

$$Re = V \rho D / \mu \qquad (2.2)$$

(V) is the entry speed of the fluid, (D) is cylinder radius, (ρ) density of the fluid, and (μ) is the fluid dynamic viscosity, as illustrated by Figure 2.12. The separation is happened extremely earlier in laminar flow ($ReD \leq 2x10^5$), it is deferent on turbulent flow shows.

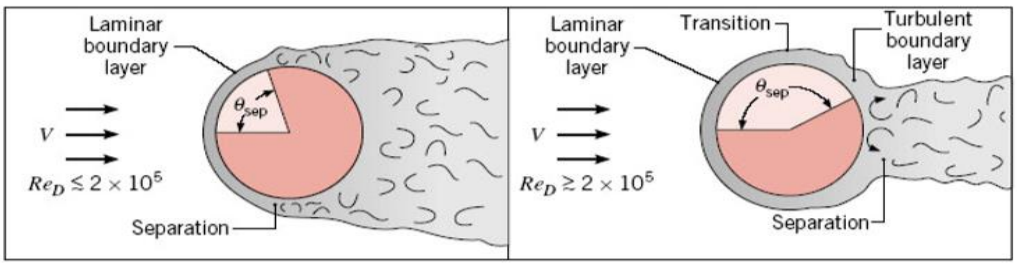

Figure 2.12: Boundary layer separated from the flow [50]

Currently, these procedures were defined; consider the flow around an airfoil and airfoils.

The location of the cross section of wings of the plane and other of the blades. It is specifically designed to use the basics discussed above before producing a lift under the exact flow procedures. Figure (2.13) shows the geometric parameters of an airfoil; there is known as follows by Pozrikdis.

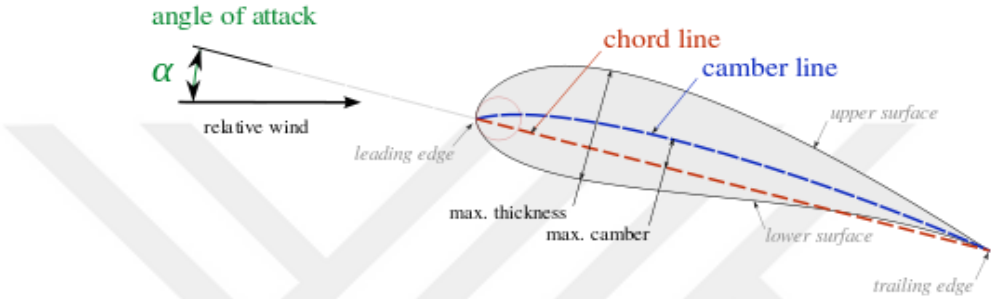

Figure 2.13: Geometric parameters of an airfoil [50]

The chord line - this is the straight line to connect the front edge to the rear edge. The chord (C) / this is the distance from the front edge to the rear edge.

The camber line/ this is place the points between the top and bottom of the airfoil surface. The camber / the maximum range of distance between the camber line and the chord line. Thickness / the airfoil thickness along the camber line.

The angle of attack / (α) is the angle between the incoming flow and the chord line.

CHAPTER 3

WIND ENERGY ASSESSMENT

The meteorological station of Misrata city is located in the west of Libya. The coordinates are latitude 32^0 22 '39. 12^0 N and longitude 15^0 05 ' 31. 26^0 E. The elevation of the site is 10 meters above the mean sea level using three cups of wind speed measuring devices. The location is near the sea, and it has available winds

The statistical wind data set was analyzed using the Weibull distribution functions in order to check shape and scale parameters at 10 meters, 30 meters, and 50 meters in height [6, 12].

3.1 Data Analysis

The meteorological station used an automatic type and measured speed at height (10) of meters. Many researches have used the Weibull method to find wind speed distribution. It is one of the most widely used methods, where a good description of speed distribution is given throughout the year, probability distribution function (PDF) possibility is expressed as [37]:

$$\mathrm{f(v)} = \frac{\mathrm{k}}{\mathrm{c}}\left(\frac{\mathrm{v}}{\mathrm{c}}\right)^{\mathrm{k-1}}\ \mathrm{e}^{-\left(\frac{\mathrm{v}}{\mathrm{c}}\right)^{\mathrm{k}}} \tag{3.1}$$

Where (k), and (C) are parameters the Weibull shape and scale parameter [13]. The density function is recognized such as cumulative distribution function (CDF) and possibility be expressed as [37]:

$$F(v) = 1 - e^{-\left(\frac{\mathrm{v}}{\mathrm{c}}\right)^{k}} \tag{3.2}$$

In order to obtain the Weibull variables, we can use several methods; also, energy pattern factor (EPF) can be expressed as:

Energy Pattern Factor (EPF):

$\overline{v}$: The mean wind speed

$$\mathrm{EPF} = \frac{1}{(\overline{v})3} \sum_{k=1}^{n} \frac{vi^3}{\mathrm{n}} \tag{3.3}$$

$$\mathrm{K}=3.957\ \mathrm{EPF}^{-0.898} \tag{3.4}$$

$$\mathrm{C} = \frac{\overline{v}\ \mathrm{k}^{2.6774}}{0.184+\mathrm{O}.816\mathrm{k}^{2.78855}} \tag{3.5}$$

Wind speed changes with altitude and predicts speed. Therefore, we can apply this function:

$$(V_2/V_1) = (H_2/H_1)^m \tag{3.6}$$

H_1 and H_2 are highs and V_1 and V_2 means speeds, also (m) is dependent on several factors, and it usually takes 0.14.

The mean wind power density of the location can be obtained as:

$$P = 1/2\ \rho\ (EPF)\ V^3 \tag{3.7}$$

To find the capacity factor (C_f), power, and energy per year out applied these functions:

$$(P)OUT\ = (P)eR\ \{\frac{e^{-\left(\frac{Qc}{c}\right)k}\ - e^{-\left(\frac{Qr}{c}\right)k}}{\left(\frac{Qr}{c}\right)k\ -\left(\frac{Qc}{c}\right)k} -\ \ e^{-\left(\frac{Qf}{c}\right)k}\ \ \} \tag{3.8}$$

Q_C, Q_r, and Q_f are the cutting in the wind speed, rated wind speed, and cut off wind speed, P_{eR} Rated electrical power, and (E rated) of energy [42].

$$\text{Capacity factor } (C_f) = P_{out} / P_{eR} \quad (3.9)$$

$$\text{Energy output } E_{out} = C_f * E_{rated} \quad (3.10)$$

3.2 Cost Analysis

To obtain the cost of electricity per kWh, the cost can be obtained by expressing this formula [13, 39]:

$$\mathrm{PVC} = \mathrm{I} + \mathrm{Comr}\left[\frac{1+\mathrm{i}}{\mathrm{r}-\mathrm{i}}\right]\mathrm{x}\left[1-\left(\frac{1+\mathrm{i}}{1+\mathrm{r}}\right)\mathrm{t}\right]\mathrm{S}\left(\frac{1+\mathrm{i}}{1+\mathrm{r}}\right)\mathrm{t} \quad (3.11)$$

Where (I) is the investment cost, (Comr) is the operation, maintenance and repair cost, (i) is the inflation rate, (r) is the Interest rate, (t) is the lifetime of the machine (in years) and (S) is the scrap value [42].

Table 3.1: Characteristics of the selected turbines [42]

Turbine Specifications	Vestas V27-225 kW	Vestas V39-500 kW	Polaris P15-50 kW
Rated Power p (kW)	225 kW/50 (kW)	500 (kW)	50 (kW)
Cut Wind Speed Qc (m/s)	3.5	4	2.5
Cut off Speed (m/s)	25	25	25
Rated Wind Speed (m/s)	14	15	10
Hub Height (m)	30	50	30
Number of Blades	3	3	3

Table 3.2: Turbine cost band [42]

Wind Turbine Size (kW)	Min. Specific Cost ($/kW)	Max. Specific Cost ($/kW)	Average Specific Cost ($/kW)
10-20	2200	3000	2600
20-200	1250	2300	1775
200 to up	700	1600	1150

Table 3.3: Wind power classification at 50 meters [12]

Resource Potential	Mean Wind Speed (m/s)*	Wind Power density (W/m^2)	Wind Power Class	
Very Poor	0 – 4.381	0 - 100	1-	1
	4.381 – 5.588	100 - 200	1+	
Poor	5.588 – 6.035	200 - 250	2-	2
	6.035 – 6.393	250 - 300	2+	
Marginal	6.393 – 6.706	300 - 350	3-	3
	6.706 – 7.018	350 - 400	3+	
Good	7.018 – 7.287	400 - 450	4-	4
	7.287 – 7.510	450 - 500	4+	
Very Good	7.510 – 7.778	500 - 550	5-	5
	7.778 – 8.002	550 - 600	5+	
Excellent	8.002 – 8.404	600 - 700	6-	6
	8.404 – 8.807	700 - 800	6+	

3.3 Results

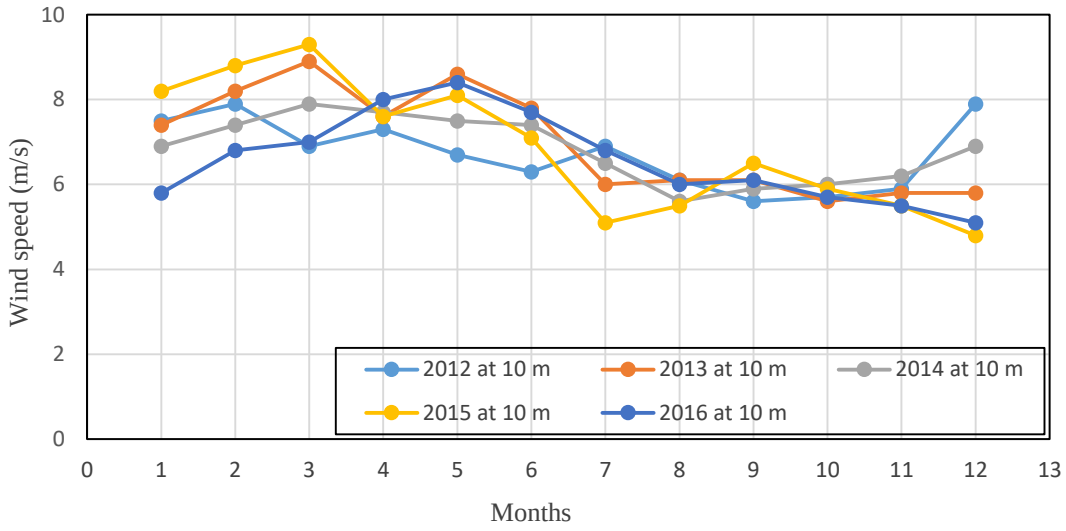

Figure 3.1: Monthly wind speed variation at 10 meters height

Figure (3.1) shows the variation of monthly wind speed between 2012 to 2016.

Observing that the minimum speed it falls between August and November, the lowest value recorded in 2015 (V=4.8 m/s), and the maximum value was recorded in March 2015 (V=9.3 m/s). Table (3.4) shows the obtained values of Weibull shape and scale parameters (k) &(C). That means speed Vm for years 2012 to 2016 used by energy pattern factor method at high 10 m. Figure (3.2) shows the density Weibull function that as the value of (C) increases for a given value of K, the shape of the distribution function obtains wider. Because this (C) is called the scale parameter, it has dimensions of speed. In addition, the plot shows that as (K) increases to 3.8 for giving the value of (C) to 7.5 m/s, the maximum of the (PDF) increases. Because this K is called the shape parameter, it is dimensionless. However, it is less when using k=3.5 and C= 7.6 m/s.

Table 3.4: Result obtained of values K, C, EPF and V_m for years 2012 to 2016 using energy pattern factor method at 10 meters height

Year	2012	2013	2014	2015	2016
C	7.5	7.9	7.6	7.6	7.3
K	3.8	3.7	3.8	3.5	3.7
EPF	1.040	1.084	1.038	1.038	1.071
V_m Data (m/s)	6.7	7	6.8	6.9	6.6
V_m Plot (m/s)	6.9	7.2	7	6.9	6.7

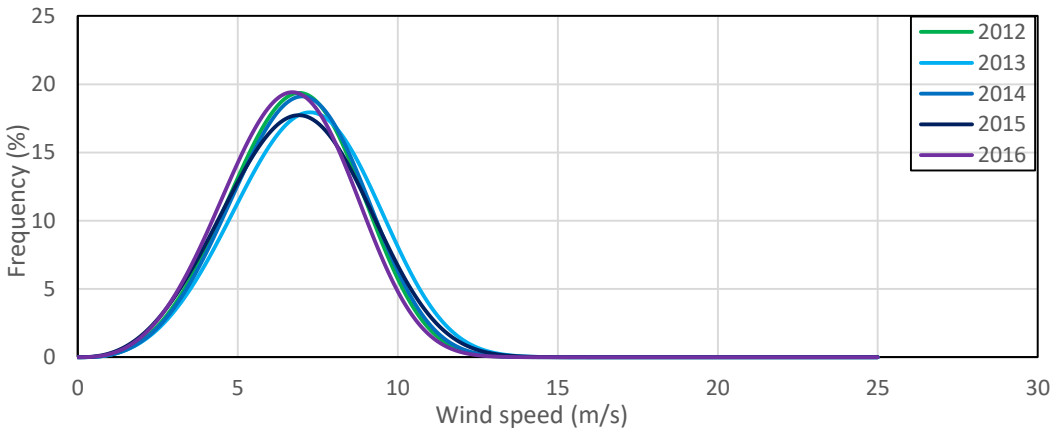

Figure 3.2: Propability wind speed density at 10 metetrs height from 2012 to 2016

Figure (3.3) shows the cumulative Weibull function. In fact, to observe, the curve covers much more area under it. Also, the Figure shows that the (CDF) for years 2012 V = 6.9 m/s, cdf = 51.73% rises than the (CDF) for others, where is 2013 V=7.2 m/s, CDF = 50.81% is the lowest value. Based on this observation, we understand the validity of the wind speed measurement for that turbine. Table (3.5) shows the value of parameters over the years at the height of 30 m. Figures (3.4) and (3.7) the Wind speeds were taken at different altitudes (30-50) meters, which is increased wind speed.

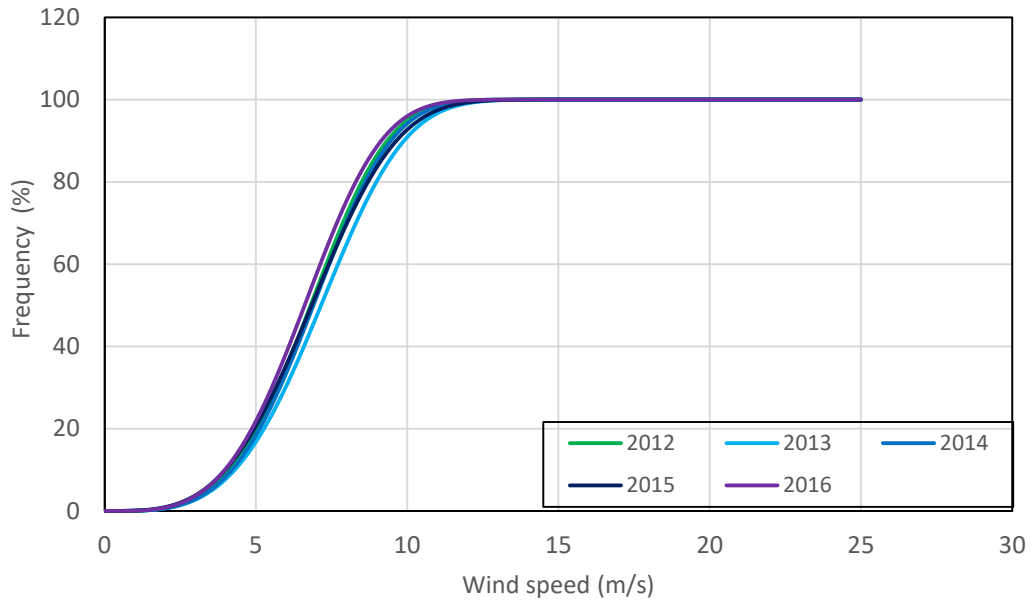

Figure 3.3: Cumulative wind speed at 10 meters height period 2012 to 2016

Table 3.5: The value of parameters over the years at height 30 meters

Year	2012	2013	2014	2015	2016
K	3.8	3.7	3.8	3.5	3.7
C (m/s)	8.8	9.2	9.0	9.0	8.7
EPF	1.040	1.084	1.038	1.138	1.071
V_m (m/s)	8.4	8.8	8.5	8.6	8.2
V_m Plot (m/s)	8.1	8.5	8.3	8.2	8.0
Freq (PDF%)	16.5	15.4	16.14	14.97	16.29
Freq (CDF%)	51.8	52.58	52.06	51.42	51.96
P (W/m^2)	338.5	407.8	362.3	384.3	335.9

To find the energy cost per year of applied function (3.11) present value cost method (PVC) and using V27-225 wind turbine:

Cost = 258750 $ I =310.500 $ comr = 3234.375 $

S = 310500*0.1 = 31050 $

r = 0.15 i = 0.12 civil cost = 20% of cost = 51750$ t= 20y

$$PVC = I + Comr\left[\frac{1+i}{r-i}\right] x\left[1-\left(\frac{1+i}{1+r}\right) t\right] S\left(\frac{1+i}{1+r}\right) t$$

PVC = 341702.1297 / 20 (y) * E (kW)

To find the energy cost per year, also applied that last function (3.11) and using P15-50 wind turbine. Table (3.6) shows the value of parameters over the years at height 30 m by using V27-225 wind turbine, observed the higher of the capacity factor present, the lower of the cost per kilowatt with the increasing rate of annual energy production. Table (3.7) shows the value of parameters over the years at the height of 30 m by using p15-50 wind turbines. Higher the capacity factor present, the lower the cost per kilowatt will be compared to using wind turbine V27-225. The tables (3.8) and (3.9) show the value of parameters over the years of wind speed at height 50 m by using V 39-500 wind turbine observer the value of power, energy and cost are best than used V27 -225.

Table 3.6: The value of parameters over the years at height 30 meters using wind V27-225 turbine

Year	2012	2013	2014	2015	2016
C_f (%)	0.17	0.23	0.19	0.21	0.17
P out (kW)	19.55	30	23.8	25.2	18.7
E (MWh)	137	202.1	161.4	175.4	137
Cost ($/kW)	0.12	0.08	0.10	0.10	0.12

Table 3.7: The value of parameters over the years at height 30 meters using wind P15-50 turbine

Year	2012	2013	2014	2015	2016
C_f (%)	0.49	0.54	0.52	0.53	0.48
P out (kW)	8.9	10.26	9.65	9.35	8.6
E (MWh)	99.97	117.54	109.64	109.94	96.30
Cost ($/kW)	0.047	0.039	0.042	0.043	0.049

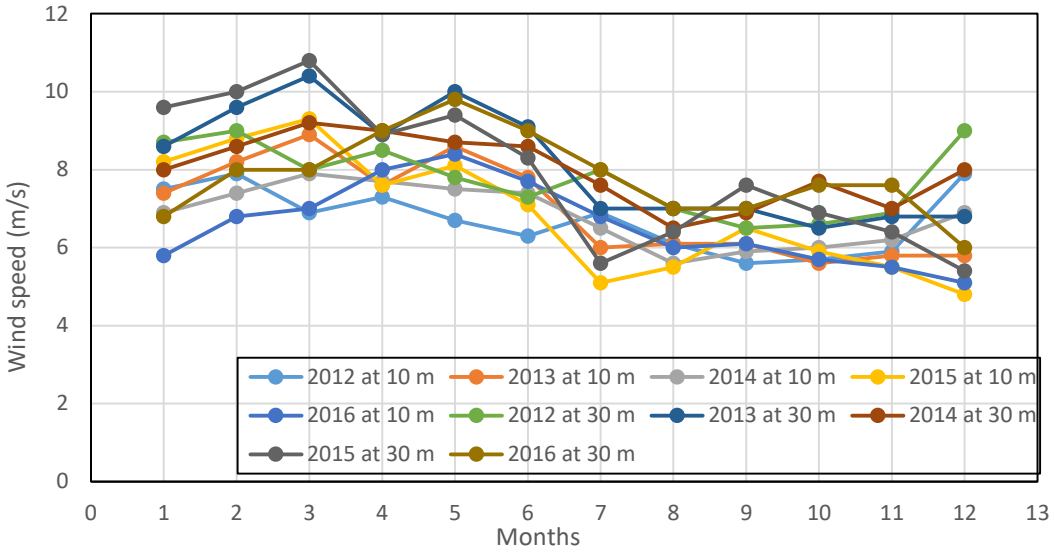

Figure 3.4: Compsrison of wind speed m/s at height of 10 meters and height 30 meters

Figure (3.5) shows the maximum (PDF) in 2012 when mean speed V = 8.1 m/s equal 16.5 and observer the minimum (PDF) in 2015 when mean speed V= 8.2 equal 14.97. Figure (3.6) shows the maximum (CDF) reached 51.96% in 2016, when the mean wind speed was equal 8 m/s and the minimum (CDF) reached 51.42% in 2015 at the mean wind speed equal 8.2 m/s. Figure (3.8) shows the maximum (PDF) reached 15.2% in 2012, when the mean wind speed equal 8.8 m/s, and observed the minimum (PDF) reached 13.7% in 2015 when the mean wind speed equal 8.9 m/s .Figure (3.9) shows maximum (CDF) reached equal 52.7 % in 2014, when the mean wind speed equal 8.9 m/. Figure (3.10) shows the compared between the value of energy when using P15-50 and using V27-225 at height 30 meters, observed the maximum energy was extracted in 2013 from applied V27-225.Figure (3.11) shows the compared between cost $/kW and capacity factor for P15-50 and V27-225, the maximum of capacity factor recorded from p15-50 in 2013 with minimum of cost. Figure (3.12) shows the maximum of energy extracted in 2015 when applied V 39-500 at 50 meters height, Figure (3.13) shows the minimum of cost $/kW and maximum of capacity

factor recorded in 2015. Figure (3.14) shows the energy obtained from V39-500 at 50 meters height is better than other turbines

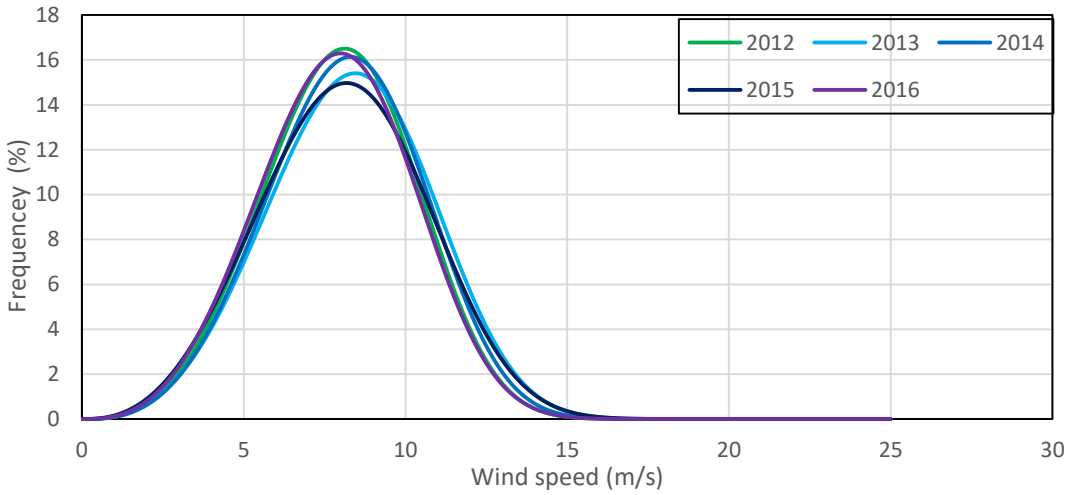

Figure 3.5: Probability wind speed density at 30 meters height period 2012 to 2016

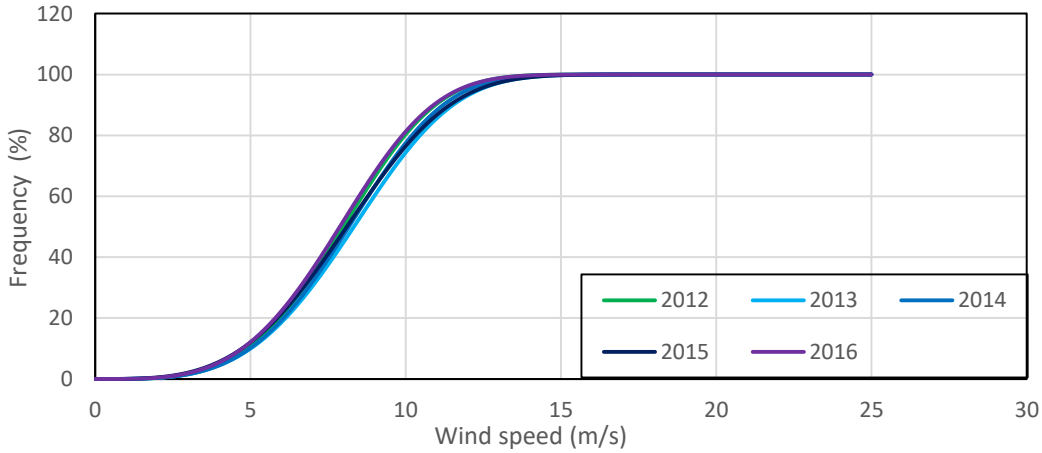

Figure 3.6: Cumulative wind speed density at 30 meters height period 2012 to 2016

Table 3.8: The value of parameters over the years wind speed at height 50 meters

Year	2012	2013	2014	2015	2016
K	3.8	3.7	3.8	3.5	3.7
C (m/s)	9.5	9.9	9.6	9.8	9.3
EPF	1.04	1.08	1.03	1.13	1.07
V_m Data (m/s)	9	9.4	9.2	9.2	9
V_m Plot (m/s)	8.8	9.1	8.9	8.9	8.5
Freq (PDF %)	15.2	14.3	15.1	13.7	15.2
Freq (CDF %)	52.2	51.9	52.7	51.0	51.1
P (W/m^2)	434	500	447	491	403

To find the energy cost per year at 50 meters height, applied last function (3.11) and using wind turbine V39-500.

Cost = 575,000 $ I =690,000 $ comr = (575,000/20) * 0.25
= 7187.5 $

S = 690,000*0.1 = 69000 $ t= 20 y r = 0.15 i = 0.12

Civil work = 20% of cost = 115,000 $

PVC = 759338.85 / 20 (y) * E (kW)

Table 3.9: The value of parameters over the years at height 50 meters using V39-500 wind turbine

Year	2012	2013	2014	2015	2016
C_f (%)	0.17	0.21	0.18	0.22	0.17
P_{out} (kW)	69.7	92.4	75.6	92.4	64.6
E (MWh)	384.8	593.9	413.1	504.9	368.6
Cost ($/kW)	0.10	0.076	0.09	0.075	0.10

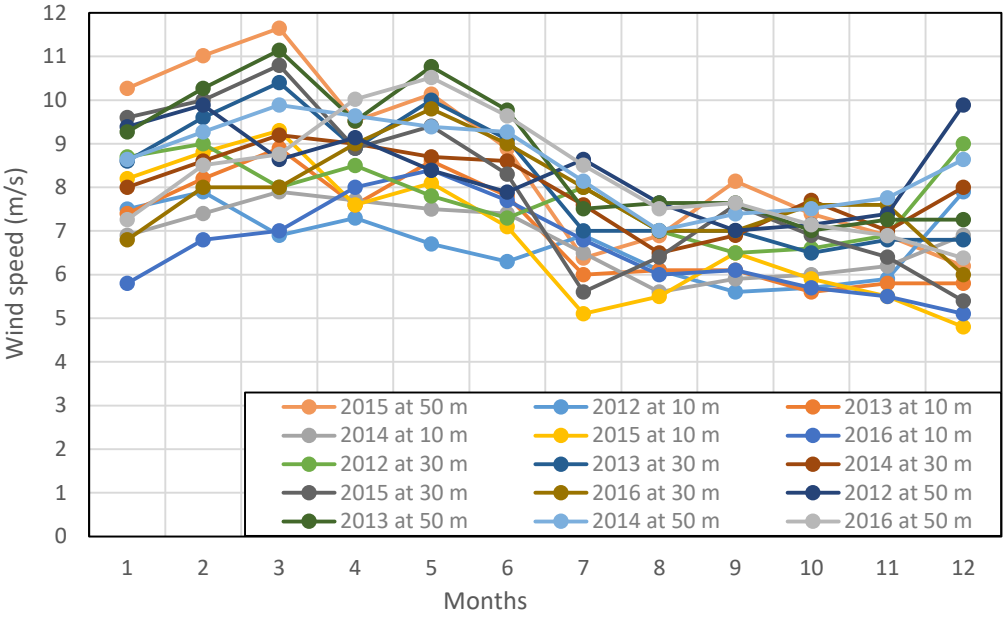

Figure 3.7: Comparison of wind speed m/s at height of 10 meters, 30 meters and 50 meters

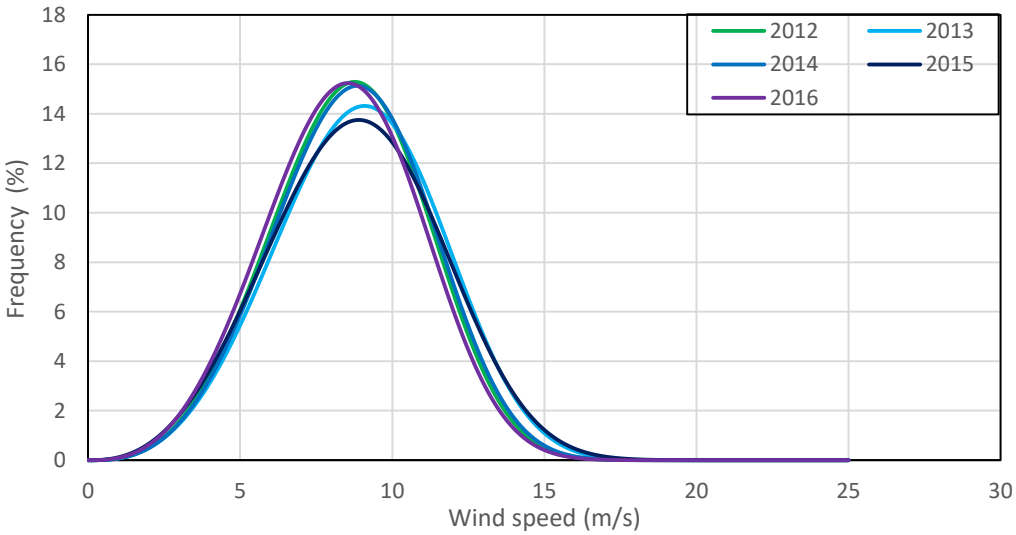

Figure 3.8: Probability wind speed density at 50 meters height from period 2012 to 2016

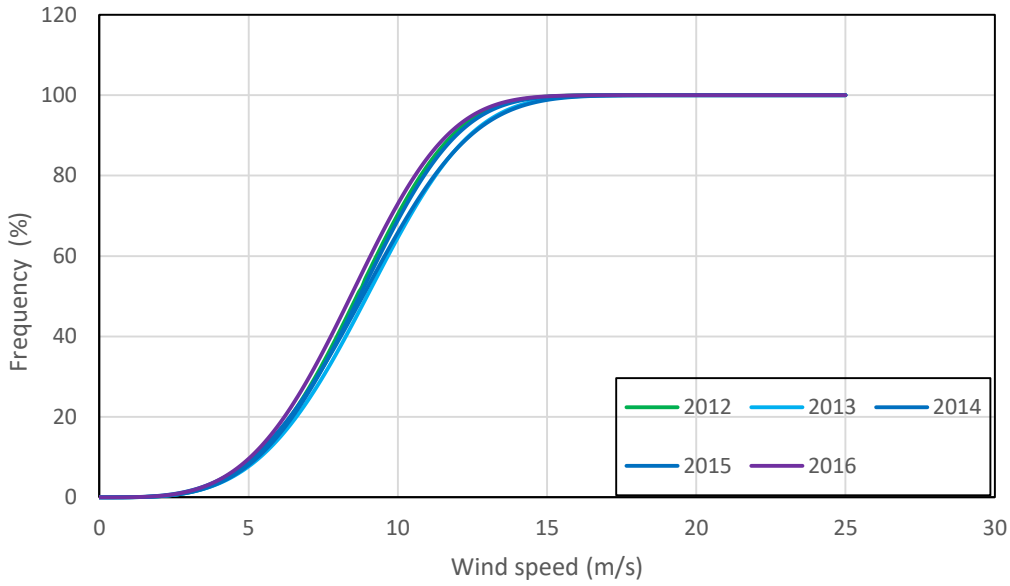

Figure 3.9: Cumulative wind speed density at 50 meters from period 2012 to 2016

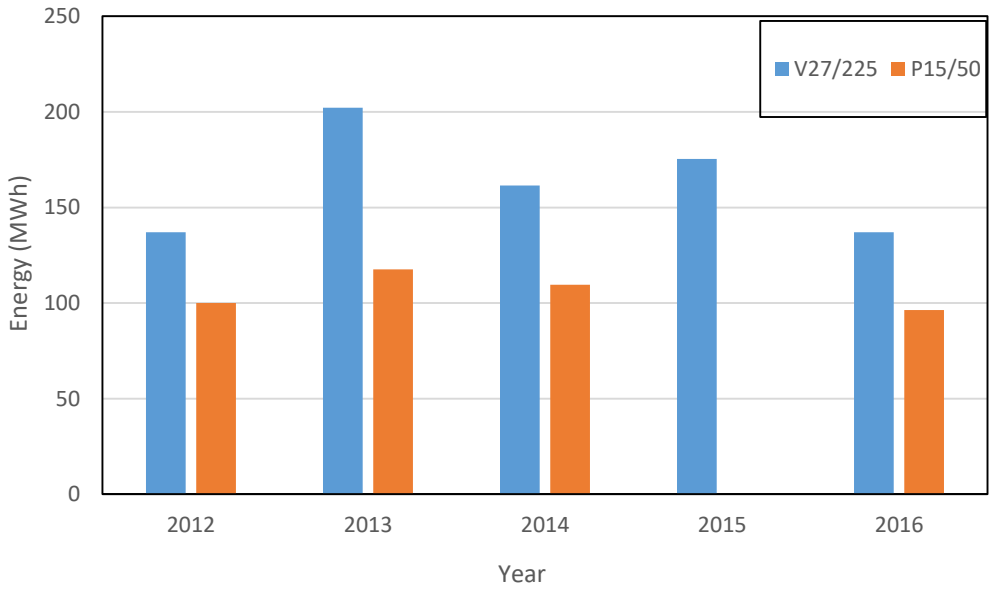

Figure 3.10: Comparison of energy value using wind turbine P15-50 and using V27-225 wind turbine at 30 meters height

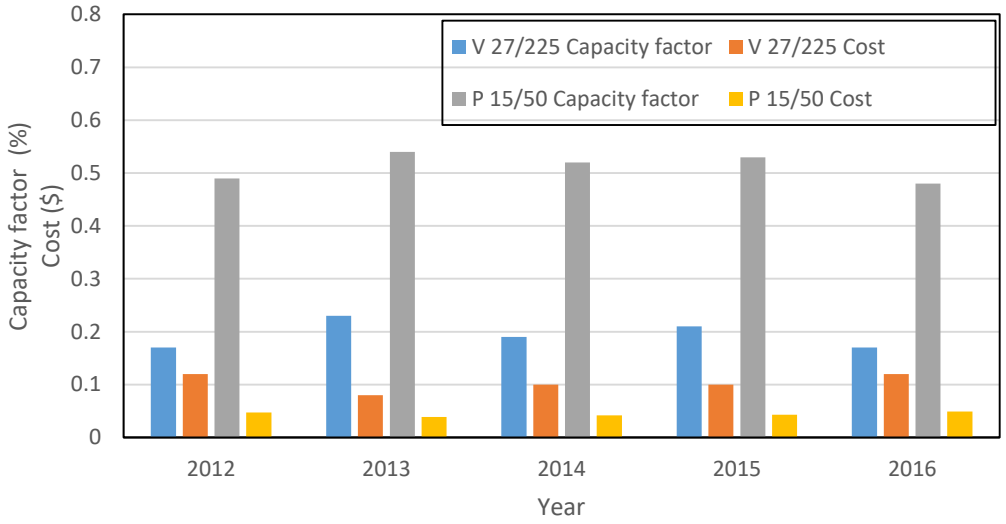

Figure 3.11: Comparison between the cost value using turbine P15-50 and using V 27-225 wind turbine at 30 meters height

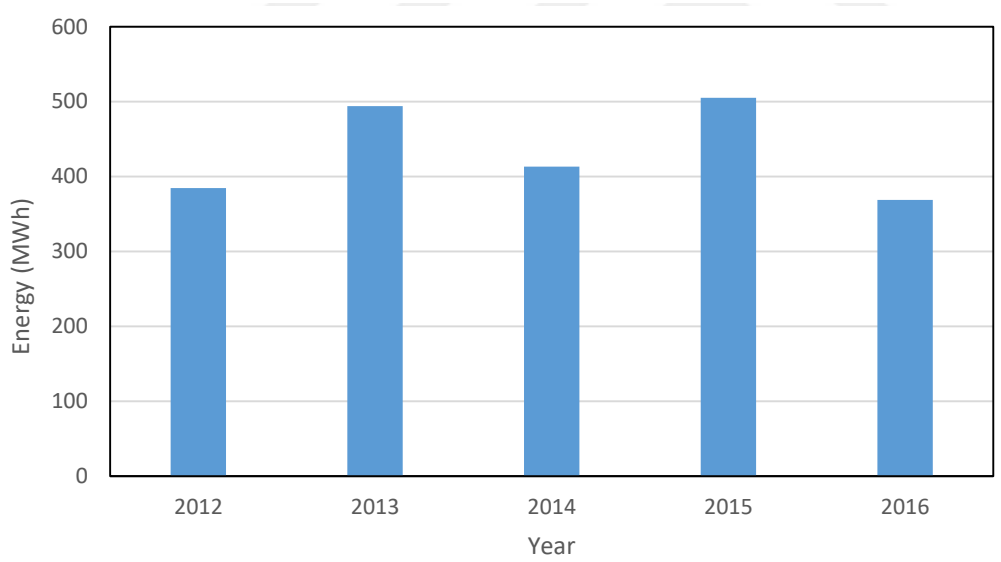

Figure 3.12: The energy value using wind turbine V 39-500 at 50 meters height

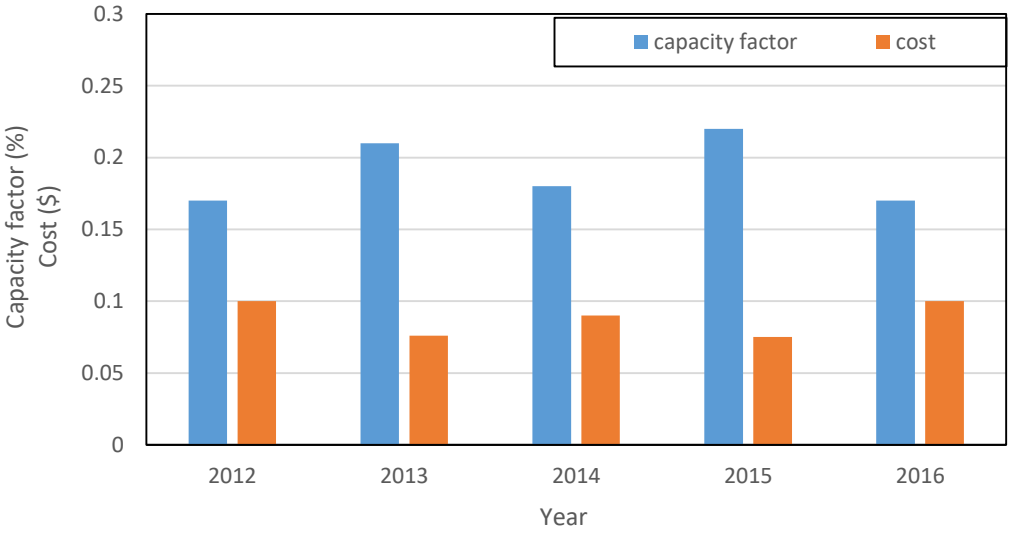

Figure 3.13: Compare the value of the capacity factor (C_f) and cost using wind turbine V39-500 at 50 meters height

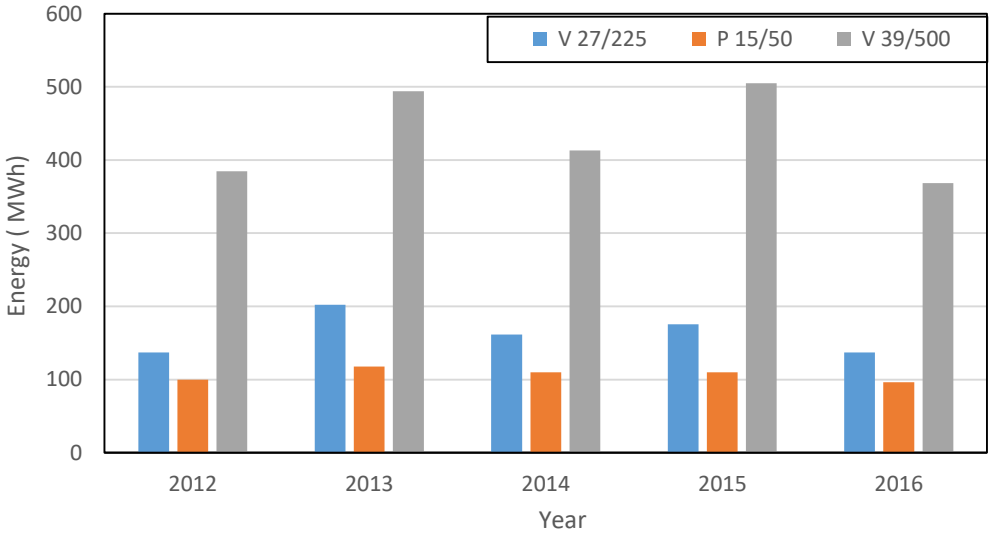

Figure 3.14: Comparison energy value using wind tuebine P15-50 and V27-225 wind turbine at 30 meters height and using V39-500 wind tuebine at 50 meters height

CHAPTER 4

BLADE ELEMENT MOMENTUM METHOD

4.1 Wind Turbine Design

This study c on the designing of small-blade wind turbine [51, 52]. Aerodynamic parameters design for blade includes the selections of the data, such as blade length, the chord length (c) and, twist angle (ϖ) from the direction of rotation [49]. Figure (4.1) shows performance parameters of the wind turbine.

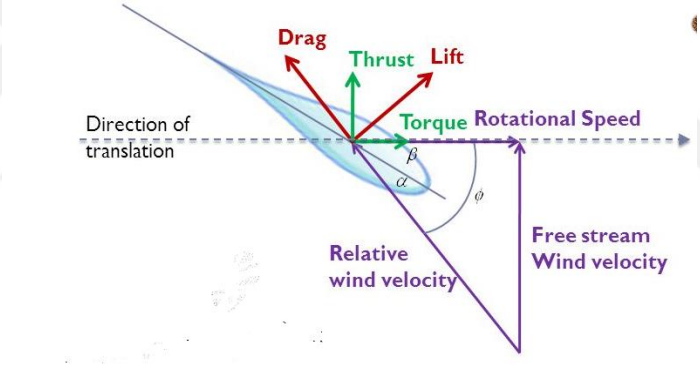

Figure 4.1: Performance parameters of the wind turbine [53]

The speed ratio must be specified for system. The speed ratio is the ratio between the rotational speed on the tip of the blade and the wind speed that comes to the turbine [51]. It is shown in the equation:

$$\lambda = \Omega r / u \tag{4.1}$$

Where Ω is the rotational speed, (r) is turbine radius, and (u) is a wind speed of incoming flow. Related to the type of wind turbine selection designed, various tip

speed ratio is recommended for the most performance [51]. This shown in Figure (4.2). The baseline at the top of the Figure appears the Betz limit, while the others represent the maximum predictions for the different types of systems [54].

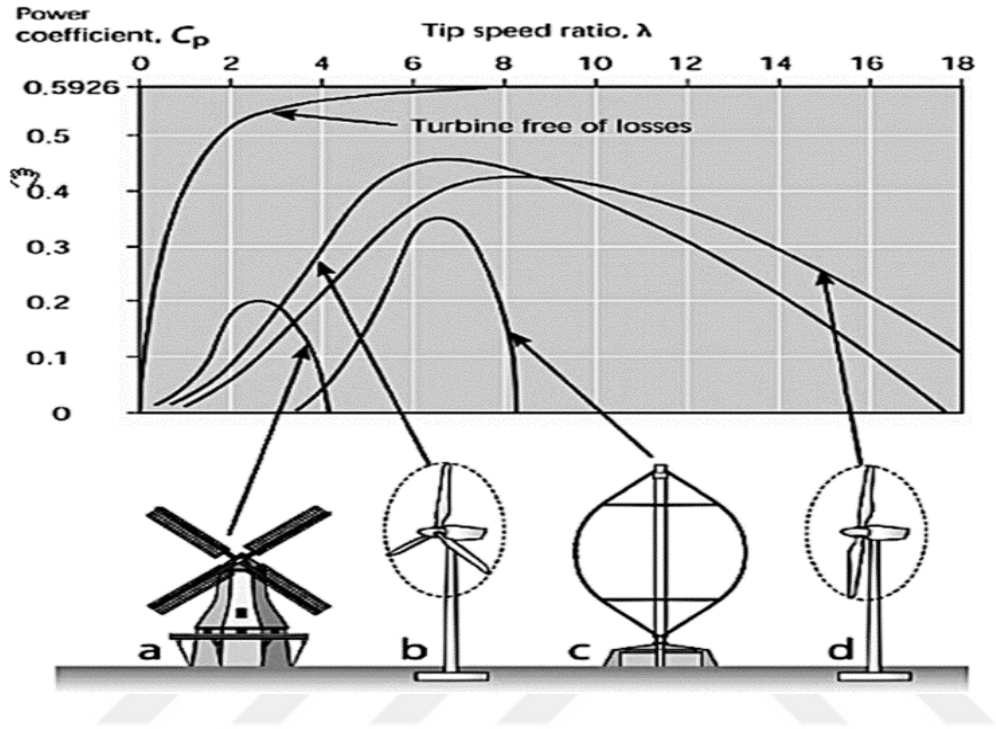

Figure 4.2: Tip speed ratio versus power coefficient [48]

When the speed ratio is decided, the airfoils are selected for various radial sections along the blade. This choice is dependent on the relative of wind speed for each section along the blade.

To calculate the relative wind speed in sections along the blade, speed triangles must be used. Speed triangles blend the rotational speed of the blade where (ωr) tip speed (u) free wind speed (m/s) and (U_{rel}) relative wind speed (m/s).

In fact, the rotational speed will grow as one action from the hub to the top of the blade, converting the relative speed and the related angles. Each section of airfoil set on has an optimum attitude of the angle of attack. Acquiring the most significant aerodynamic performance of the wind turbine the angle of twist, it should be selected

in order that the airfoil is always at its optimum attitude angle of attack, which proceeds from hub to top while the blade rotation at the range design of speed ratio [49].

That the lift force generated will increase with the angle of attack up to a stall point. However, the drag grows the maximum of ratio L/D related to the angle for optimum attack design of blade wind turbine [51].

4.2 Introduction

BEM method describes the process of the calculation for wind turbine blades [43]. This process is useful to be used for every analysis of the designing new machines or the existing machines. Many methods are useful; however, this way has the advantage because it is simple and easy to use. BEM method design is used to complete the design and, it can perform by using data for lift and drag type for the airfoil.

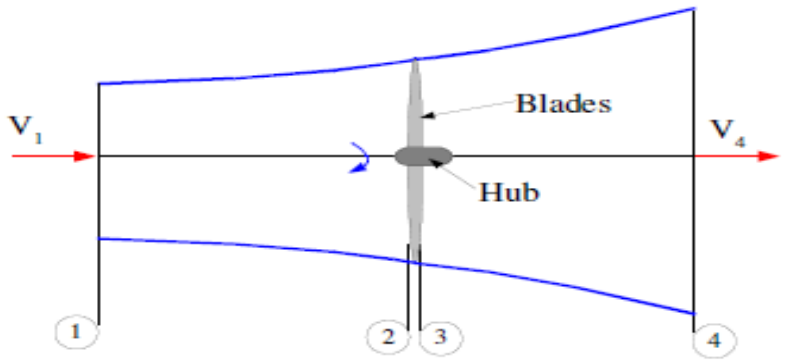

Figure 4.3: Blade element theory [22]

4.3 Blade Element Momentum Theory

Using two methods to test how a wind turbine works. First, a momentum balance is used on an annular of a rotating flow tube passing across a turbine [51]. Then to

determine the results of the force by the airfoil lift and drag coefficients at different divided elements along the blade. Using a series of processes that are solved iteratively.

4.3.1 Axial Force

Figure (4.3) shows the flow tube around a wind turbine. Four zones are shows, zone1 is upstream of the turbine, zone 2 is before the blades, zone 3 is just after the blades, and zone 4 is downstream of the blades, between zone 2 and zone 3. Power is obtained from the wind, and there is a change in the value of pressure as a result.

Presume $p_1=p_4$ and that $V_2=V_3$. Also, presume between 1 and 2, and between 3 and 4, the stream is frictionless then applies Bernoulli's equation. After some process of algebra:

$$p_2 - p_3 = 1/2\ \rho\ (V^2 1 - V^2 4) \tag{4.2}$$

We found that force:

$$dF_x = (p_2 - p_3)\ dA \tag{4.3}$$

$$\Rightarrow dF_x = 1/2\ \rho\ (V^2 1 - V^2_4)\ dA \tag{4.4}$$

(a) is indicative of the axial induction factor:

$$a = V_1 - V_2\ /V_1 \tag{4.5}$$

so this too:

$$V_2 = V_1\ (1-a) \tag{4.6}$$

$$V_4 = V_1\ (1-2a) \tag{4.7}$$

Obtained axial force:

$$dF_x = 1/2\ \rho V21\ [4a\ (1-a)]\ 2\pi rd. \tag{4.8}$$

4.3.2 Rotary Annular Flow Tube:

To consider the rotary flow theory of the current tube shown in the Figure (4.4). Four zones are shown in Figure (4.3) the turbine upstream, (2) just ahead of the blades, (3) directly after of the blades, and 4 downstream of the blades. Between (2) and (3), the rotation motion of the turbine rotates the blade wake.

Consider that the angular momentum is kept in this annular flow of stream tube. It is shown in Figure (4.4). The active blade's rotation with an angular speed (ω) and the rotation of the blades with an angular speed of (Ω), then:

.

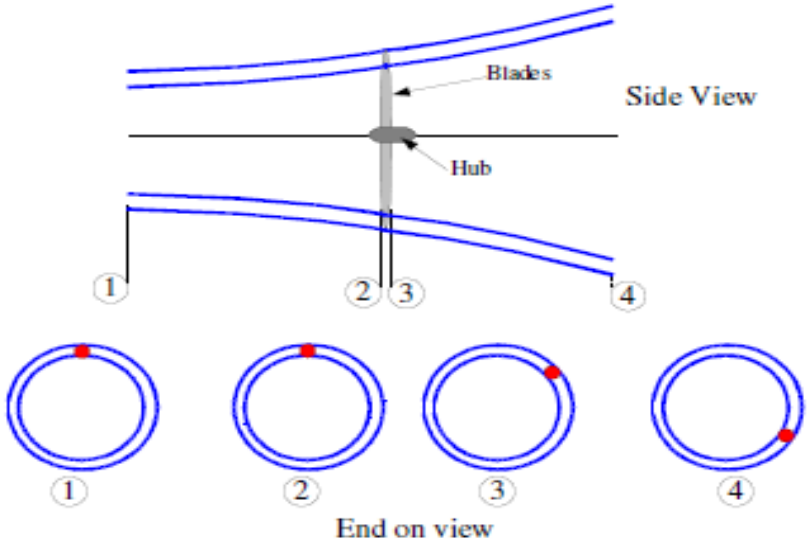

Figure 4.4: Rotating annular flow tube at different flow position [53]

$$\text{Inertia of moment } I=mr^3 \tag{4.9}$$

$$\text{Angular of moment } L= I\,\omega \tag{4.10}$$

$$\text{Torque } T = dl/dt \tag{4.11}$$

$$T = dl\omega/dt = d(mr^2\,\omega)/dt \quad = dm/dt\, r^2\,\omega \tag{4.12}$$

For element with torque as:

$$dt = d\dot{m}\ \omega r^2 \tag{4.13}$$

For rotation annular of element

$$d\dot{m} = \rho A V_2 \tag{4.14}$$

$$d\dot{m} = \rho\ 2\pi r dr V_2 \tag{4.15}$$

$$dt = \rho\ 2\pi r dr V_2\ \omega r^2 = \rho\ V_2\ \omega r^2\ 2\pi r dr \tag{4.16}$$

Define angular induction factor

$$á = \omega / 2\Omega \tag{4.17}$$

$$dT = 4\ á\ (1\text{-}a)\ \rho\ V\ \Omega\ r^3\ \pi r\ dr \tag{4.18}$$

The Blade Element Method (BEM) is used to calculate the blade performance [55]. BEM is dependent on dividing a designed wind turbine blade to elements, as shown in Figure 4.5. Where data of the airfoil is used to determine the lift and drag for each element along the blade. The data for this technique is the angle of attack for each element, the length of the chord, and the lift-drag diagram curve for the airfoil used on each element. Using the forces under design conditions to calculate the total torque produced by the system design. Then, the torque estimated can be used to predict the theoretical power. This process assumes that there is no three-dimensional stream flow along the blade. The computer software used to apply (BEM) to selected specified blade designs.

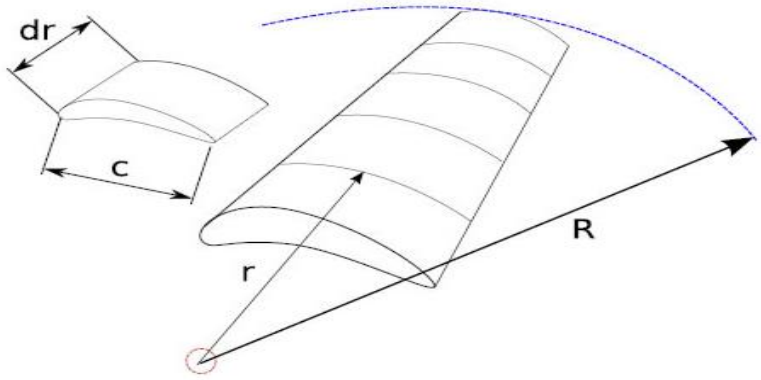

Figure 4.5: Model of blade element theory [53]

The design of the horizontal axis wind turbine carried out by using blade element momentum is generally followed as [27, 45, 52]:

Momentum theory; to acquiring (dFX) and (dT) for each element on the blade, it can be applied the following equations on each element axial force:

$$dFX = \rho U^2[4a(1-a)]\pi r dr \tag{4.19}$$

Angular torque:

$$dT = 4\acute{a}(1-a)\rho U\Omega r^3\,\pi dr \tag{4.20}$$

When (u) is wind speed, (ρ) is density, (a) and (á) are axial and induction factor.

The blade is divided to several sections figure (4.5) showen, and each element will have a different flow like different rotational speed (ωr), a different chord (C_r), different twist angle (θ_r) and determined each one and calculated the overall performance characteristics by numerical integration along of the blade span finally. Therefore, we can obtain an induction factor and tangential factor as given below:

$$\text{Tip speed ratio } \lambda = \frac{\omega r}{U} \tag{4.21}$$

Relative angle:

$$\Phi_r = (2/3)\tan^{-1} * (1/\lambda_r) \tag{4.22}$$

To determine of optimal twist angle:

$$\theta_r = \Phi_r - \alpha_d \tag{4.23}$$

To determine blade solidity and chord: where (B) number of blades, (r) is radius and lift coefficient design Lc, d

$$\sigma = \frac{BC}{2\pi r} \tag{4.24}$$

$$\text{Chord (Cr)} = \frac{8r\pi sin\Phi r}{Nb\ Lc,d} * \frac{1-\lambda_r \tan \Phi r}{\tan \Phi r + \lambda_r} \tag{4.25}$$

$$\text{Induction factor } a = \frac{1}{\frac{4Ftipsin^2 \Phi r}{\sigma(CL \sin\Phi r + CD \sin\Phi r)} + 1} \tag{4.26}$$

$$\text{Tangential factor } \acute{a} = \frac{1}{\frac{4Ftip \sin \Phi r \cos \Phi r}{\sigma(CL \sin\Phi r - CD \cos\Phi r)} + 1} \tag{4.27}$$

To find the incoming flow angle Φ_r :

$$\text{Relative speed Urel} = \frac{U(1-a)}{\sin \Phi r} \tag{4.28}$$

$$\tan \Phi r = \frac{\lambda(1+\acute{a})}{(1-a)} \tag{4.29}$$

Where: C_L and C_D are obtained from (x) foil program. Moreover, the attack of angle can be determined as:

$$\alpha = \phi - \beta \tag{4.30}$$

Where: β is Twist angle (blade pitch angle + local twist angle):

To calculate the lift and the drag:

$$L = 1/2\rho Vrel^{2}\, cCL \tag{4.31}$$

$$D = 1/2\rho Vrel^{2}\, cCD \tag{4.32}$$

Lift and drag are determined in the same tendency according to the flow. However, the best way to divide the forces in the normal and tangential direction compared to the rotor speed. To determine the forces as:

$$PN = L.\cos(\Phi) + D.\sin(\Phi) \tag{4.33}$$

$$PT = L.\sin(\Phi) - D.\cos(\Phi) \tag{4.34}$$

The thrust forces and moment can be determined as follows:

$$dT = (NB)\,(PN)\,dr \tag{4.35}$$

$$dM = (r)\,(NB)\,(PT)\,dr \tag{4.36}$$

And, where (NB) is the number of blades

The Power and Reynolds number from each element determine as:

$$dP = dM\,\omega \tag{4.37}$$

$$Re = U_{rel}\, C / \nu \tag{4.38}$$

ν: is kinematic viscosity [$\nu = 14.8\text{x}10^{-6}$ (m^2/s)]

4.4 Blade Element Theory Correction Factors

The blade element theory does not contain any loss at the tip and hub; otherwise, it is not suitable for the axial induction factor greater than 0.5.

The important correction factors contained in the blade element theory [53].

4.4.1 Tip Loss Correction (Prandtl)

As a result, the vortex of effects at the blade tips, an expression for the afford losses over the span of the blade takes to be factored into the analyses [56, 57]. However, it does have an effect on rotor performance; the correction can be obtained as:

$$Ftip = 2/\pi \cos^{-1}\ (eXp(-f)) \tag{4.39}$$

$$f = \frac{B(R-r)}{2rsin\Phi r} \tag{4.40}$$

Therefore, the last equations will be changed into this formulation as:

$$dFX = 4Ftip\ \rho U^2[a(1-a)]\pi r dr \tag{4.41}$$

$$dT = 4Ftip\ 4á(1-a)\rho U\Omega r^3\ \pi dr \tag{4.42}$$

Induction factor $a = \frac{1}{\frac{4Ftipsin^2\ \Phi r}{\sigma(CL\ sin\Phi r + CD\ sin\Phi r)}+1}$ (4.43)

Tangential factor $á = \frac{1}{\frac{4Ftip\ sin\ \Phi r cos\ \Phi r}{\sigma(CL\ sin\Phi r - CD\ cos\Phi r)}+1}$ (4.44)

4.4.2 Glauert Correction

The blade element theory (BEM) for the axial induction factor is less than 0.4. Also, when the induction factor is more than 0.4. Then, the wind will be turbulent.

According (Glauert and Spera), is further modified as [58]:

1- When a<ac, where ac is the critical value and is equal to 0.2.

Induction factor $a = \frac{1}{\frac{4Ftipsin^2\ \Phi r}{\sigma(CL\ sin\Phi r + CD\ sin\Phi r)}+1}$ (4.45)

2- Where a>ac

$$a = 0.5[2 + k(1 - 2ac) - \sqrt{k(1 - 2ac) + 2)^2 + 4(kac^2 - 1)}] \quad (4.46)$$

$$K = \frac{4Ftipsin^2\,\Phi r}{\sigma(CL\,\sin\Phi r + CD\,\sin\Phi r)} \quad (4.47)$$

4.4.3 Hub Loss Correction

The hub loss is used for correcting speed; the reason is that vortex happened near the hub. The hub loss is a model of Prandtl tip loss[59].

$$Fhub = 2/\pi \cos^{-1}\,(eXp(-fhub)) \quad (4.48)$$

$$fhub = \frac{B(r - Rhub)}{2rsin\Phi r} \quad (4.49)$$

Where,

$$F = Ftip * Fhub \quad (4.50)$$

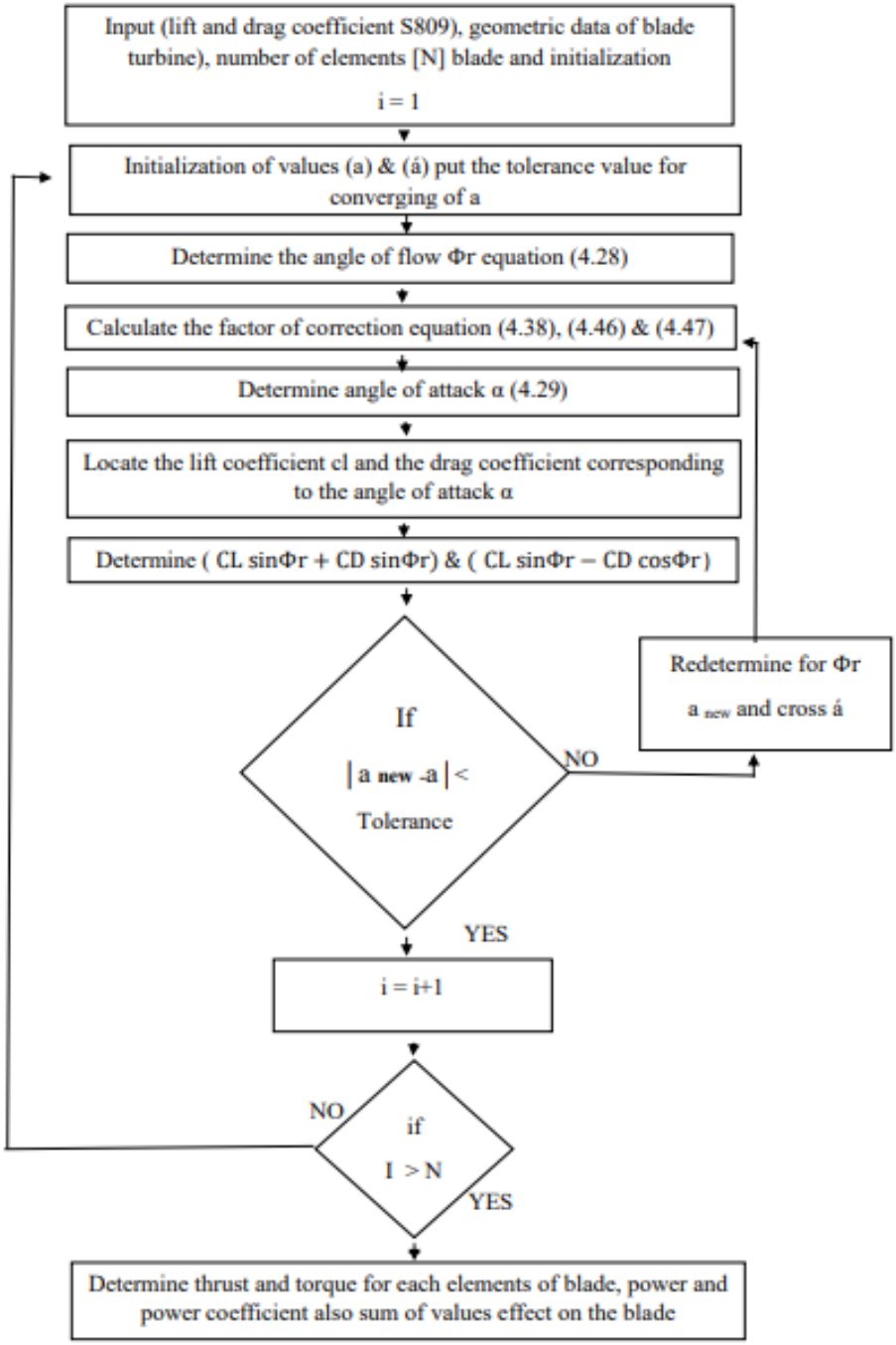

Figure 4.6: Blade element theory process chart

4.5 S809 NREL Lift & Drag Coefficient Data with Different Reynolds Number

Blade element theory (BEM) request on (C_L), and (C_D) use to determine the angle of attack (AoA) by using experimental to predicted (C_L), and (C_D) for S809 airfoil from different wind tunnel tests are conducted at the University of Ohio State, the University of Colorado State and the University of Delft Technology for various values of Reynolds numbers are recorded in the reports. Figures (4.7)and(4.8)show the relation between C_L and C_D with the angle of attack (AoA) and Reynolds number from the experimental results[60]. Rate of C_L and C_D are close in all measures of the minimize angles of attack; however, the bigger angles of attack are different in the same of Reynolds number experiments are conducted in various universities [61].

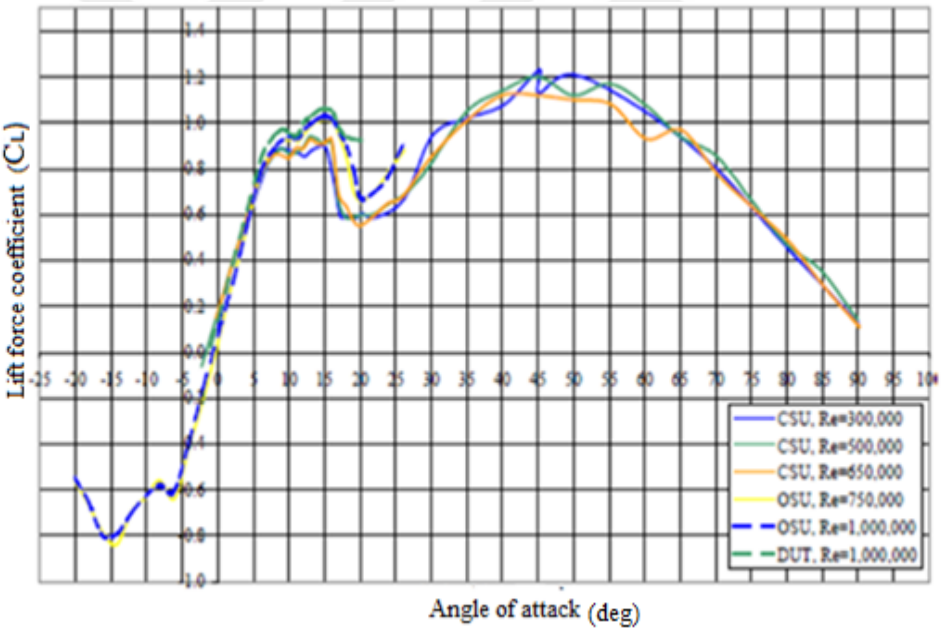

Figure 4.7: NERL S809 lift coefficients with different Reynolds number

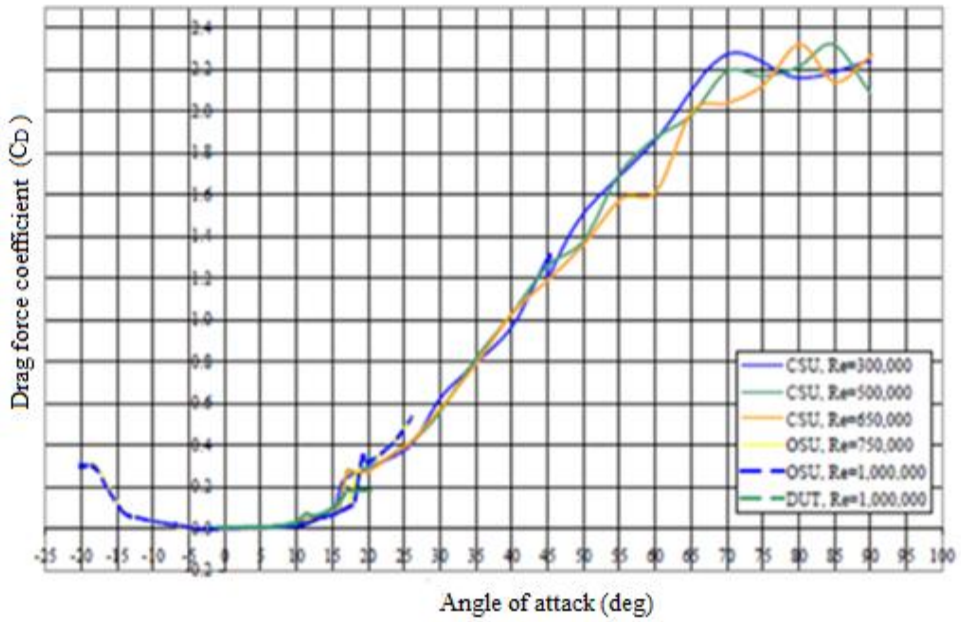

Figure 4.8: NERL S809 drag coefficients with different Reynolds number [61]

CHAPTER 5

VALIDATION STUDY

5.1 Introduction

In this chapter, Q blade software program and Matlab software program code based on BEM theory are used. The BEM theory model is mostly applied by the researcher community to design a blade of horizontal axis wind turbines and estimate their performance [23, 26, 27, 45, 31]. This code has been checked and validated with Phase VI wind turbine S809 airfoil wind turbine [62, 63]. The code can estimate the wind turbine power curve, thrust, and power coefficient. As results were compared with the empirical experimental of S809 two blades and three blades of a wind turbine [63]. The Q Blade program is firstly used in 2010 at Fluid Mechanics Chair (TU Berlin). Motivation [64]. It was to make a single tool compromised of all functions necessary for wind turbine simulation and design without having to import, transfer, or operation data from other sources shown in Figure (5.1). In order to stimulate scientific research in the field of wind energy [41], this program has been provided free use and has been granted a license to use that; license (GPL).

The software of Q Blade was used to analysis of blade wind turbine. Moreover, it will be concentrated on the horizontal axis blade of the wind turbine (HAWT). By utilized Q Blade software program as following [64, 65]:

- Definition and simulation of turbine
- Extrapolation of Lift and Drag polar
- Design airfoil and analysis

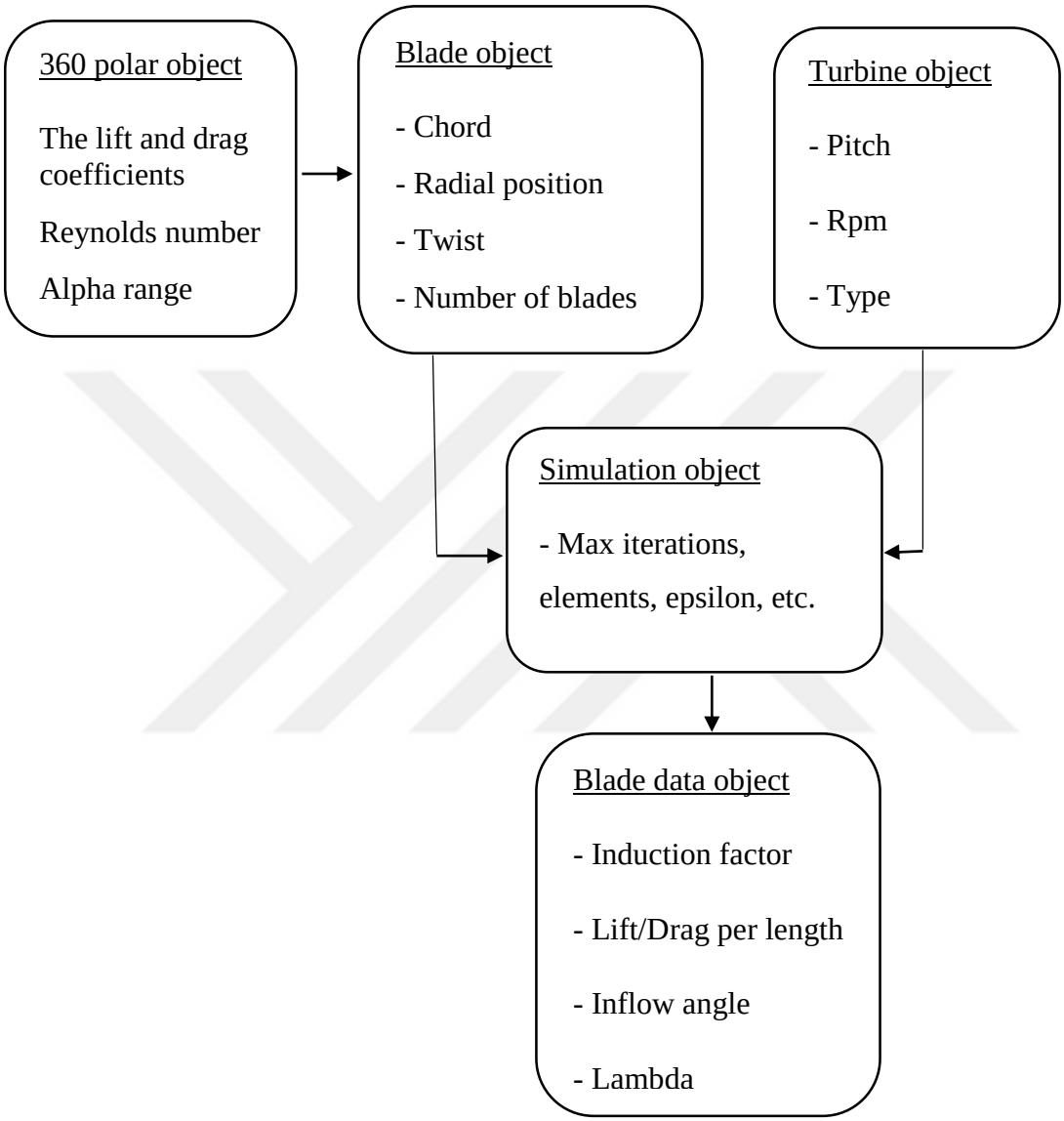

Figure 5.1: Q blade modules [64]

Click the airfoil of design tag and add data S809 profile, where it is available to use a simulation profile of ones or more different data profiles and the possibility of downloading from another source

5.2 Analysis of X Foil

Choosing X foil to Direct Analysis and click define X Foil Polar Button and input the value of Reynolds Number and to click on. After that, it acquired the window at which we input the beginning and ending angle of attack with the difference of angle. Then, will obtain the values of results for lift and drag coefficient with angle of attack.

5.3 Polar Extrapolation to (3600)

When designing any aerofoil, it must be performed with a range angle of attacks. In order to obtain these results of all angles attacks, we used this extrapolation.

Rotor design of HAWT [24]; it is used for Blade wind profile design. Values are entered in their positions, chord, elements of sections, and Polar design. In addition, we can add multiple numbers of sections and view the rotor of the blade.

5.4 HAWT Simulation using BEM

Using the BEM theory of blade wind turbine analysis, that we can obtain several relationships available in the program and calculate the impact of force and torque on the sections of the blade, which are related to angular rotor sections [24]. Next, click OK to obtained account values in numerous figures.

5.5 Experimental Data of S809 and Results

Table 5.1Data of experimental[57]

Number of Blades	2
Rotor Diameter	10.06 m
Rotational Speed	72 r/min
Cut-in Wind Speed	5 m/s
Cut out Wind Speed	25 m/s
Rated Power	10.0 kW
Blade Type	Variable Chord and Twist
Root Extension	1.258 m
Blade Pitch	3 Degrees
Blade Profile	NREL VI S809

Table 5.2 Data of experimental[61]

Number of Blades	3
Rotor Diameter	10.06 m
Rotational Speed	72 r/min
Cut-in Wind Speed	6 m/s
Cut-out Wind Speed	20 m/s
Rated Power	19.8 kW
Blade Type	Variable Chord and Twist
Root Extension	1.258 m
Blade Pitch	5 Degrees
Blade Profile	NREL VI S809

Table 5. 3 Geometric of two blades[61]

Section	nce r(m)	Chord length(m)	Twist (deg)
1	0.508	0.218	0
2	0.660	0.218	0
3	1.343	0.728	18.074
4	1.510	0.711	14.292
5	1.648	0.697	11.909
6	1.952	0.666	7.979
7	2.257	0.636	5.308
8	2.343	0.627	4.715
9	2.562	0.605	3.425
10	2.867	0.574	2.083
11	3.172	0.543	1.150
12	3.476	0.512	0.494
13	3.781	0.482	-0.015
14	4.023	0.457	-0.381
15	4.086	0.451	-0.475
16	4.391	0.420	-0.920
17	4.696	0.389	-1.352
18	4.780	0.381	-1.469
19	5.029	0.358	-1.775

Table 5. 4 Geometric of three blades[61]

Section	Radial Distance r(m)	Chord Length (m)	Twist (deg)
1	0.508	0.218	0.00
2	0.660	0.218	0.00
3	0.883	0.183	0.00
4	1.008	0.349	6.7
5	1.067	0.441	9.9
6	1.133	0.544	13.4
7	1.257	0.737	20.0
8	1.522	0.710	14.0
9	1.798	0.682	9.67
10	2.075	0.654	6.75
11	2.352	0.626	4.48
12	2.628	0.598	3.48
13	2.905	0.570	2.40
14	3.181	0.542	1.51
15	3.458	0.514	0.76
16	3.735	0.486	0.09
17	3.772	0.483	0.00
18	4.011	0.459	-0.55
19	4.288	0.431	-1.11
20	4.656	0.403	-1.55
21	4.841	0.375	-1.84
22	5.030	0.356	-2.00

Figures (5.2) and (5.3) show the simulation of the S809 lift coefficient and drag coefficient after input data. It was performed by X foil Qblade software[65][66], as the results following observed from figures the maximum of lift coefficient at 20 degrees of angle attack and fall down. After that, the air separation, Figures (5.4) and (5.7) show design of two blades, and three blades airfoil by using geometric for both obtained from tables (5.3) and (5.4). Figures (5.5) and (5.8) show for both two blades and three blades, it agrees between

the power curve of correction and power curve without correction, for Q blade software simulation between 5 to10 m/s of wind speed. After that, there is a fall slightly of wind speed from 12 m/s to 15 m/s there is a cubic relationship between

power and wind speed when increase wind speed doubles the power increasing eight times and this is effect during speeds that lower than 15 m/s and at wind speed rated, so that leads to result in the comparatively flat area of the power curve, there is an improvement rated power by using correction coefficients to overcoming the losses that happened near the hub and top of the blade. From Figures (5.6) and (5.9) show the blade element method, which gives a reasonably accurate indication of the thrust force affect the blade to many speeds of wind energy [46]. Figures (5.10) and (5.11) show the superlative between the power curve of Q blade software simulation, the power curve of the Matlab software simulation, and points of experimental. The result, the of power curve of the Matlab software simulation to most points showed accuracy best than the power curve of Q blade software simulation when it is supported on points of experimental [65, 66].

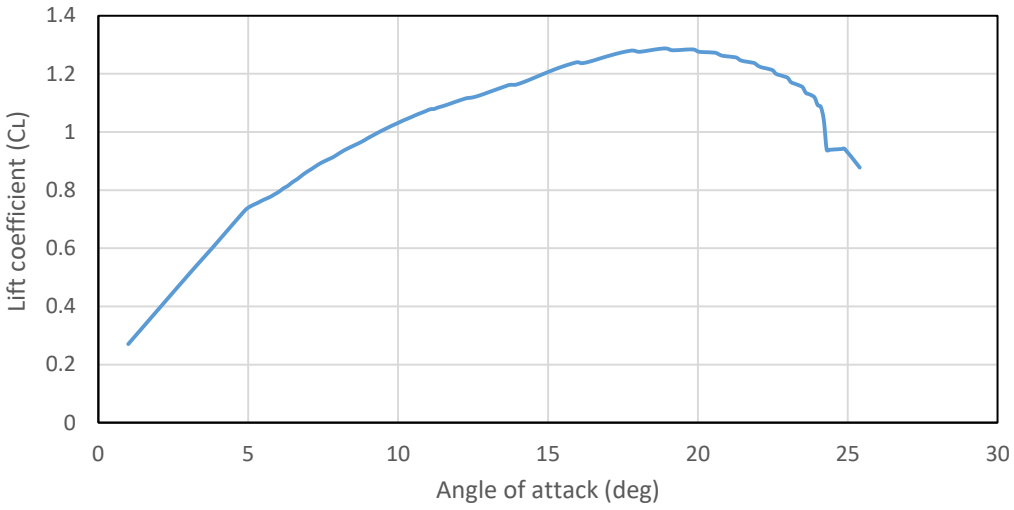

Figure 5.2: Simulation lift coefficient with angle of attack NETL VI S809

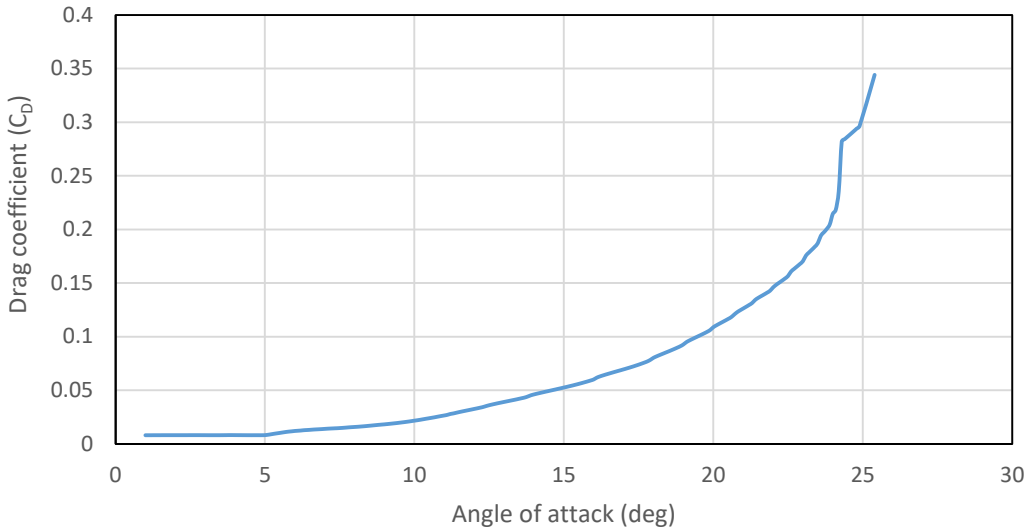

Figure 5.3: Simulation drag coefficient with angle of attack NERL VI S809

Two Blades:

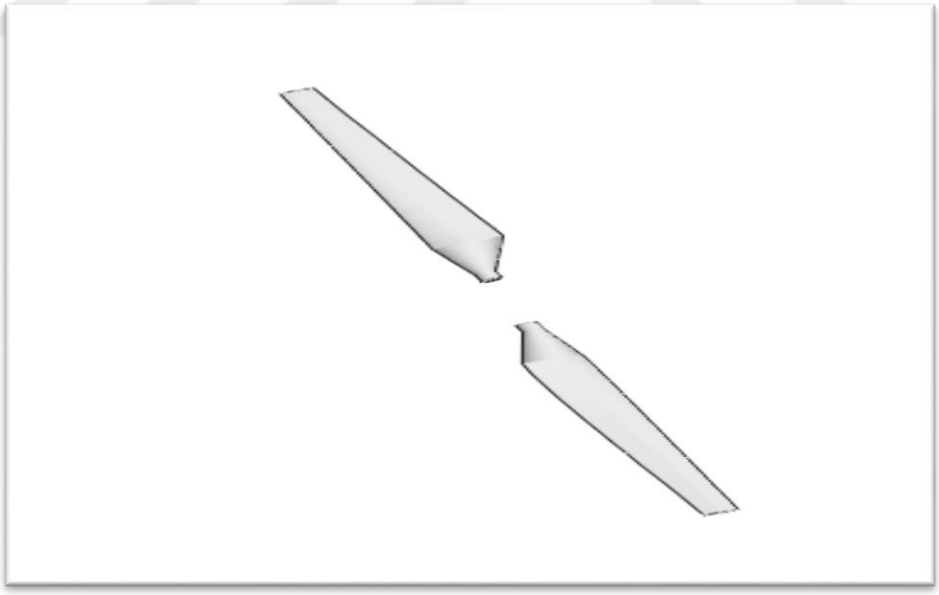

Figure 5.4: Design two blades by Q blade software

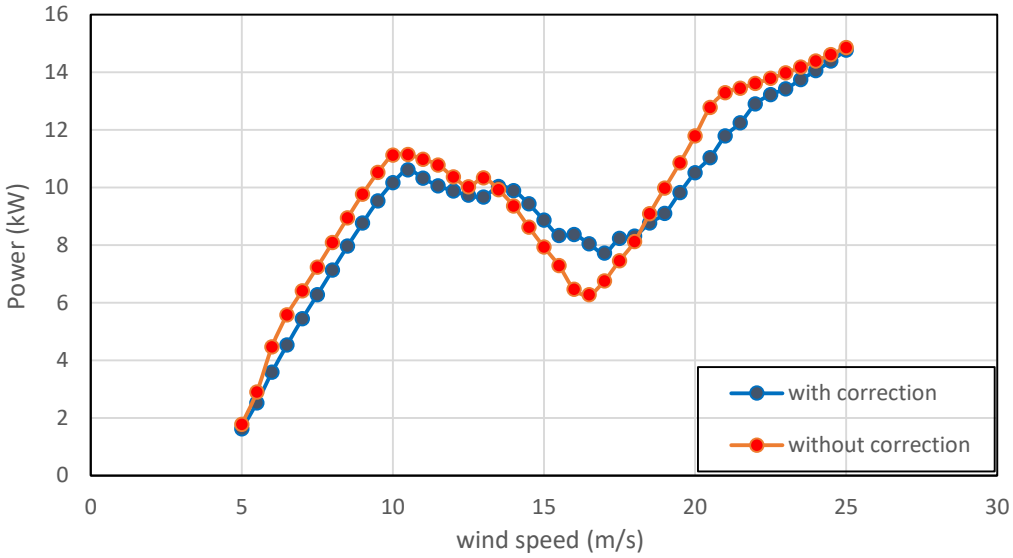

Figure 5.5: The effect of wind speed on the power

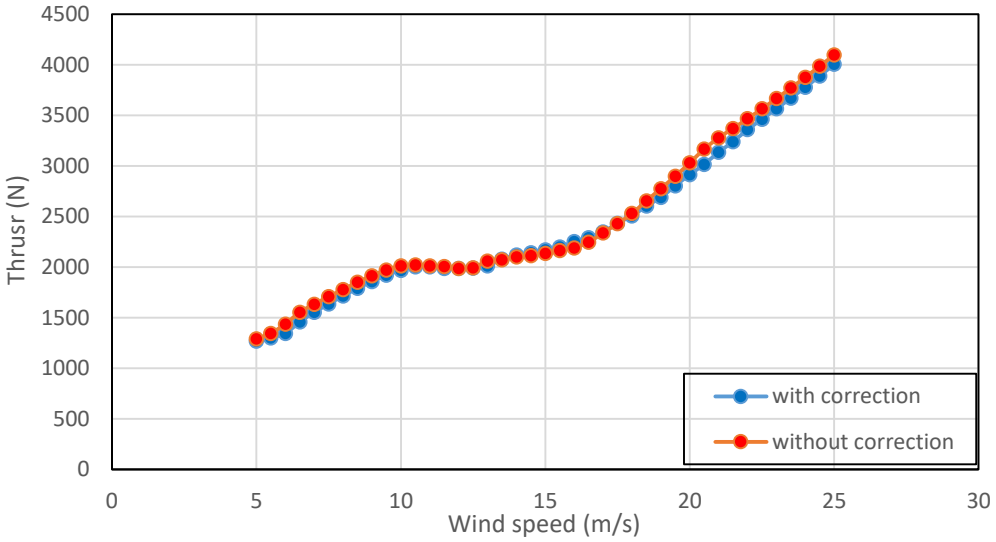

Figure 5.6: The effect of wind speed on the thrust

Three Blades:

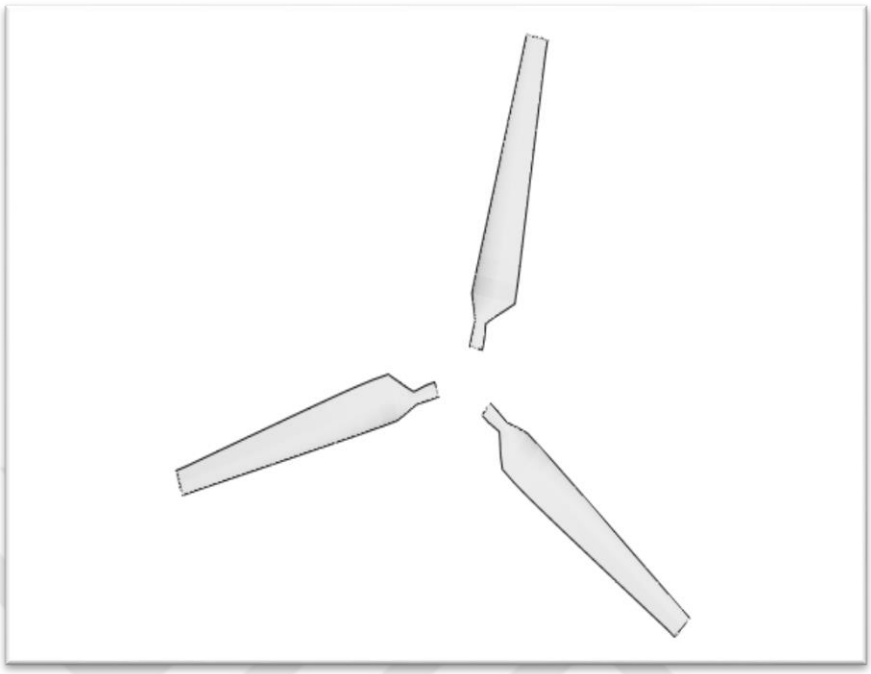

Figure 5.7: Design of three blades by Q blade software

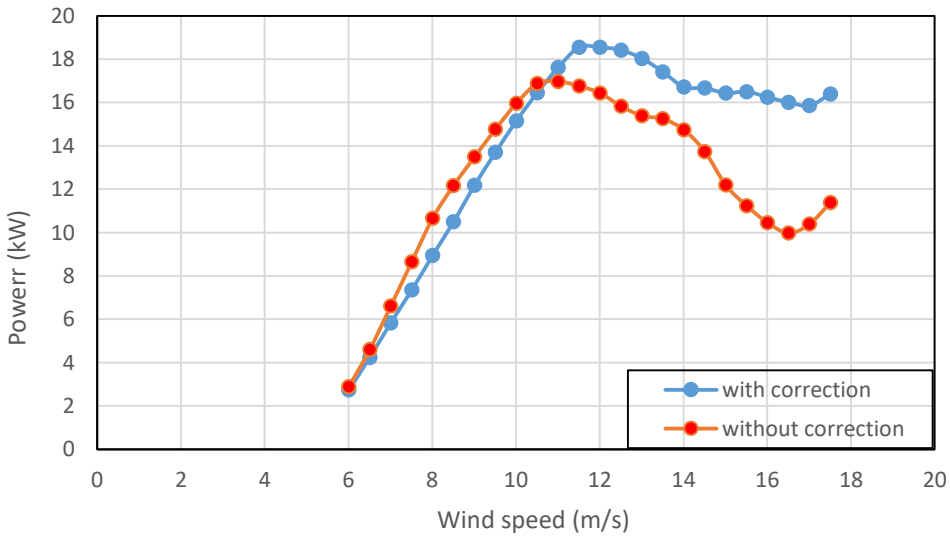

Figure 5.8: The effect of wind speed on the power

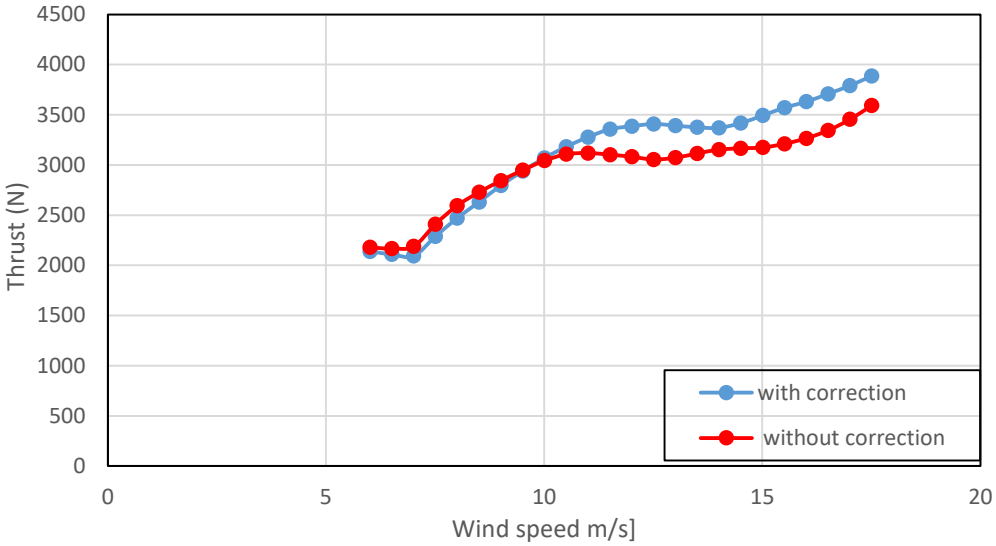

Figure 5.9: The effect of wind speed on the thrust

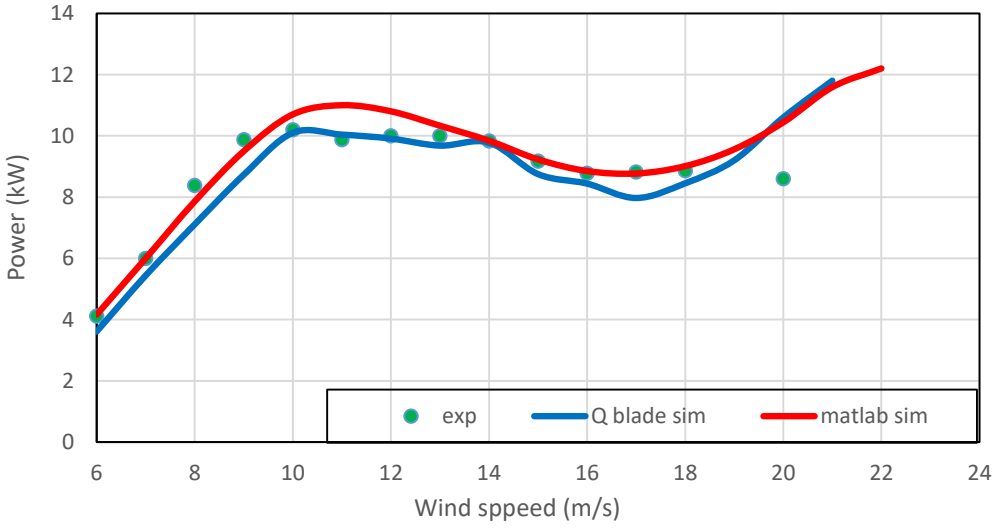

Figure 5.10: Wind speed comparison on the NERL S809 power of two blades with the simulation of Matlab software and Q blade software

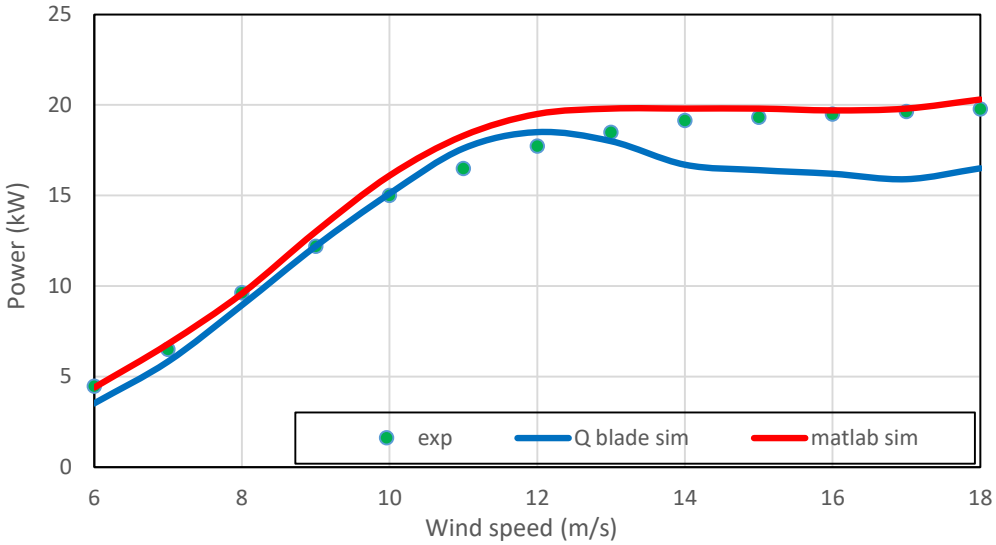

Figure 5.11: Wind speed comparison on NERL S809 power of three blades with the simulation of Matlab software and Q blade software

CHAPTER 6

WIND TURBINE DESIGN

6.1 Introduction

Rising costs of electricity production lead to higher energy prices; therefore, this pushed people to become more energy independent. Energy generated from the wind; can be one of the most affordable domestic renewable energy systems [1, 2, 11]. This chapter will be observing the best production power and best price of kilowatts that can be obtained by using many blades turbines designs applied the airfoil S809 [62] and related designs with the study site at mean wind speed and altitude of 30 meters from the Earth's surface[62]. In order to obtain a small design for an axis wind turbine that can be used for farms and residential areas and study that effect of (change chord and fixed twist angle) and (change twist angle and fixed chord) on the power generated where it had been studied with multiple values of a twist angle which a resulted in that power and cost per kilowatt of energy [36].

6.2 Wind Turbine Design

Designing of 5 m rotor wind turbine by applying (blade element theory) and neglecting the drag force to obtain a twist of angle and chord. NERL S809 was selected [52]. The Reynolds number is $1x10^{6,}$ and angle attack 6.25, with specification speed ratio 6 agree with maximum power coefficient for experimental of S809, the number of blades 3, mean wind speed equal 8 m/s corresponded to the location of study at height 30 m. Firstly design the chord by using the lift coefficient

Cʟ 1.1. Secondly, change the design of the chord with new lift coefficients 1.2 and 1.3, with fixing the twist angle. The process did with x foil Q blade airfoil software construction and Matlab software. The curves of values, power, thrust, power coefficient, and cost per kilowatt of energy for each design as following:

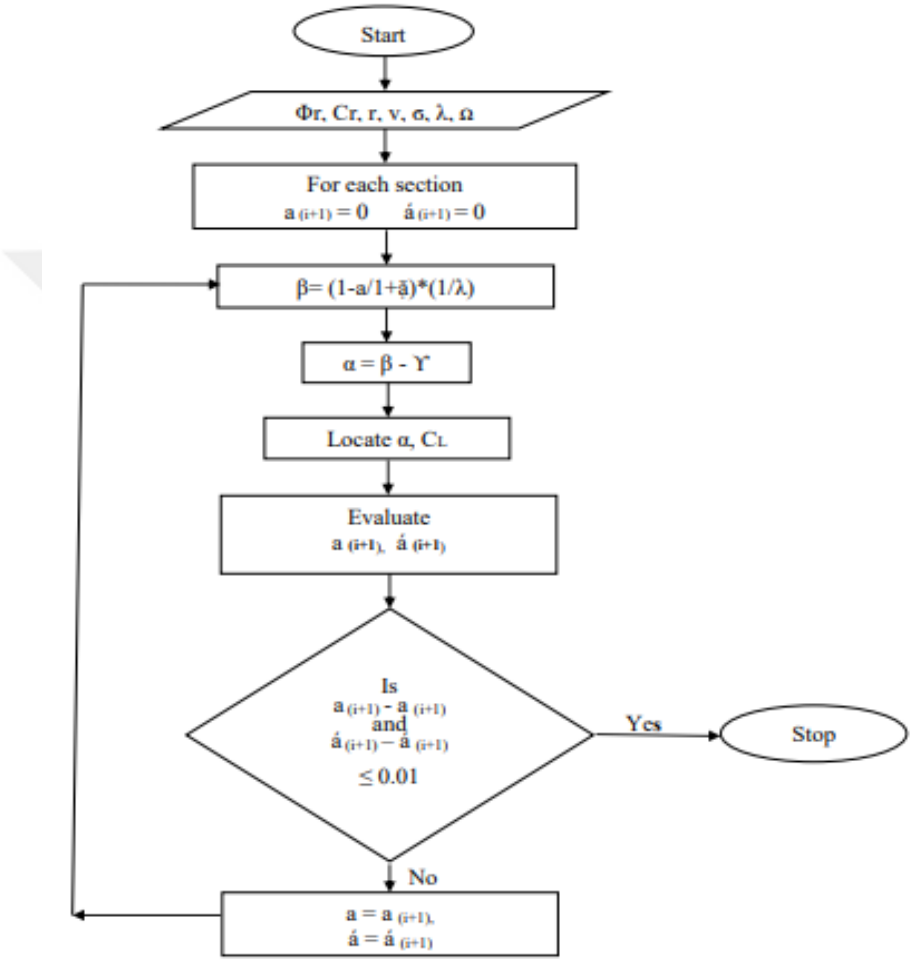

Figure 6.1: Determining parameters of design A, B&C process chart

6.3 Results

Tabel (6.1) shows design the geometric of three blades parameters with C_L chord 1.1, in which we divided blade into eighteen elements and applied (BEM) to find a chord and twist angle. Tables (6.2) and (6.3) show respectively geometric of three blades parameters with lift coefficient (C_L) after fixed twist angle and then changing chord design with lift coefficients 1.2 and 1.3 to obtain optimal power at mean wind speed at 8 m/s. While table (6.4) shows the total results of three typys of design,for the power, thurst, and power coefficient. The best result of the power record is in 7.84 kW at 8 m/s of mean wind speed with the design lift coefficient 1.1. Figures (6.2),(6.3) and (6.4) show values of parameters induction factor, tangent factor, twist angle, chord relationship with radius, respectively. Also, the twist angle and solidity have a relationship with tip speed ratio for three types of lift coefficients 1.1,1.2 and 1.3. Figures (6.5),(6.6) and (6.7) show respectively that baseline had obtained from the relationship between wind speed and power, power coefficien and thrust. When the wind speed has been increasing , the mentioned parameters are increasing, especially at the high wind speeds. These advantages are shown in the first design C_L 1.1.

Table 6.1: Geometric of three blades parameters with Cʟ 1.1

Section	Radial Distance r(m)	Local Tip Speed Ratio	Chord Length(m)	Twist (deg)
1	0.75	0.9	0.8747	25.8776
2	1.0	1.2	0. 8094	20.4044
3	1.25	1.5	0.7292	16.3207
4	1.5	1.8	0.6534	13.2216
5	1.75	2.1	0.5871	10.8187
6	2.0	2.4	0. 5304	8.9151
7	2.25	2.7	0.4824	7.3769
8	2.5	3.0	0.4415	6.1120
9	2.75	3.3	0.4064	5.0556
10	3.0	3.6	0.3762	4.1613
11	3.25	3.9	0.3499	3.3954
12	3.5	4.2	0.3269	2.7324
13	3.75	4.5	0.3066	2.1534
14	4.0	4.8	0.2886	1.6435
15	4.25	5.1	0.2726	1.1912
16	4.5	5.4	0.2582	0.7873
17	4.75	5.7	0.2452	0.4246
18	5.0	6.0	0.2334	0.0972

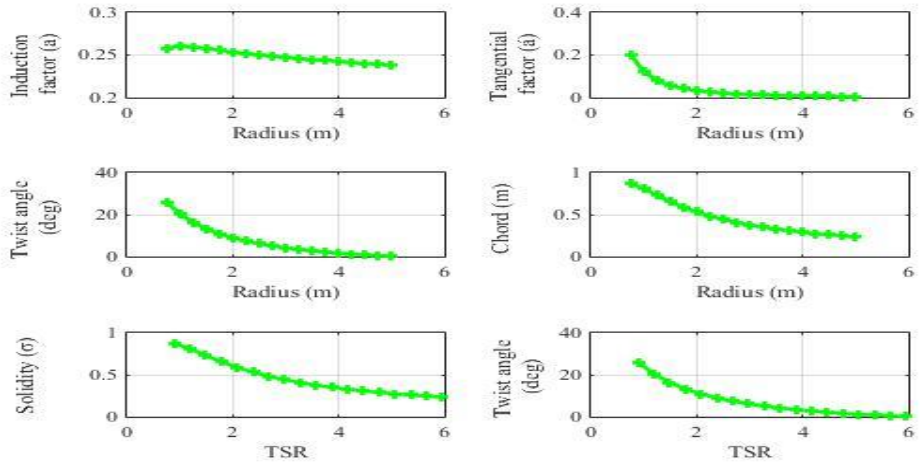

Figure 6.2: Value of parameters with Cʟ 1.1

Table 6. 2: Geometric of three blades parameters with Cʟ 1.2

Section	Radial Distance r(m)	Local Tip Speed Ratio	Chord Length(m)	Twist (deg)
1	0.75	0.9	0.8018	25.8776
2	1.0	1.2	0.7419	20.4044
3	1.25	1.5	0.6684	16.3207
4	1.5	1.8	0.5989	13.2216
5	1.75	2.1	0.5381	10.8187
6	2.0	2.4	0. 4862	8.9151
7	2.25	2.7	0.4422	7.3769
8	2.5	3.0	0.4047	6.1120
9	2.75	3.3	0.3725	5.0556
10	3.0	3.6	0.3448	4.1613
11	3.25	3.9	0.3207	3.3954
12	3.5	4.2	0.2997	2.7324
13	3.75	4.5	0.2811	2.1534
14	4.0	4.8	0.2646	1.6435
15	4.25	5.1	0.2499	1.1912
16	4.5	5.4	0.2367	0.7873
17	4.75	5.7	0.2248	0.4246
18	5.0	6.0	0.2140	0.0972

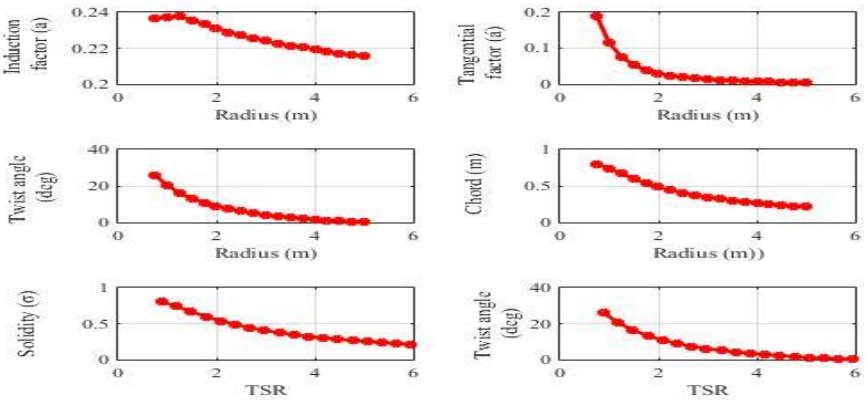

Figure 6.3: Value of parameters with Cʟ 1.2

Table 6.3: Geometric of three blades parameters design with Cʟ 1.3

Section	Radial Distance r(m)	Local Tip Speed Ratio	Chord Length(m)	Twist (deg)
1	0.75	0.9	0.7401	25.8776
2	1.0	1.2	0.6849	20.4044
3	1.25	1.5	0.6170	16.3207
4	1.5	1.8	0.5529	13.2216
5	1.75	2.1	0.4967	10.8187
6	2.0	2.4	0. 4488	8.9151
7	2.25	2.7	0.4082	7.3769
8	2.5	3.0	0.3735	6.1120
9	2.75	3.3	0.3439	5.0556
10	3.0	3.6	0.3123	4.1613
11	3.25	3.9	0.2961	3.3954
12	3.5	4.2	0.2766	2.7324
13	3.75	4.5	0.2595	2.1534
14	4.0	4.8	0.2442	1.6435
15	4.25	5.1	0.2307	1.1912
16	4.5	5.4	0.2185	0.7873
17	4.75	5.7	0.2075	0.4246
18	5.0	6.0	0.1975	0.0972

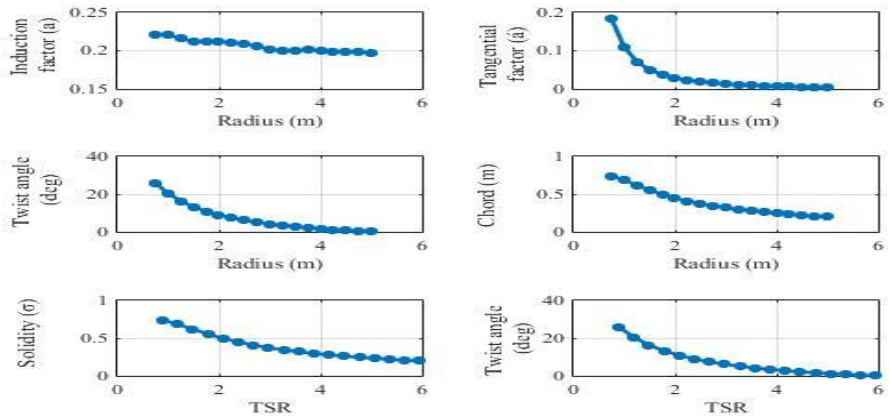

Figure 6.4: Values of parameters with Cʟ 1.3

Table 6. 4: Total values of parameters design

Parameters	Chord C_L =1.1 V = 8 (m/s)	Chord C_L =1.2 V = 8 (m/s)	Chord C_L =1.3 V = 8 (m/s)
Total Power, P (kW)	7.84	7.12	6.78
Total Thurst (N)	1335	1184	1109
Total Power Coefficient (Cp)	0..37	0.34	0.32

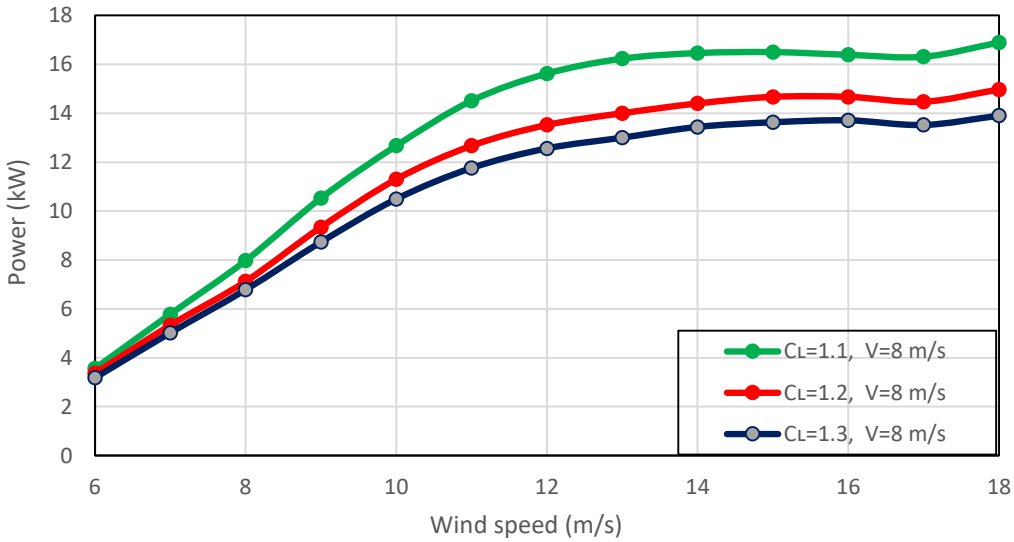

Figure 6.5: Wind speed comparison on three blades of power turbine for site design with different C_L 1.1,1.2 & 1.3

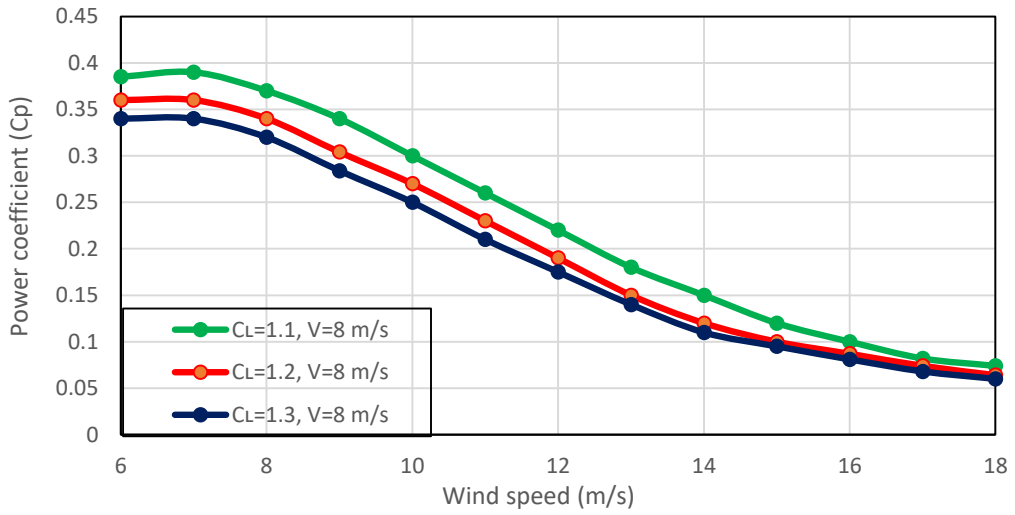

Figure 6.6: Wind speed comparison on three blades of power coefficient turbine for site design with different Cʟ 1.1, 1.2 & 1.3

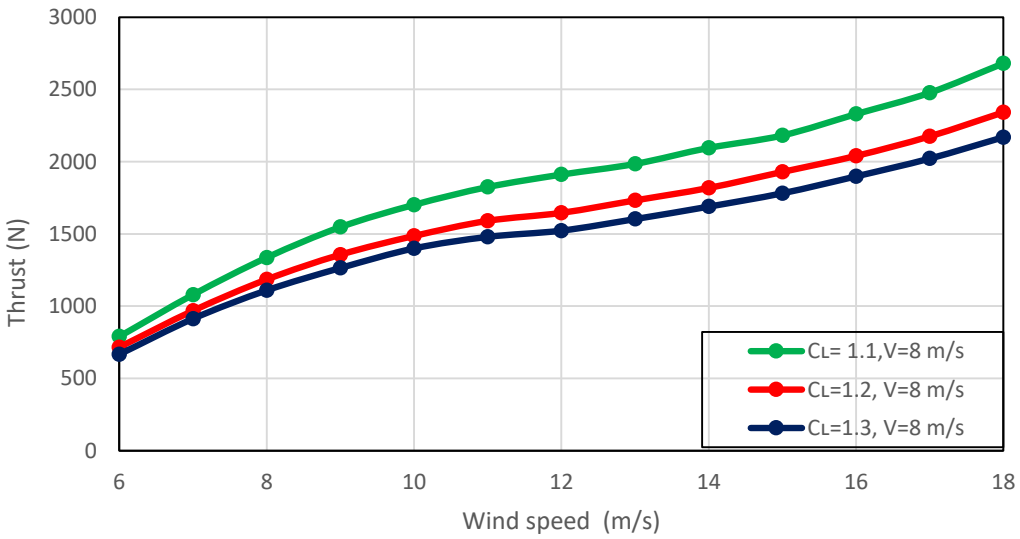

Figure 6.7: Wind speed comparison on three blades of thrust turbine for site design with different Cʟ 1.1, 1.2 & 1.3

6.4 Wind Energy Cost Analysis

The wind turbine of [P10-20 kW] generates electricity was selected to conduct as a model for calculating the cost of rated power generated from designed turbines, which was mentioned in changing the last design of chord, and fixed twist angle with three types of design (C_L= 1.1,1.2 and 1.3). To calculate the cost of energy that is related to Misrata city by characteristics shape, scale parameters, and capacity factor (parameters of K and C at 30 m height) per kWh. The cost can be obtained by expressing the formula (3.11). Table (6.5) shows the characteristics of the selected wind turbine; it is close to the designed turbines in terms of diameter, height, and rated power. The tables (6.7), (6.8), and (6.9) show the power, energy, and cost per Kw, when related, the rated power for each design with parameters (K, C and C_f) of Misrata city between 2012 to 2016 showed in Table (6.6). Therefore, the best cost result was recorded with the design C_L1.1 in 2013; also, the maximum rated power and maximum capacity factor recorded in the same year. Figure (6.8) shows compared between costs which had got form three types of design at period 2012 to 2016 with three types of design C_L (1.1, 1.2 and 1.3) that applied P10-20 kW so we observed minimum cost recorded with design C_L1.1 in 2013 by 0.038 $ it was better than from other years.

Table 6.5: Characteristics of the selected wind turbine

Characteristics	P10-20 kW
Diameter (m)	10
Cut- in Wind Speed (m/s)	2.5
Rated Wind Speed (m/s)	10
Cut off Wind Speed (m/s)	25

Table 6.6: Characteristics of the shape, scale parameters and capacity factor selected the city of Misrata at height 30 meters

Year	2012	2013	2014	2015	2016
K	3.8	3.7	3.8	3.5	3.7
C	8.8	9.2	9	9	8.7
Capacity Factor (%)	0.49	0.54	0.52	0.53	0.48

Table 6.7: Mean annual of power (kW/year) and annual out of energy (kWh/year) for Cʟ 1.1 with rated power 16.5 Kw

Year	2012	2013	2014	2015	2016
Power kW/y	8	8.9	8.6	8.7	7.9
Energy (kWh/y)	70080	77964	75336	76212	69204
Cost ($/kW)	0.042	0.038	0.039	0.0389	0.043

Table 6.8: Mean annual of power (kW/year) and annual out of energy (kWh/year) for Cʟ 1.2 with rated power 14.6 Kw

Year	2012	2013	2014	2015	2016
Power (kW/y)	7.2	7.9	7.6	7.7	7
Energy (kWh/y)	62669	69063	66505	67784	61390
Cost ($/kW)	0.047	0.043	0.045	0.044	0.048

Table 6.9: Mean annual of power (kW/year) and annual out of energy (kWh/year) for Cʟ with rated power 13.6kW

YEAR	2012	2013	2014	2015	2016
Power (kW/y)	6.7	7.3	7	7.2	6.5
Energy (kWh/y)	58376	64333	61950	63142	57185
Cost ($/kW)	0.051	0.046	0.048	0.047	0.052

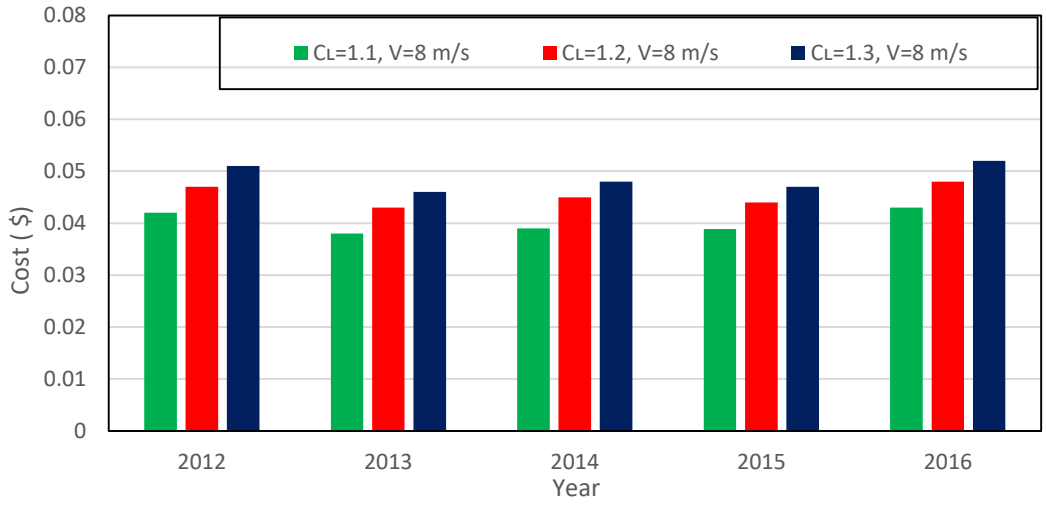

Figure 6.8: Comparison of costs at year period 2012 to 2016 with CL 1.1, 1.2 & 1.3 using P10-20 kW

6.5 Design by Changing Twist Angle for Three Blades Wind Turbine

Many changes were conducted on the main design of three blades experimental S809 shown in (table 5.4 NERL VI S809 geometric) by varying range of twist angle between (-4 & +4 degrees) with a fixed chord to obtain a better value of power at mean wind speed 8 m/s. The best result was observed with increasing (-1, -2, and -4 degrees) of all span of the blade. Table (6.10) show the values of total power, thrust, and power coefficient after changing the range of twist angle for three blades experimental S809. In fact, that observed the maximum total power, which recorded at mean wind speed 8m/s is equal 10.06 kW, total thrust is equal 2110 N, and total power coefficient is also equal 0.47 with increasing twist angle -2 degrees on all the span of the blade is better when compared with other design at the same mean wind speed. Figures (6.9), (6.10) and (6.11) show the respective relationship between wind speed and power, wind speed and thrust, wind speed, and power coefficient; it is observed that the maximum rated power recorded 18.3 kW with increasing twist

angle -1 degree on all of the spans of the blade. There is increasing for a baseline of thrust with twist angle -4 degrees when compared with other designs and fall slightly between wind speed 11 m/s to 14 m/s because it happened the stall. Also, there is a decrease for the baseline of power coefficient with twist angle -1 degree at lower speeds compared to other designs [54].

Table 6.10: Parameters after changing range of twist angle for three blades experimental S809

Twist Angle With Increasing	-1 (deg)	-2 (deg)	-4 (deg)
Total Power (kW)	9.97	10.06	10.01
Total Thrust (N)	2007	2110	2274
Total Power Coefficient (Cp)	0.462	0.47	0.467

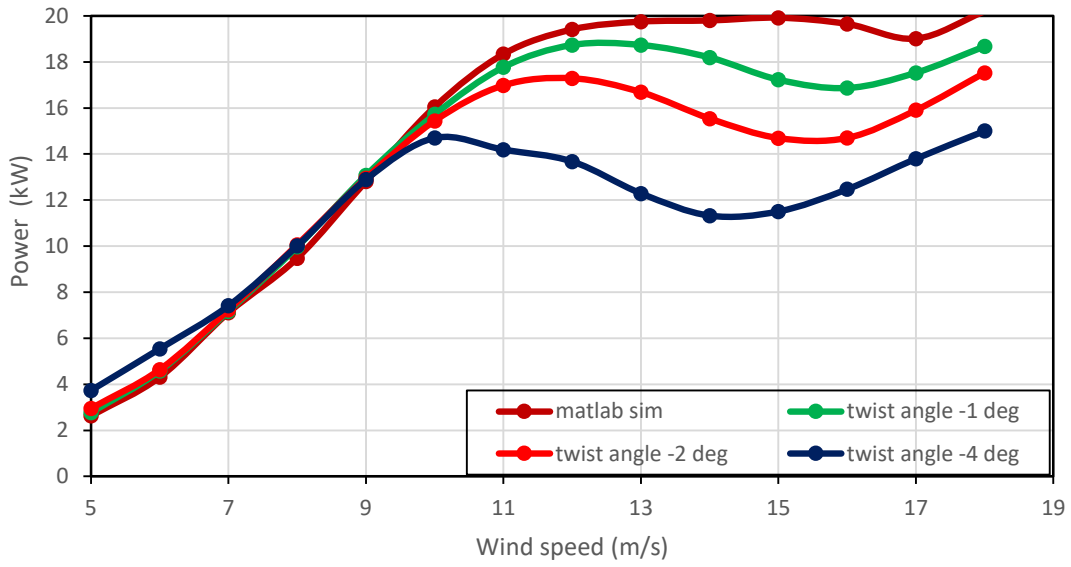

Figure 6.9: Comparison of power with a varying twist angle

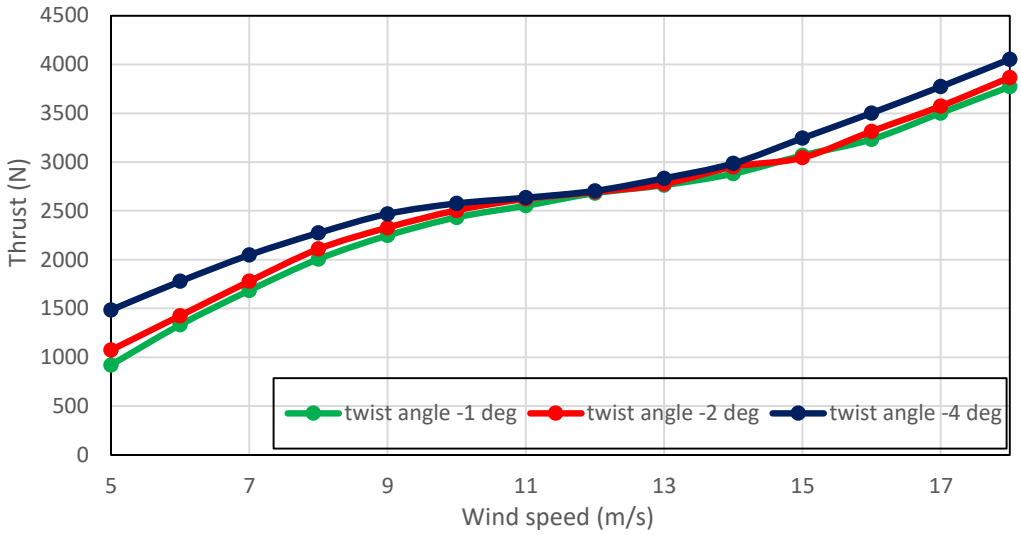

Figure 6.10: Comparison of thrust with a varying twist angle

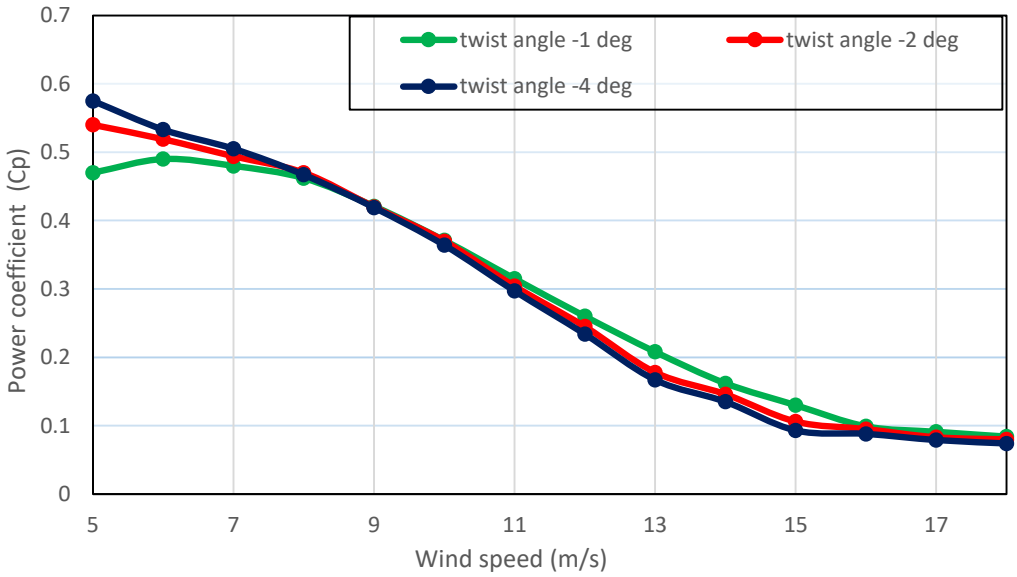

Figure 6.11: Comparison of power coefficient with a varying twist angle

6.6 Design by Changing Twist Angle for Two Blades Wind Turbine

Many changes were conducted on the main design two blades experimental S809 (table 5.3 NERL VI S809 geometric) by changing range of twist angle between (-4 & +4 degrees) with a fixed chord to obtain a better value of power at mean wind speed at 8 m/s. which we observed the best result with increasing the twist angle +2, -2, and -4 degrees of all span of blade Table (6.11) shows the values of total power, thrust, and power coefficient after changing range of twist angle for two blades experimental S809. In fact, that was observed the maximum power recorded at mean wind speed 8 m/s is equal 7.804 kW, thrust is equal 1373 N, and power coefficient is equal 0.31 with increasing twist angle +2 degrees on all the span of the blade are better with compared with other design at the same mean wind speed. Figures (6.12), (6.13) and (6.14) show respectively relationship between wind speed and power, wind speed and thrust, wind speed and power coefficient; it was observed that the maximum rated power recorded 13 kW with increasing twist angle (+2 degrees); however, we did not observe that there is an enhance in power at mean wind speed 8 m/s when it compared with the experiment S809 was equal 8.3 kW. But, we observed that there was an enhanced of rated power. There is an increase in the baseline of thrust with twist angle -4 degrees when compared with other designs and fall slightly between wind speed 11 m/s to 14 m/s because happened the stall. Also, there is a decrease in the baseline of power coefficient twist angle +2 degrees at lower speeds compared to other designs [54].

Table 6.11: Parameters after changing range of twist angle for blades S809 experimental

Twist Angle Increasing	+2 (deg)	-2 (deg)	-4 (deg)
Total Power (kW)	7.804	7.775	7.334
Total Thrust (N)	1373	1583	1644
Total Power Coefficient (Cp)	0.31	0.3095	0.2945

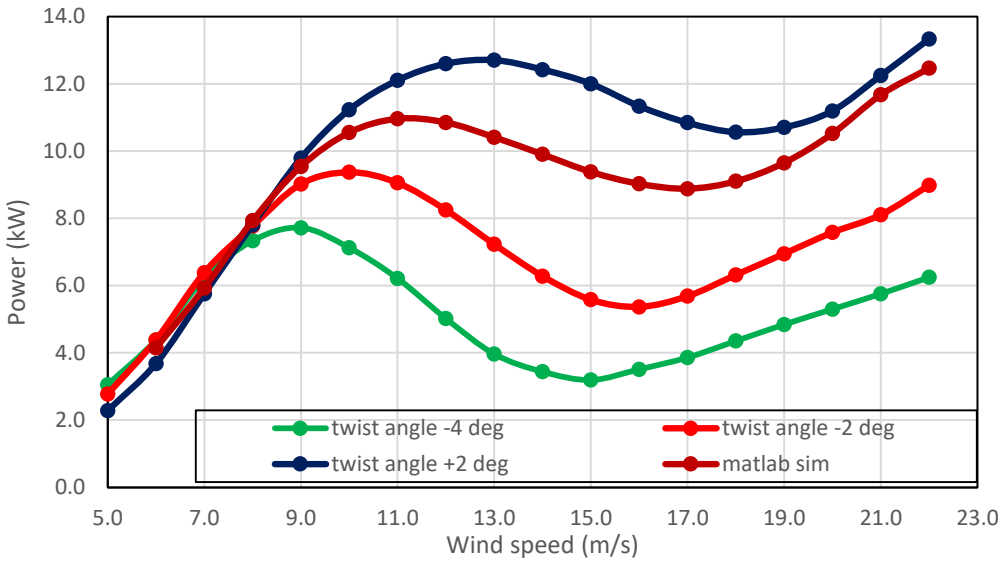

Figure 6.12: Comparison of power with a varying twist angle

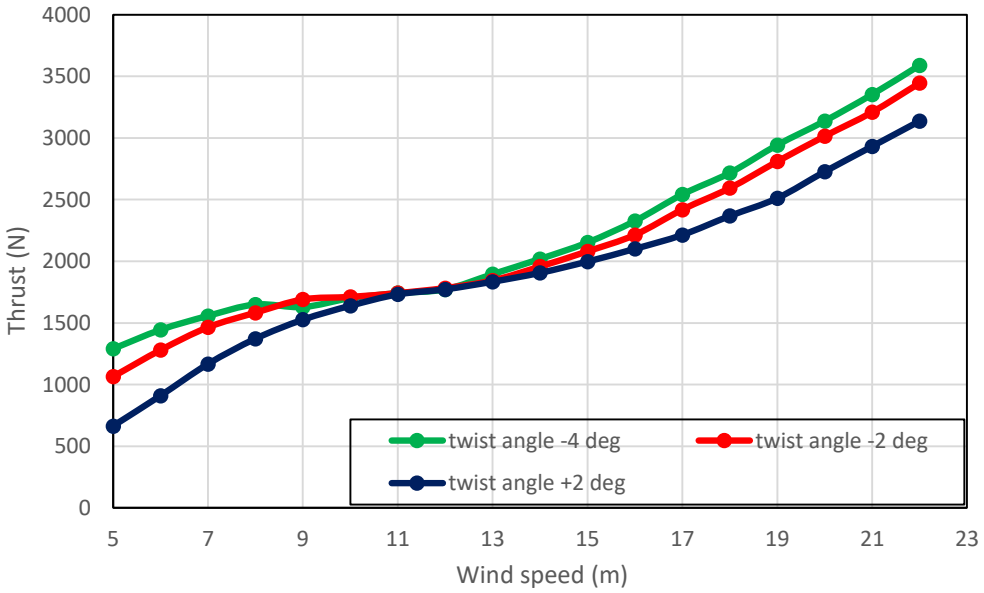

Figure 6.13: Comparison of thrust with a varying twist angle

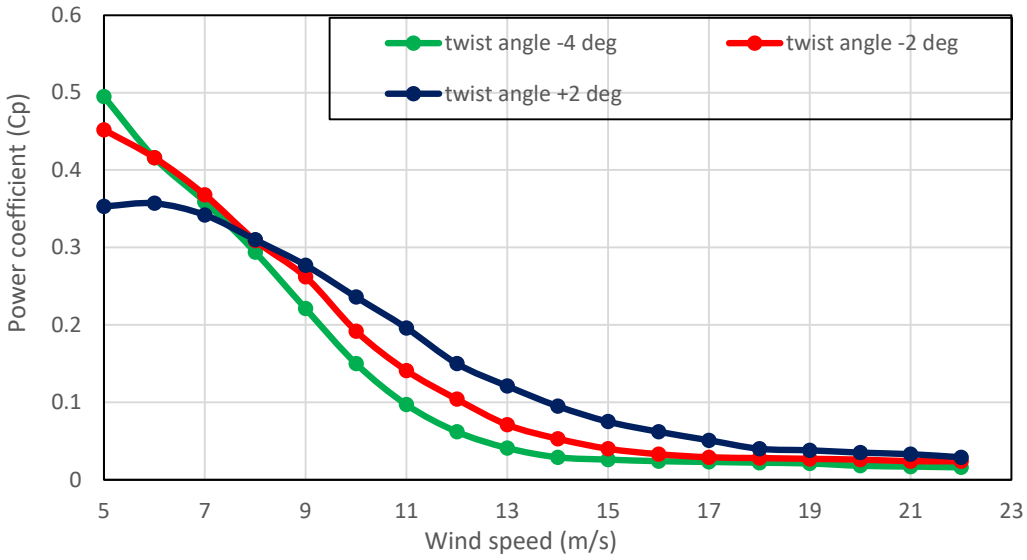

Figure 6.14: Comparison of power coefficient with a varying twist angle

6.7 Design by Changing the Tip Speed Ratio (TSR) of Three Blades of a Wind Turbine

BEM theory applied to design of blade with (fixed chord and change twist angle) changing for three types of twist angle A, B, and C with an angle of attack equal (αd) 6.25 degrees, wind speed equal 8 m/s agree with mean of wind speed of Misrata city, location, Reynolds number is equal $1x10^6$, TSR is equal respectively 7, 8 and 10 by using the NERL VI of three blades experimental S809 and choosing five sections of the chord as a reference to obtain optimal power resulting at mean wind speed equal 8 m/s. Table (6.12) shows the geometric of three blades experimental S809 with changing twist angle and fixed chord for three types of design (A, B, and C), the twist angle, changing between values 15.335 degrees to -2.446 degrees. Table (6.13) shows the results of values for total power, thrust, and power coefficient after changing the range of twist angle for three blades experimental S809[67]. The optimal power recorded with design B at mean wind speed 8 m/s is equal 10.2 kW

and the power coefficient is equal 0.476 there is an enhance when it is compared with the NERL VI data. Figures (6.15), (6.16) and (6.17) show Respectively the maximum rated power recorded with design A which is equal 21.5 kW; it is better than the rated power of experimental, and aother designs (B &C), the thrust is increasing for the baseline design C and fall slightly between 11m/s to 13 m/s as a result happened the stall and we have acquired lower value of power coefficient from design A at lower speeds than other designs. Tables (6.14),(6.15) and (6.16) show respectively mean annual of power (kW/year), annual out of energy (kWh/year) and cost of energy for three types designs (A, B and C) with rated power (21.5 Kw, 20.5 Kw and 18 kW). The maximum power was equal 11.61 kW/y and energy equal 101703.6 kW.h/y with minimum cost 0.029 $ that recorded in 2013 when it is related with parameters (C, K, and Cf) of Misrata location from the period (2012 to 2016) that recorded with design (A). Table 6.17 shows mean annual of power (kW/year), annual out of energy kWh/year) experimental S809 and cost with rated power 19.8 kW when it compared these results with results that got from design A, B, and C. It has been observed an enhance in design A. Figure (6.18) shows compared between the costs for three types of designs (A, B and C) period 2012 -2016 and cost that results from experimental S809. When related to parameters (C, K, and C_f) of Misrata location it was observed that the maximum cost recorded with design C equals 0.39 $ in 2016.

Table 6.12: Geometric of S809 experimental three blades parameters with varying twist angle and fixed chord

Radius (m)	Chord (m)	Twist Angle (deg) (A)	Twist Angle (deg) (B)	Twist Angle (deg) (C)
1.1335	0.544	15.335	13.11	9.707
2.257	0.636	5.521	4.13	2.124
3.172	0.543	2.258	1.29	- 0.243
4.023	0.457	0.5	- 0.321	- 1.499
5.029	0.358	- 0.829	- 1.5	- 2.446

Table 6.13: Parameters after a varying range of twist angle for three blades S809 experimental

Parameters	Experimental NERLVI S809	Design A	Design B	Design C
Total Power (kW)	9.63	9.972	10.2	10.12
Total Thrust (N)	1750.4	1875	1973	2089
Total Power Coefficient (Cp)	0.45	0.465	0.476	0.472

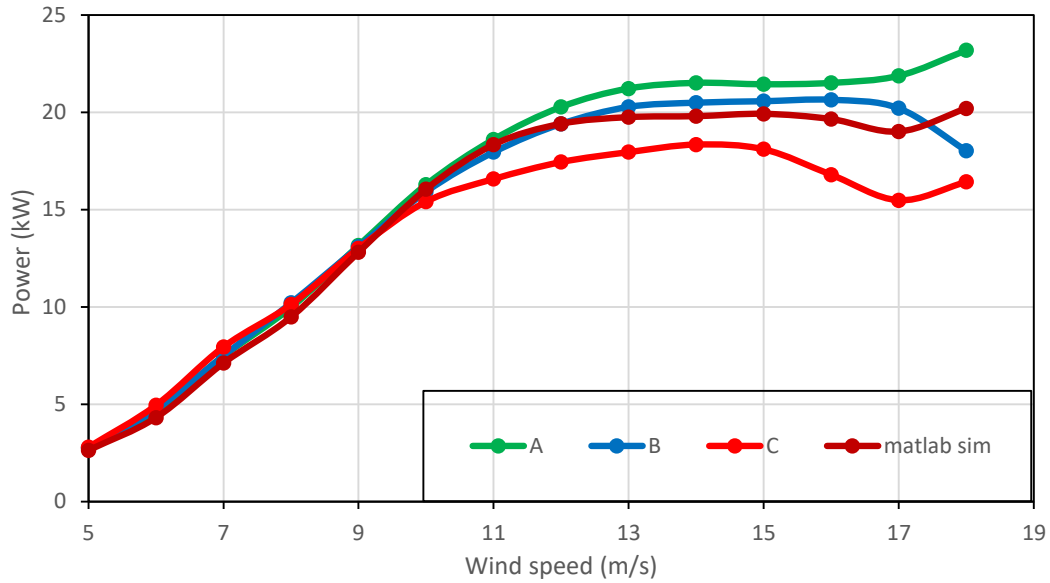

Figure 6.15: Comparison of power with a varying twist angle of design A, B, C and baseline of NERL S809

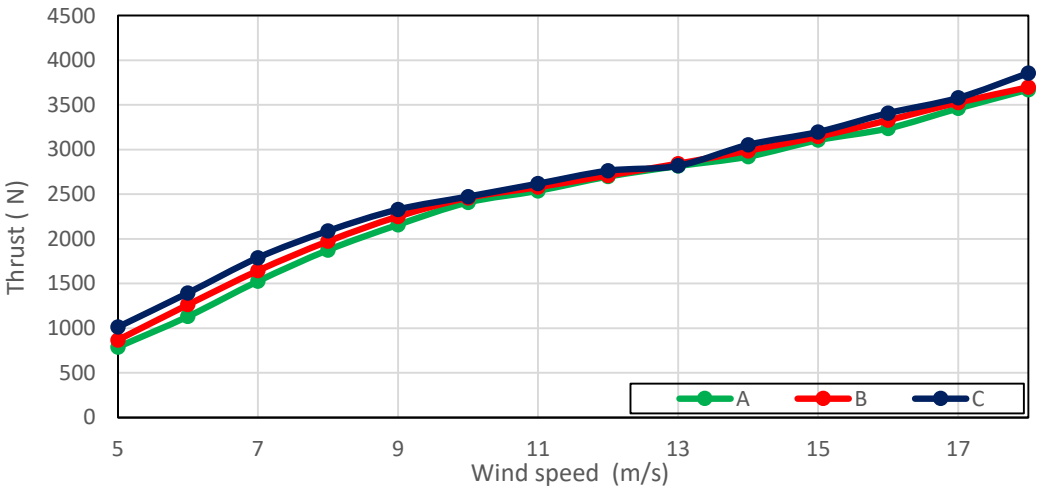

Figure 6.16: Comparison of thrust with a varying twist angle of design A, B, C and baseline of NERL S 809

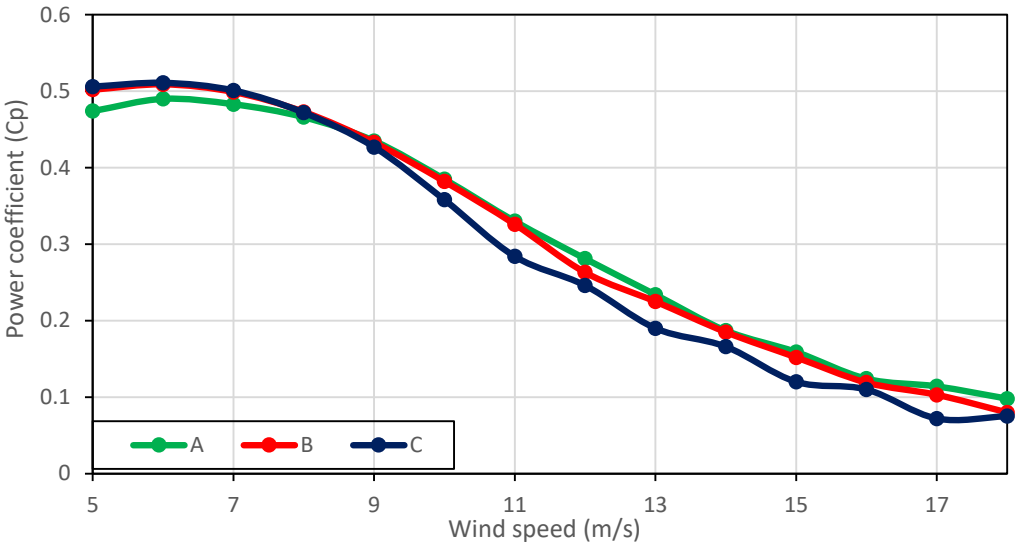

Figure 6.17: Comparison of power coefficient with a varying twist angle of design A, B, C and baseline of NERL S 809

6.8 Cost Analysis

Table 6.14: Mean annual of power (kW/year) and annual out of energy (kWh/year) for design A with rated power 21.5 kW

Year	2012	2013	2014	2015	2016
Power (kW/y)	10.535	11.61	11.18	11.395	10.32
Energy (kWh/y)	92286.6	101703.6	97936.8	99820.2	90403.2
Cost ($/kW)	0.032	0.029	0.030	0.029	0.032

Table 6.15: Mean annual of power (kW/year) and annual out of energy (kWh/year) for design B with rated power 20.5 kW

Year	2012	2013	2014	2015	2016
Power (kW/y)	10.45	11.07	10.66	10.865	9.84
Energy KWh/y)	87994.2	96973.2	93381.6	95177.4	75686.4
Cost ($/kW)	0.033	0.030	0.031	0.031	0.034

Table 6.16: Mean annual of power (kW/year) and annual out of energy (kWh/year) for design C with rated power 18 Kw

Year	2012	2013	2014	2015	2016
Power (kW/y)	8.82	9.72	9.36	9.54	8.46
Energy (kWh/y)	77263.2	851472	81993.6	83570.7	75686.4
Cost ($/kW)	0.038	0.034	0.036	0.0355	0.039

Table 6.17: Mean annual of power (kW/year) and annual out of energy (kWh/year) for experimental S809 with rated power 19.8 kW

Year	2012	2013	2014	2015	2016
Power (kW/y)	9.702	10.692	10.296	10.494	9.504
Energy kWh/y)	84989.5	93661.9	90192.9	91927.4	83255.04
Cost ($/kW)	0.035	0.032	0.033	0.032	0.036

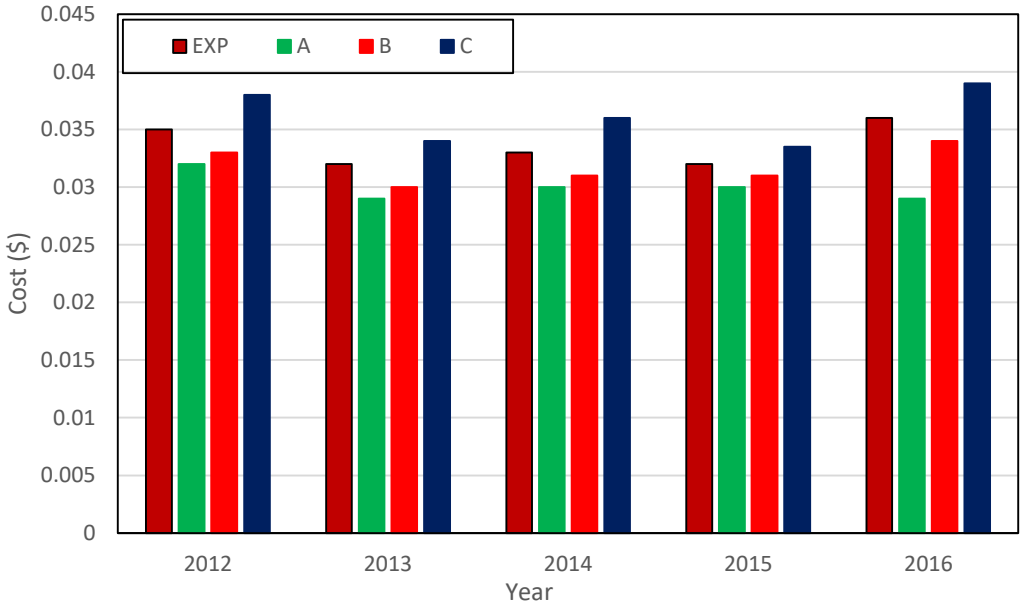

Figure 6.18: Comparison of costs at year period 2012 to 2016 with designs A, B , C, and EXP S809 using P10-20 kW

CHAPTER 7

SUMMARY AND CONCLUSION

In this study wind speed assessment, economic and of several axis wind turbines related to parameters location were performed. In conclusion, the Weibull distribution was used in the method of energy pattern factor (EPF), which was a good technique to performed in wind speed analysis from wind speed data obtained it from Misrata city for five years from 2012 to 2016. In addition, the results shown a good location for generating energy from wind. It was found addition of the annual energy values for the cost, got a high of 30 m using the turbine type P15-50, was better than the turbine type V27- 225. The average annual energy obtained through the use V39-500 at altitude of 50 m, it was considered to be the best comparison to turbines V 27-225 and P 15-50.

The design and simulation of HAWT by, Q Blade software was easy and practical which conducted compared to other simulation methods it has been several blade profiles such as NACA profile, additionally was easy to the obtained values of lift coefficient and drag coefficient against the angle of attack according to Reynolds number.

BEM code for HAWT was including three important corrections: tip loss Correction, Glauert Correction and Bhul Correction. These corrections were used to avoid the losses that effect of performance parameters for blade turbine. The code was validated by the results obtained from the Matlab code power curve simulation against data of NREL S809 phase-VI.

Results from the design of three blades axis wind turbine shown that fixed twist angle and change the chord with a lift coefficient 1.1, the power was an extract better

when compared with lift coefficients 1.2&1.3. In addition, the minimum cost obtained from the same design when related with the location. The second design was performed on the three blades NERL VI S809 with different twist angle and fixed chord. The results shown an improvement in the power extracted and power coefficient at mean wind speed of location especially when compared with NERL VI at the same wind speed.

The third designing was using the NERL VI two-blades when the twist angle has been changed by proper twist angle, observed the power curve improvement at high wind speeds especially when the twist angle was changed by an appropriate value. The forth designing shows the maximum power extracted obtained from design three blades with proper TSR which lead to the improvement in performance, Possibility leads to an important rise in the generation power turbine and power coefficient specially at mean wind speed location also showed that minimum value of cost per kilowatt-hour related with location parameters.

Hence, the BEM theory with modification factors, it was ideal for HAWT code design. In addition, to estimated blade performance and a good comparison was made between blade aerodynamic forces simulation. The designing for wind turbines can be analyzed using other theories such as the CFD method data including for different Reynolds numbers, moreover many airfoils can be added to the database.The studies must be conducted in other regions in Libya using other methods and increase the interest in alternative energy, specializations created colleges and training centers.

REFERENCES

[1] A. Khalil, A. Khalil, and A. Asheibi, “The chances and challenges for renewable energy in Libya the chances and challenges for renewable energy in Libya,” 4th International Conference on Renewable Energy Research and Applications, Palermo, Italy, 22-25 Nov 2015.

[2] M. M. A. Ahmed and M. M. A. Ahmed, “Future prospects of the krg,” Iraqi Kurds and Nation-Building,”January,pp.195–211, 2012, doi: 10.1057/9781137034083_12.

[3] R. A. Felseghi, E. Carcadea, M. S. Raboaca, C. N. Trufin, and C. Filote, “Hydrogen fuel cell technology for the sustainable future of stationary applications,” Energies, vol. 12, no. 23, 2019, doi: 10.3390/en12234593.

[4] A. Mostafaeipour, M. Jadidi, K. Mohammadi, and A. Sedaghat, “An analysis of wind energy potential and economic evaluation in Zahedan, Iran,” Renew. Sustain.Energy Rev.,vol.30,pp.641–50,2014,doi:10.1016/j.rser.2013.11.016.

[5] R. D. Prasad, R. C. Bansal, and M. Sauturaga, “Wind energy analysis for vadravadra site in Fiji Islands: a case study,” IEEE Trans. Energy Convers., vol. 24, no. 3, pp. 750–757, 2009, doi: 10.1109/TEC.2009.2025326.

[6] A. M. A. Mohamed, A. Al-Habaibeh, and H. Abdo, “An investigation into the current utilisation and prospective of renewable energy resources and technologies in Libya,” Renew Energy, vol. 50, pp. 732–740, 2013, doi: 10.1016/j.renene.2012.07.038.

[7] H. Salah, A. Embirsh, and E. Yousuf, “Future prospects of the wind energy in libya,” International Journal of Scientific and Research Publications, vol. 7, no. 10, pp. 163–164, 2017.

[8] A. Khalil, Z. Al Faituri, and A. Asheibi,“The economic feasibility of

photovoltaic systems for electricity production in libya," 7th Int. Renew. Energy Congr. IREC'2016, February, 2016.

[9] W. El-Osta, M. Belhag, M. Klat, I. Fallah, and Y. Kalifa, "Wind farm pilot project in Libya," Renew. Energy, vol. 6, no. 5–6, pp. 639–642, 1995, doi: 10.1016/0960-1481(95)00061-N.

[10] M. M. A. Ahmed, "Iraqi Kurds and nation-building," Iraqi kurds and nation-building, pp. 1–274, 2016, doi: 10.1057/9781137034083.

[11] A. Asheibi and A. Khalil, "The renewable energy in libya: present difficulties and remedies," World Congr. Renew. Energy, September, 2013.

[12] M. Salem Elmnefi and A. M. Bofares, "An analysis of wind speed distribution at Benina, Benghazi, Libya," Appl. Mech. Mater., vol. 492, pp. 550–555, 2014, doi: 10.4028/www.scientific.net/AMM.492.550.

[13] M. Ali Elfarra and S. Silini, "Analysis of wind power generation in four sites using different weibull parameters," Int. J. Renew. Energy Res., vol. 8, no. 3, 2018.

[14] O. Kaplan and M. Temiz, "The analysis of wind speed potential and energy density in Ankara," Conf. Renew. Energy Res. Appl., pp. 919–923,2016

[15] S. Basile, R. Burlon, and F. Morales, "Joint probability distributions for wind speed and direction. A case study in Sicily," 2015 Int. Conf. Renew. Energy Res. Appl. Icrera 2015,vol. 5, pp. 1591–1596, 2015, doi: 10.1109/ICRERA.2015.7418675.

[16] O. Charrouf, A. Betka, A. Taleb-Ahmad, and G. Amar, "Wind energy potential and economic analysis of wecs in four selected locations in Algeria," 5th Int. Conf. Renew. Energy Res. Appl., pp. 118–123, 2016

[17] A. Hossieni, V. Rasouli, and S. Rasouli, "Wind energy potential assessment in order to produce electrical energy for case study in Divandareh, Iran," 3rd

Int. Conf. Renew. Energy Res. Appl. Icrera 2014, pp. 133–137, 2014, doi: 10.1109/ICRERA.2014.7016544.

[18] P. K. Chaurasiya, V. Warudkar, and S. Ahmed, “Wind energy development and policy in India: a review,” Energy Strateg. Rev., vol. 24, no. November 2016, pp. 342–357, 2019, doi: 10.1016/j.esr.2019.04.010.

[19] S. Madhu and S. Payal, “A review of wind energy scenario in India,” Int. Res. J. Environ. Scie., vol. 3, no. 4, pp. 87–92, 2014.

[20] R. Bharvirkar and A. Phadke, “Reassessing wind potential estimates for India : economic and policy implications,” Environmental Energy Technologies Division, July, 2011.

[21] H. M. Naser, O. Nagata, S. Sultana, and R. Hatano, “Carbon sequestration and contribution of CO2, CH4 and N2O fluxes to global warming potential from paddy-fallow fields on mineral soil beneath peat in Central Hokkaido, Japan,”Agric., vol. 10, no. 1, pp. 1–18, 2020, doi: 10.3390/agriculture10010006.

[22] A. M. Bofares and M. S. Elmnefi, “Design and performance of horizontal axis wind turbine using blade element momentum theory (BEMT),” Appl. Mech.Mater.,vol.492,pp.10612,2014,doi:10.4028/www.scientific.net/AMM.492.106.

[23] S. Liu and I. Janajreh, “Development and application of an improved blade element momentum method model on horizontal axis wind turbines,” Int. J. Energy Environ. Eng., vol. 3, no. 1, pp. 1–10, 2012, doi: 10.1186/2251-6832-3-30.

[24] C. J. Bai, F. B. Hsiao, M. H. Li, G. Y. Huang, and Y. J. Chen, “Design of 10 kW horizontal-axis wind turbine (HAWT) blade and aerodynamic investigation using numerical simulation,” Procedia Eng., vol. 67, pp. 279–287, 2013, doi: 10.1016/j.proeng.2013.12.027.

[25] S. Allsop, C. Peyrard, P. R. Thies, E. Boulougouris, and G. P. Harrison, “Hydrodynamic analysis of a ducted, open centre tidal stream turbine using blade element momentum theory,” Ocean Eng., vol. 141, no. June, pp. 531–542, 2017, doi: 10.1016/j.oceaneng.2017.06.040.

[26] I. Journal, F. Technological, P. R. Mishra, and B. Patel, “Design and simulation of horizontal axis wind,” International Journal For Technological Research In Engineering, vol. 2, no. 9, pp. 2033–2036, 2015.

[27] N. Tenguria, N. Mittal, and S. Ahmed, “Investigation of blade performance of horizontal axis wind turbine based on blade element momentum theory (BEMT) using NACA airfoils,” Int. J. Eng. Sci. Technol., vol. 2, no. 12, pp. 25–35, 2011, doi: 10.4314/ijest.v2i12.64565.

[28] G. Corbetta, “Wind energy scenarios for 2030,” Ewea, no. July, pp. 1–8, 2015.

[29] A. Duffy and B. Cleary, “Wind energy development in the Ireland.,” IEA Wind Task 26 - Wind Technol. Cost, Perform. Trends Denmark, Ger. Ireland, Norway, Eur. Union, United States 2007–2012. NREL/TP-6A20-64332, pp. 75–100, 2015.

[30] L. Söder et al., “Review of wind generation within adequacy calculations and capacity markets for different power systems,” Renew. Sustain. Energy Rev., vol. 119, no. November 2019, 2020, doi: 10.1016/j.rser.2019.109540.

[31] M. Borg and M. Collu, “A comparison between the dynamics of horizontal and vertical axis offshore floating wind turbines,” Philos. Trans. R. Soc. A Math. Phys. Eng. Sci., vol. 373, no. 2035, 2015, doi: 10.1098/rsta.2014.0076.

[32] R. Clare and I. D. Mays, “Development of vertical axis wind turbine,” Proc. Inst. Civ. Eng. (London). Part 1 - Des. Constr., vol. 86, no. January, pp. 857–878, 1989, doi: 10.1680/iicep.1989.3160.

[33] L. Deisadze, D. Digeser, C. Dunn, and D. Shoikat, “Vertical axis wind

turbine evaluation and design," Engineering, vol. 1, no. April, pp. 1–81, 2013.

[34] G. Abdalrahman, W. Melek, and F. S. Lien, "Pitch angle control for a small-scale Darrieus vertical axis wind turbine with straight blades (H-Type VAWT),"Renew.Energy,vol.114,pp.1353–1362,2017,doi: 10.1016/j.renene.2017.07.068.

[35] A. H. Algifri, "Wind energy potential in Aden-Yemen," Renew. Energy, vol. 13, no. 2, pp. 255–260, 1998, doi: 10.1016/S0960-1481(97)00069-4.

[36] A. K. Azad, M. G. Rasul, M. M. Alam, S. M. Ameer Uddin, and S. K. Mondal, "Analysis of wind energy conversion system using Weibull distribution,"ProcediaEng.,vol.90,pp.725–732,2014,doi: 10.1016/j.proeng.2014.11.803.

[37] D. Kidmo Kaoga, S. Doka Yamigno, D. Raidandi, and N. Djongyang, "Performance analysis of Weibull methods for estimation of wind speed distributions in the adamaoua region of Cameroon," Int. J. Basic Appl. Sci., vol. 3, no. 3, pp. 298–306, 2014, doi: 10.14419/ijbas.v3i3.3081.

[38] E. DOKUR and M. KURBAN, "Wind speed potential analysis based on Weibull distribution," Balk. J. Electr. Comput. Eng., vol. 3, no. 4, pp. 231–235, 2015, doi: 10.17694/bajece.72748.

[39] H. O. Aboh, P. M. Gyuk, and M. K. O. Onwumere, "The use of energy pattern factor (EPF) in estimating wind power density," Sci. World J.,vol. 11, no. 3, pp. 27–30, 2016.

[40] M. Sessarego and D. Wood, "Multi-dimensional optimization of small wind turbine blades,"Renewables Wind.Water,Sol.,vol.2,no.1, 2015, doi: 10.1186/s40807-015-0009-x.

[41] C. Y. Joukovski,"Parametric airfoil catalog, part i an aerodynamic and geometric comparison between parametrized and point cloud airfoils" Tomas

Melin. 2013.

[42] S. Gaddada and S. P. K. Kodicherla, “Wind energy potential and cost estimation of wind energy conversion systems (WECSs) for electricity generation in the eight selected locations of Tigray region (Ethiopia),” Renewables Wind. Water, Sol., vol. 3, no. 1, 2016, doi: 10.1186/s40807-016-0030-8.

[43] Vaisala, “User’s guide tacmet weather station MAWS201M,” p. 174, 2006.

[44] Emadwiandr, J. Chem. Inf. Model. “Electrical power systems track ,” Erasmus Wind Energy, vol. 53, no. 9, pp. 1689–1699, 2013, doi: 10.1017/CBO9781107415324.004.

[45] S. Rehman, M. Mahbub Alam, L. M. Alhems, and M. Mujahid Rafique, “Horizontal axiswind turbine blade design methodologies for efficiency enhancement a review,” Energies,vol. 11, no. 3, 2018, doi: 10.3390/en11030506.

[46] S. O. Oyedepo, M. S. Adaramola, and S. S. Paul, “Analysis of wind speed data and wind energy potential in three selected locations in South-East Nigeria,” Int. J. Energy Environ. Eng., vol. 3, no. 1, pp. 1–11, 2012, doi: 10.1186/2251-6832-3-7.

[47] K. Kara, M. E. Gunduz, J. W. Kim, and L. N. Sankar, “Effects of circulation control on power production for large scale wind turbines,” 51st AIAA Aerosp. Sci. Meet. Incl. New Horizons Forum Aerosp. Expo. 2013, no. January, 2013, doi: 10.2514/6.2013-1105.

[48] M. M. Moh Saad, N. Asmuin, and M. Ó. Óskarsdóttir, “Ageneral description and comparison of horizontal axis wind turbines and vertical axis wind turbines,” IOSR J. Eng. www.iosrjen.org ISSN, vol. 04, no. 08, pp. 2250–3021, 2014.

[49] E. A. Efkirn, T. M. Lazim, W. Z. W. Omar, N. A. R. N. Mohd, and M. M.

Takeyeldein, “Aerodynamic analysis of horizontal axis wind turbine using blade element momentum theory for low wind speed conditions,” vol. 2, pp. 12–16, 2015.

[50] A. S. L. Frank P. Incroper, David P. Dewitt, Theodore L. Bergman, “Fundamentals of heat and mass transfer,” Incropera, Lavine, DeWitt - 2011

[51] A. Tahir, M. Elgabaili, Z. Rajab, N. Buaossa, A. Khalil, and F. Mohamed, “Optimization of small wind turbine blades using improved blade element momentum theory,” Wind Eng., vol. 43, no. 3, pp. 299–310, 2019, doi: 10.1177/0309524X18791395.

[52] P. J. Schubel and R. J. Crossley, “Wind turbine blade design,” Energies, vol. 5, no. 9, pp. 3425–3449, 2012, doi: 10.3390/en5093425.

[53] G. Ingram, “Wind turbine blade analysis using the blade element momentum method.,” October, vol. 1.1, no. c, pp. 1–21, 2011.

[54] W. Wisnoe, W. Kuntjoro, F. Mohamad, R. E. Mohd Nasir, N. F. Reduan, and Z. Ali, “Experimental results analysis for UITM BWB baseline-I and baseline-II UAV running at 0.1 mach number,” Int. J. Mech., vol. 4, no. 2, pp. 23–32, 2010.

[55] S. Ehrich, C. M. Schwarz, H. Rahimi, B. Stoevesandt, and J. Peinke, “Comparison of the blade element momentum theory with computational fluid dynamics for wind turbine simulations in turbulent inflow,” Appl. Sci., vol. 8, no. 12, pp. 1–15, 2018, doi: 10.3390/app8122513.

[56] E. Branlard and M. Gaunaa, “Development of new tip-loss corrections based on vortex theory and vortex methods,” J. Phys. Conf. Ser., vol. 555, no. 1, 2014, doi: 10.1088/1742-6596/555/1/012012.

[57] W. Z. Shen, R. Mikkelsen, J. N. Sørensen, and C. Bak, “Tip loss corrections for wind turbine computations,” Wind Energy, vol. 8, no. 4, pp. 457–475, 2005, doi: 10.1002/we.153.

[58] J. R. P. Vaz, J. T. Pinho, and A. L. A. Mesquita, “An extension of BEM method applied to horizontal-axis wind turbine design,” Renew. Energy, vol. 36, no. 6, pp. 1734–1740, 2011, doi: 10.1016/j.renene.2010.11.018.

[59] J. T. Lee, H. G. Kim, Y. H. Kang, and J. Y. Kim, “Determining the optimized hub height of wind turbine using the wind resource map of South Korea,” Energies, vol. 12, no. 15, 2019, doi: 10.3390/en12152949.

[60] M. A. Miller, S. Duvvuri, W. D. Kelly, and M. Hultmark, “Rotor solidity effects on the performance of vertical-axis wind turbines at high Reynolds numbers,” J. Phys. Conf. Ser., vol. 1037, no. 5, 2018, doi: 10.1088/1742-6596/1037/5/052015.

[61] J. M. Jonkman, “Modeling of the UAE wind turbine for refinement of FAST _ AD modeling of the UAE,” Contract, no. December, 2003.

[62] Y. He and R. K. Agarwal, “Shape optimization of NREL S809 airfoil for wind turbine blades using a multi-objective genetic algorithm,” 32nd AIAA Appl. Aerodyn. Conf., vol. 2014, 2014, doi: 10.2514/6.2014-2845.

[63] H. Sogukpinar and I. Bozkurt, “Numerical calculation of aerodynamics wind turbine blade S809 airfoil and comparison of theoretical calculations with experimental measurements and confirming with NREL data,” AIP Conf. Proc., vol. 1935, 2018, doi: 10.1063/1.5025958.

[64] P. R. Mishra and Brijesh Patel, “Design and simulation of horizontal axis wind turbine using open source software Q-Blade,” Int. J. Technol. Res. Eng., vol. 2, no. 9, pp. 2033–2036, 2015.

[65] M. Alaskari, O. Abdullah, and M. H. Majeed, “Analysis of wind turbine using Qblade software,” IOP Conf. Ser. Mater. Sci. Eng., vol. 518, no. 3, 2019, doi: 10.1088/1757-899X/518/3/032020.

[66] V. R. Ponakala and G. A. Kumar, “Design and simulation of small wind turbine blades in Q-Blade,” International Journal of Engineering.,vol. 5, no.

4, pp. 1095–1103, 2017.

[67] M. Asli, B. Mashhadi Gholamali, and A. Mesgarpour Tousi, “Numerical analysis of wind turbine airfoil aerodynamic performance with leading edge bump,” Math. Probl. Eng., vol. 2015, 2015, doi: 10.1155/2015/493253.

APPENDIX A

A. Location and Wind Speed Data for Misrata City

Table A.1: Monthly wind speed m/s data at 10 meters height of misrata weather station

YEAR	1	2	3	4	5	6	7	8	9	10	11	12
2012	07.5	07.9	06.9	07.3	06.7	06.3	06.9	06.1	05.6	05.7	05.9	07.9
2013	07.4	08.2	08.9	07.6	08.6	07.8	06.0	06.1	06.1	05.6	05.8	05.8
2014	06.9	07.4	07.9	07.7	07.5	07.4	06.5	05.6	05.9	06.0	06.2	06.9
2015	08.2	08.8	09.3	07.6	08.1	07.1	05.1	05.5	06.5	05.9	05.5	04.8
2016	05.8	06.8	07.0	08.0	08.4	07.7	06.8	06.0	06.1	05.7	05.5	05.1

Figure A.1: Location of Misrata city [Wikipedia]

Table A.2: Probability of wind speed at 10 m period 2012/2016

V (m/s)	2012	2013	2014	2015	2016
0	0	0	0	0	0
1	0.1796162	0.176512	0.170803	0.288976	0.23639
2	1.2432948	1.14043	1.182649	1.620822	1.524333
3	3.7769069	3.335287	3.596938	4.337514	4.425474
4	7.9519429	6.879137	7.595743	8.325976	8.965525
5	13.14116	11.33085	12.6282	12.8333	14.25783
6	17.675373	15.52578	17.16485	16.47117	18.39532
7	19.350344	17.8296	19.10871	17.71308	19.22361
8	16.91228	16.99572	17.12325	15.82146	15.95224
9	11.432029	13.18077	11.99185	11.53397	10.18748
10	5.7373377	8.092908	6.316252	6.704632	4.812672
11	2.0371976	3.807122	2.390805	3.023417	1.606091
12	0.4846412	1.321963	0.617641	1.025632	0.359604
13	0.0727344	0.325146	0.102864	0.253122	0.051057
14	0.0064504	0.054171	0.01038	0.043852	0.004326
15	0.0003151	0.005827	0.000594	0.005135	0.000205
16	7.86E-06	0.000385	1.79E-05	0.000391	5.07E-06
18	4.73E-10	3.12E-07	1.76E-09	5.25E-07	3.29E-10
19	9.59E-13	3.41E-09	4.89E-12	8.49E-09	7.39E-13
20	7.05E-16	1.81E-11	5.15E-15	7.49E-11	6.34E-16
21	1.70E-19	4.41E-14	1.88E-18	3.44E-13	1.91E-19
22	1.22E-23	4.59E-17	2.17E-22	7.84E-16	1.85E-23
23	2.34E-28	1.90E-20	7.14E-27	8.42E-19	5.25E-28
24	1.08E-33	2.93E-24	6.04E-32	4.05E-22	3.95E-33
25	1.06E-39	1.56E-28	1.18E-37	8.31E-26	7.18E-39

Table A.3: Probability of wind speed at 30 m period 2012/2016

V (m/s)	2012	2013	2014	2015	2016
0	0	0	0	0	0
1	0.097867	0.100477	0.089859	0.159963	0.123548
2	0.679321	0.650781	0.6239	0.900632	0.799606
3	2.08648	1.921063	1.918326	2.441944	2.353731
4	4.516599	4.053443	4.163905	4.830043	4.932208
5	7.891971	6.980899	7.31554	7.872986	8.380225
6	11.70162	10.32474	10.95097	11.07977	12.1104
7	14.96244	13.36474	14.21719	13.70107	15.11702
8	16.48405	15.19105	16.02225	14.94066	16.28946
9	15.47451	15.07533	15.53269	14.30642	15.00032
10	12.15733	12.91039	12.75061	11.91939	11.61268
11	7.809778	9.390796	8.68061	8.532649	7.400742
12	3.991107	5.691448	4.781115	5.169861	3.787994
13	1.572907	2.811829	2.071124	2.606434	1.51454
14	0.461918	1.105291	0.683913	1.07324	0.458848
15	0.097385	0.336713	0.166392	0.353789	0.10193
16	0.014161	0.077284	0.028754	0.091408	0.01603
17	0.001361	0.012971	0.003394	0.018103	0.00172
18	8.26E-05	0.001542	0.000263	0.002685	0.000121
19	3.02E-06	0.000126	1.27E-05	0.000291	5.36E-06
20	6.33E-08	6.78E-06	3.71E-07	2.25E-05	1.43E-07
21	7.20E-10	2.33E-07	6.15E-09	1.21E-06	2.21E-09
22	4.22E-12	4.94E-09	5.55E-11	4.39E-08	1.87E-11
23	1.20E-14	6.19E-11	2.58E-13	1.05E-09	8.34E-14
24	1.57E-17	4.40E-13	5.87E-16	1.61E-11	1.86E-16
25	8.86E-21	1.71E-15	6.16E-19	1.53E-13	1.96E-19

Table A.4: Probability of wind speed at 50 m period 2012/2016

V (m/s)	2012	2013	2014	2015	2016
0	0	0	0	0	0
1	0.0472786	0.047717	0.044958	0.082599	0.06391
2	0.6565256	0.618364	0.6244	0.930527	0.827396
3	3.028085	2.742234	2.881611	3.79064	3.655879
4	8.7664693	7.744878	8.354668	10.03684	10.23509
5	19.28265	16.81174	18.42942	20.62333	21.8503
6	34.838016	30.32715	33.45359	35.41588	38.37003
7	53.669884	47.229	51.88673	52.75799	57.52209
8	72.138827	64.9236	70.33514	69.77953	75.42058
9	86.457666	80.20733	85.06121	83.58836	88.57898
10	94.939894	90.85628	94.14176	92.66915	95.94044
11	98.624113	96.67451	98.30194	97.39507	98.95262
12	99.743456	99.08705	99.65618	99.28908	99.81459
13	99.969229	99.8191	99.95424	99.85637	99.97879
14	99.997782	99.97533	99.99625	99.97932	99.99853
15	99.999911	99.9978	99.99982	99.99796	99.99994
16	99.999998	99.99988	100	99.99987	100
17	100	100	100	99.99999	100
18	100	100	100	100	100
19	100	100	100	100	100
20	100	100	100	100	100
21	100	100	100	100	100
22	100	100	100	100	100
23	100	100	100	100	100
24	100	100	100	100	100
25	100	100	100	100	100

Tbale A.5: Cumulative of wind speed at 10 m period 2013/1016

V (m/s)	2012	2013	2014	2015	2016
0	0	0	0	0	0
1	0.0472786	0.047717	0.044958	0.082599	0.06391
2	0.6565256	0.618364	0.6244	0.930527	0.827396
3	3.028085	2.742234	2.881611	3.79064	3.655879
4	8.7664693	7.744878	8.354668	10.03684	10.23509
5	19.28265	16.81174	18.42942	20.62333	21.8503
6	34.838016	30.32715	33.45359	35.41588	38.37003
7	53.669884	47.229	51.88673	52.75799	57.52209
8	72.138827	64.9236	70.33514	69.77953	75.42058
9	86.457666	80.20733	85.06121	83.58836	88.57898
10	94.939894	90.85628	94.14176	92.66915	95.94044
11	98.624113	96.67451	98.30194	97.39507	98.95262
12	99.743456	99.08705	99.65618	99.28908	99.81459
13	99.969229	99.8191	99.95424	99.85637	99.97879
14	99.997782	99.97533	99.99625	99.97932	99.99853
15	99.999911	99.9978	99.99982	99.99796	99.99994
16	99.999998	99.99988	100	99.99987	100
17	100	100	100	99.99999	100
18	100	100	100	100	100
19	100	100	100	100	100
20	100	100	100	100	100
21	100	100	100	100	100
22	100	100	100	100	100
23	100	100	100	100	100
24	100	100	100	100	100
25	100	100	100	100	100

Table A.6: Cumulative of wind speed at 30 m period 2012/201

(m/s)	2012	2013	2014	2015	2016
0	0	0	0	0	0
1	0.025758	0.02716	0.02365	0.045714	0.033397
2	0.35818	0.352395	0.32891	0.515981	0.433159
3	1.661095	1.570008	1.526174	2.115634	1.92712
4	4.875128	4.484177	4.48518	5.684785	5.485394
5	11.01433	9.945472	10.1603	11.99746	12.08638
6	20.8095	18.58882	19.28265	21.48849	22.34497
7	34.23747	30.49611	31.94229	33.96258	36.0676
8	50.15031	44.91186	47.22729	48.42664	51.96219
9	66.34973	60.22362	63.21206	63.21206	67.81412
10	80.31712	74.36977	77.51624	76.44762	81.25213
11	90.31745	85.58697	88.27835	86.71435	90.76292
12	96.12174	93.09368	94.93989	93.52401	96.262
13	98.77845	97.25112	98.24813	97.32718	98.79593
14	99.70849	99.11541	99.52991	99.08555	99.70136
15	99.94934	99.77632	99.90572	99.74631	99.94493
16	99.99385	99.95687	99.9864	99.94422	99.99272
17	99.9995	99.99385	99.99865	99.99051	99.99934
18	99.99997	99.99937	99.99991	99.99878	99.99996
19	100	99.99996	100	99.99988	100
20	100	100	100	99.99999	100
21	100	100	100	100	100
22	100	100	100	100	100
23	100	100	100	100	100
24	100	100	100	100	100
25	100	100	100	100	100

Table A.7: Cumulative of wind speed at 50 m period 2012/2016

V (m/s)	2012	2013	2014	2015	2016
0	0	0	0	0	0
1	0.0192579	0.020706	0.018507	0.033934	0.026095
2	0.2679057	0.268767	0.257468	0.383248	0.338601
3	1.244499	1.199172	1.196243	1.574676	1.508914
4	3.6676643	3.437153	3.527144	4.251277	4.312196
5	8.3546684	7.675602	8.042234	9.050384	9.574809
6	16.006566	14.51137	15.43308	16.4372	17.92966
7	26.900237	24.22032	26.00122	26.50853	29.49757
8	40.575635	36.52672	39.3568	38.8292	43.60878
9	55.704025	50.48155	54.27439	52.39643	58.75946
10	70.335143	64.57974	68.89502	65.81111	72.96441
11	82.54582	77.1618	81.31588	77.64781	84.44961
12	91.193004	86.96597	90.31745	86.88774	92.33061
13	96.286994	93.54254	95.77798	93.20173	96.83512
14	98.727928	97.27941	98.49182	96.93349	98.93523
15	99.656176	99.04624	99.57101	98.81612	99.71585
16	99.928945	99.72807	99.90572	99.61539	99.94156
17	99.989137	99.93843	99.98449	99.89668	99.99101
18	99.998813	99.98921	99.99815	99.97746	99.999
19	99.999911	99.99857	99.99985	99.99608	99.99992
20	99.999996	99.99986	99.99999	99.99947	100
21	100	99.99999	100	99.99994	100
22	100	100	100	100	100
23	100	100	100	100	100
24	100	100	100	100	100
25	100	100	100	100	100

B. S809 Airfoil Data

Table B.1: Lift coefficient vs angle of attack S809 EXP [X Foil &Re10^6

Angle of attack α (deg)	Lift coefficient (C_L)
1	0.27
2	0.389
3	0.508
4	0.624
5	0.739
6	0.792
7	0.865
8	0.924
9	0.979
10	1.03
11	1.07
12	1.11
13	1.14
14	1.16
15	1.21
16	1.24
17	1.26
18	1.28
19	1.29
20	1.28

Table B.2: Drag coefficient vs angle of attack S809 EXP [X foil&Re10^6]

Angle of attack α (deg)	Drag coefficient (C_D)
1	0.00804
2	0.0081
3	0.00809
4	0.00814
5	0.00815
6	0.012
7	0.014
8	0.0157
9	0.0182
10	0.0216
11	0.0265
12	0.0325
13	0.0391
14	0.0461
15	0.0525
16	0.0601
17	0.0695
18	0.0802
19	0.0927
20	0.109

Table B.3: Data experimental S809 three blades

WIND SPEED (V) [m/s]	POWER (P) [KW]
5.4	2.63
6.3	4.47
7.2	6.83
8	9.63E
8.9	12.2
10.3	15
11.2	16.5
12.1	17.7
13	18.5
14.3	19.1
15.2	19.3
16.1	19.5
17	19.6
17.9	19.8

Table B.4: Data experimental S809 two blades

WIND SPEED (V) [m/s]	POWER (P) [kw]
6.01	4.12
7.21	6.16
8.02	8.38
9.09	9.88
10.1	10.2
11.0	9.88
12.2	10
13.09	10
13.82	9.84
15.02	9.18
16.21	8.78
17	8.82
18.19	8.86
20.03	8.6

CURRICULUM VITAE

PERSONAL INFORMATION

Surname, Name: Benghuzzi, Abdulhamid
Nationality: Libya
Date and Place of Birth: 18 December 1969, Ejdabya
Marital Status: Married
Phone: 05395601109
email: hameid2006@yahoo.com

EDUCATION

Degree	Institution	Year of Graduation
MS	TIMS Corrosıon Engineering	2008
BS	BSU Mechanical Engineering	1992
High School	Alfatih High School, Ejdabya	1998

WORK EXPERIENCE

Year	Place	Enrollment
2014-Present	THK University	Ph.D Student
2009-2013	HIEG Dept. of Mechanical Eng.	Research Assistant
1998 July	Misrata	Intern Eng. Student
1996 August	Ejdabya	Intern Eng. Student

FOREIGN LANGUAGES

English

PUBLICATIONS

M. Elmnefi and A. Benghuzzi, "An Analysis Of Wind Speed Distributıon And Economical Evalution At Misrata City, Libya" 10th Ankara International Aerospace Conference 18-20 September 2019 – METU, Ankara Turkey